Project funded by EUROPEAN UNION

PONTOS

Black Sea CROSS BORDER COOPERATION

Copernicus assisted environmental monitoring across the Black Sea Basin – PONTOS

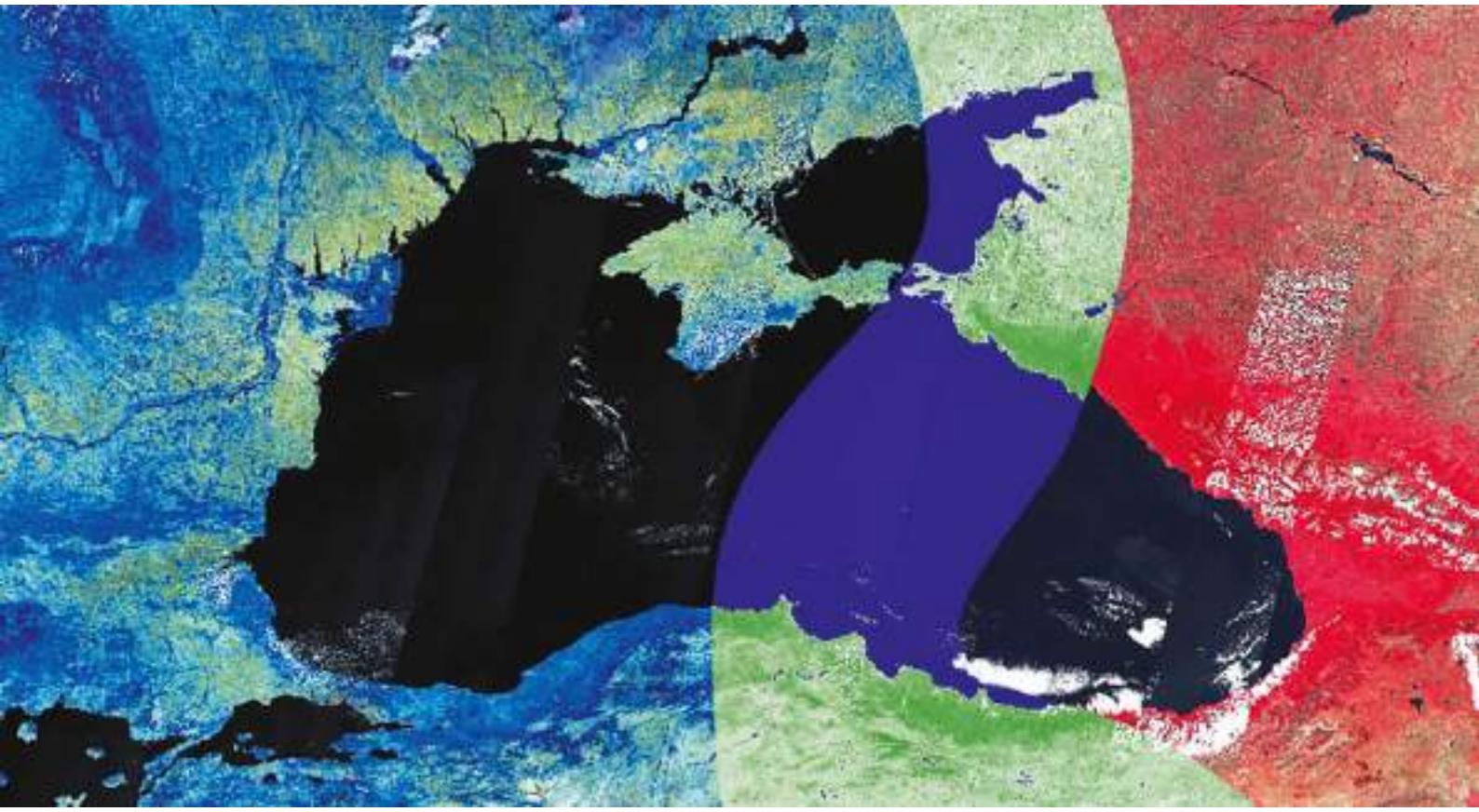

Report on Dynamics of Ukrainian Coastal Line Changes for 1980-2020

Deliverable D.T1.2.1

PONTOS – UA-1 (Ukraine)

Ukrainian coastal zone from Danube Delta to the Great Adzhalyk Estuary (Odessa bay)

Table of Contents

1. Introduction

The problem of destruction of marine coastal zones, which are the most densely populated and developed areas in the world, is in focus of attention of many researchers globally (e.g. Cherkez, 1996; Cherkez et al., 2006; Freiberg et al., 2012; Luijendijk et al., 2018; Tatui et al., 2019) whose efforts are concentrated on studies of natural and anthropogenic factors' influence on intensity of shore erosion, which is caused first of all by changing of sea level and coastline abrasion, as well as revealing of critical coastline areas with maximal intensity of coast destruction processes. Besides, in line with the EU Marine Strategy Framework Directive, coastal abrasion has been chosen one of impact indicators for coastal ecosystems of European seas, having special importance for the Black Sea. The main impact of coastal abrasion on the marine environment is due to large amount of suspended matter entering coastal waters thus decreasing transparency and causing siltation, which dramatically damages coastal algal and seagrass communities and completely destroys natural processes of their reproduction. There are abrasion and cumulative types of coasts, which differ in prevailing processes and forming of different relief forms, which are characteristic of each type (Cherkez, 1996; Freiberg et al., 2012). The problem of coasts erosion is especially important for shallow north-western part of the Black Sea (NWBS), where intensity of coast destruction varies within broad limits for different parts of the coast and different periods of observation (Atlas, 2006). According to the authors (Shuiskiy and Vikhovanets, 1989; Zelinskiy et al, 1993, Safranov et al, 2017), coastal abrasion is the main mechanism of coastline formation in the NWBS. It has been shown that intensity of coastline forming processes is different for separate NWBS areas and depends on lithological composition of sea cliffs rock, sea level, wave's direction and intensity, composition, direction and intensity of sediments flow, economic activities. Light and easily corrodible rocks dominate in the NWBS coasts. That is why more that 75% of sedimentary material is carried out from the coastal zone to the open sea driven by differentiation processes (Shuiskiy and Rotar, 1975; Zelinskiy et al, 1993). It has been established that qualitative characteristics of beach drifting in the NWBS are characterized by high spatiotemporal variability from -1.5 to +5 m/ year. This is true for all the NWBS areas but the Danube River deltaic part, where beach drifting could reach +180 m/ year (Atlas, 2006). At that it should be pointed out that instrumental studies have been brought down to a minimum in past decades due to economic reasons; the available sets of historical instrumental data are discontinued; observation points are located along the NWBS coast unevenly; local geological, hydrological, meteorological and economic conditions of the coast are very rarely taken into account. Therefore to study how the sea ecosystems are affected by intensity of shore (beach) drifting, currently remote sensing techniques (RST) are widely used (Cherkez et al., 2013; Gazyetov et al., 2015; Luijendijk et al., 2018; Tatui et al., 2019). Using RST we are able not only assess coastal destruction, but also perform quantitative estimation of coastal areas increase/ decrease, quantify suspended terrigenous matter, nutrients and toxicants carried into the open sea and then accumulated in other coastal areas and/ or in bottom sediments.

As was shown in (Cherkez et al, 2020) Maximal changes of coastline position in the North-Western part of the Black Sea were registered in the Danube Delta, areas of the Sasyk and Dniester Limans and Odesa Bay for the 1983-2013 years. Land area in those locations grew more than 16 km^2. In the other NWBS areas decrease of land terrain was observed, i.e. destruction of coasts, which made about 5 km^2. At that, it should be noted that the biggest changes were taking place in the past decade.

Aim of the work has been to study different coast areas' growth/ reduction resulting from coastlines position dynamics changes under abrasion and accumulation processes in pilot area UA1 in the North-Western Black Sea (NWBS) influenced by natural and anthropogenic factors over 1980-2020 using LANDSAT satellite images .

As other partners we used several open-source databases for retrieving satellite images, such as:

- Earth Explorer (https://earthexplorer.usgs.gov/)
- Copernicus Open Access Hub (https://scihub.copernicus.eu/), and
- Planet Explorer (https://www.planet.com/explorer/).

Furthermore, remote sensing information can be integrated with Geographical Information Systems (GIS) as a helpful tool for analyzing and extracting more reliable and consistent information by using satellite imagery as base data. The satellite image processing methods to extract the shoreline position may be applied using tools as the Geographical Information System software (e.g., QGIS, ArcGIS). Several techniques have been documented to evaluate the shoreline movement, mainly with the use of GIS software. The most common are the transect-based and the point-based approaches. Both techniques are capable to calculate the short- and long-term shoreline changes. Extraction and application of the transect-based approach became more easily applied with the Digital Shoreline Analysis System (DSAS), created by the United States Geological Survey USGS (Thieler et al., 2009).

The present study presents the methodology applied for the identification of the coastal erosion and accretion hotspots in the PONTOS project pilot area UA1. The shoreline change analysis covers the period 1980 to 2020. A common methodological framework was developed by all partners, consisting of four main steps:

a) the creation of a list containing all data sources, referring to each coastal area of interest,

b) the retrieval of all historic satellite images,

c) the historical shoreline extraction from the historical satellite images, and

d) the execution of an algorithm to estimate the statistical parameters related to shoreline change over time.

2. Background

2.1. Geology and Geomorphology

2.2.

The north-western Black Sea coastal zone is developing under the complicated natural conditions. Its state is significantly influenced by the peculiarities of geological structure, lithology, tectonics and neotectonics, geomorphology, climatic and hydrological conditions of the area. The relief of the north-western Black Sea coast was formed under conditions of complicated interaction between exogenous, endogenous and anthropogenic factors resulting at regional morphostructural and morphosculptural features. Morphostructures reflect the influence of endogenous factors on the formation of the relief. Morphosculptures are formed under the leading role of exogenous processes, which are genetically and spatially subordinated to morphoclimatic zonation and are controlled by morphostructural conditions.

Modern geomorphology of the northwestern Black Sea coast was formed in the Neogene-Quaternary time on the background of intensive and differentiated neotectonic movements. Types and forms of the relief, nature and development of the coast demonstrate a clear dependence on the geological structure. The relief was formed under the influence of denudation processes, erosion-accumulative activity of watercourses, abrasion of the Black Sea, changes in climatic conditions (Zelinskiy I.P. et al, 1993; Cherkez, E.A. et al, 2012). Anthropogenic processes resulting from civil engineering, hydrotechnical, land reclamation and other economic activities are a powerful factor of modern geomorphogenesis and determine the anthropogenic variability of the natural relief. The northwestern coast from the Danube Delta to Karkinitska Bay is located within the southern edge of the Black Sea lowlands. The flat surface of the loess watershed is gently sloping to the sea, has small heights (5 to 50 m), is characterized by weak dissection of the relief by the ravine-beam network and deeply incised river valleys, lakes and estuaries.

The studied coastal zone can be divided into two major areas by the shore type: 1) Zhebryiany-Ochakiv – the estuary-lagoon type: leveled shore stretching from southwest to northeast; 2) Dnipro-Karkinitskyi area (from the Kinburn Spit to the Dzharylgach Island) - abrasive-accumulative shores in loose clay-sandy deposits, shore contour is large-bay or lobed, stretching from northwest to southeast [Zenkovych V.P., 1958]. The coastline of the first area is interrupted by large estuaries - Dniester, Sukhyi, Khadzhibey, Kuyalnyk, Malyi Adzhalyk and Velykyi Adzhalyk, Tiligul, Berezan and Dnipro-Bug. The Dnipro-Karkinitskyi area has a complex dissected configuration and is characterised by the development of bars, spits and islands. The largest landforms are represented by the Kinburn Spit, the Yegorlyk Bay and the Tendra Bay. The Black Sea estuaries appeared as the result of seawater encroachment into the mouths of river valleys and erosive lowlands in the land relief.

During the late Pleistocene-Holocene, numerous bays and coves of various shapes were formed. Later on, most of the estuaries were blocked from the sea by spits and sandbars. Thus, the classic estuarine type of coast was formed.

The estuaries of the first area are extending northeast, while the estuaries of the second area have meridional extension. This is due to the tectonic movements of orthogonal and diagonal nature associated with deep faults.

Having access to the Black Sea coast, the valleys of rivers, estuaries and ravines contribute to the high dismemberment of the coastal slopes, where their density makes ca. 0.5 km/km^2. Due to erosion, abrasion and landslides, the Black Sea coastal slopes have the form of a complex wavy line with maximal height up to 54 m above sea level within Odesa city and minimal at the mouths of rivers and estuaries. The amplitude of the coastal relief dissection averages to ca. 30 m with maximal values reaching 60 m [Geology of the shelf of Ukrainian SSR, 1982].

Slow immersion of the coastline causes continuity of abrasion and landslide processes. The avalanches of the undermined cliffs form sliding terraces and cones of talus at the foot of the slope. Aeolian forms (heaps, dunes, hills) are typical for spits and sandbars.

The northwestern part of the coast is characterised by a platform (transgressive) type of shelf, which has the form of slightly hilly plain and considerable width. The continental slope edge (isobath 100-200 m) is 100-200 km far from the shoreline. The main most clearly defined large elements of the shelf are large sloping planes with relics of erosive relief (Fig. 2.1) [Shmuratko V.I. 2016.]. Depressions are represented by wide well-developed paleo-valleys of the big rivers Dnipro, Dniester and Sarata [Zenkovych V.P. П. 1960.; Shmuratko V.I. 2016.]. In some places their width reaches 20-30 km and the relative elevation is up to 30 m. They are trough-shaped. Paleochannels can be seen in their axial zones.

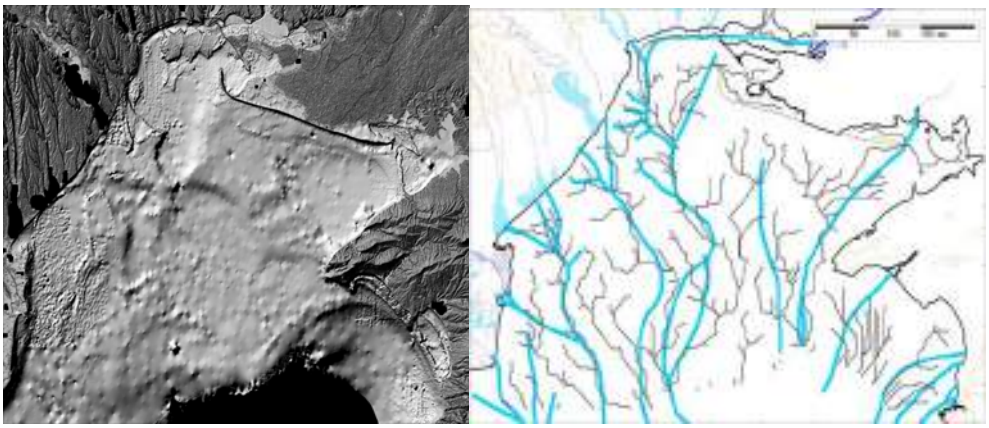

Fig. 2.1. Shadow relief model left-hand side) built based on the digital database [Shmuratko V.I. 2016.] and hydrographic network of the epoch of last glaciation maximum of the Black Sea north-western shelf (right-hand side). Blue lines show the network of rivers identified using geological and geophysical methods; thin dark grey lines - hydrographic network calculated based on morphometric features of the modern shelf relief [Shmuratko V.I. 2016.]

Odesa Trench, which has an asymmetrical trough-like shape, also belongs to the negative forms of the relief. It is 4 to 9 km wide and its average depth is 12-15 km. The trench was made by waters of the Paleo-Dnipro and its tributary, the Paleo-Southern Bug, in the late Pleistocene. In addition to the alluvial forms making the basis of the shelf, the forms of marine genesis are important - areas of abrasion terraces (benches), banks and underwater coastal barriers composed of marine sand and shell deposits.

There is an abrasion terrace (bench) on the underwater slope of the abrasive shore, which is the result of waves influence on the Neogene rocks in the Late Pleistocene-Holocene. The abrasion terrace is up to 6 km wide. There is no abrasion terrace in front of the estuaries. The outer edge of the bench lies at depths of 10-15m. In Odesa section of the coast it is composed of meotic clays partially disturbed by landslide processes.

The largest accumulative forms of the northwestern shelf are the Odesa Bank and the Dniester Bank. The Odesa Bank is separated from the land by the Odesa Trench in the north and is 5 km far from the shoreline. The Dniester Bank is located within the Dniester Upland on the shelf 12 km far from the shore and stretches in meridional direction.

Brief overview of the northwestern Black Sea coast natural conditions and the peculiarities of the current shelf relief shows that abrasion and accumulation processes have been widespread in the history of the coast in the studied area development during the Holocene.

The Black Sea has a great variety of shore types, but the main feature of their differences, used by most authors of classifications [Shuiskiy, Vykhovanets, 1989, 2009; Kaplin et al, 1991; Shuiskiy, 2000; Ignatov, 2010], are the wave-formed abrasion and accumulative genetic types, which differ from each other in the formation of different relief forms, characteristic of each type of shore. Due to abrasion processes, the destruction of coastal slopes in the form of landslides and avalanches takes place and a type of shore is defined as abrasion-landslide or abrasion-avalanching. Accumulative shore type appears due to sediments accumulation, however, depending on changes in the intensity and dynamic indicators of sediment flow, as well as hydrological conditions of the sea, the type of accumulative shore can be defined as accretion, erosion or dynamically stable. Such division of shores into characteristic types allows, as an integral characteristic of abrasion and accumulation processes intensity, the of use indicators of shoreline movement magnitude and speed, which are determined using field instrumental or space images processing methods. .

2.3. Coastline Dynamics

High degree of modern coastal zone dynamism has been revealed. According to the Black Sea State Regional Geological Enterprise, out of 87 km of abrasive shores in Odesa Region about 50% are being eroded at the rate of up to 1.0 m/year; 2% of the length of the coast has the erosion rate of more than 1.5 m/year. The highest levels of abrasion are observed in the area from Cape Burnas to the Budakskyi Estuary, where loess-like rocks flake away above sea level (Zelinskiy et al, 1993). This abrasion site (abrasion and landslide monitoring station “Lebedivka”) of the seacoast has the length of 20 km, out of which 18 km are abrasion and landslide slopes of living rock. During the period of observations (2006-2012) the average coastline retreat rate was 1.45 m per year with the maximum value of 9.0 m/year. Among the accumulative coastal forms, the sandbar areas of the Dniester Estuary and the Alibey-Burnas Estuary suffer the most threatening destruction. The most significant erosion of the Dniester Estuary sandbar occurs in the vicinity of Zatoka village and to the southwest of it; the rate of coastline retreat there makes 0.9 - 2.3 m/year. Relatively stable segments of the coast are located in the northeastern part of the Budakskyi Estuary, on the Dniester Estuary sandbar to the northeast up to the valley of the Baraboy River (Vykhovanets et al, 2018). This is due to the fact that the foot of the coastal ledge is protected by a full profile beach. The increase in the height of the cliff and appearance of limestones in its outcrop in the Sukhyi Estuary area caused the decrease in the average rate of abrasion to 0.5-0.7 m per year (Safranov et al, 2017). In the segment of coast between the Sukhyi Estuary and the Tiligul Estuary, where the rocks of the coastal slope contain clays of the Meotian tier and Upper Pliocene, as well as limestones of the Pontic tier, abrasion has an average rate of 0.2-2.0 m per year. Thus, in the area of town Chornomorsk the coastline retreats with an average speed of 0.5 m per year. Average long-term rate of coastline retreat in the area between the Kuyalnyk Estuary and the Tiligul Estuary is ca.0.5 m per year. At the same time in the western part of the area the maximum value reaches 5 m, while near the Tiligul Estuary it makes ca. 1.5 m (Safranov, et al, 2017). The limestone blocks that accumulate at the foot of abrasive-landslide slopes reduce the rate of abrasion. In some areas that suffer significant anthropogenic impact, the rate of cliff erosion exceeds 1.5 m per year. Those areas are located on the southern outskirts of Fontanks village to the west of Hrygorivka Port.In general, quantitative characteristics of shoreline movements in the northwestern part of the Black Sea coast have high spatio-temporal variability, on average from -3.0 to +3.0 m/year in all areas except the Danube Delta, where the changes of coastline position can reach up to +180 m/year (Fig. 2.2A).

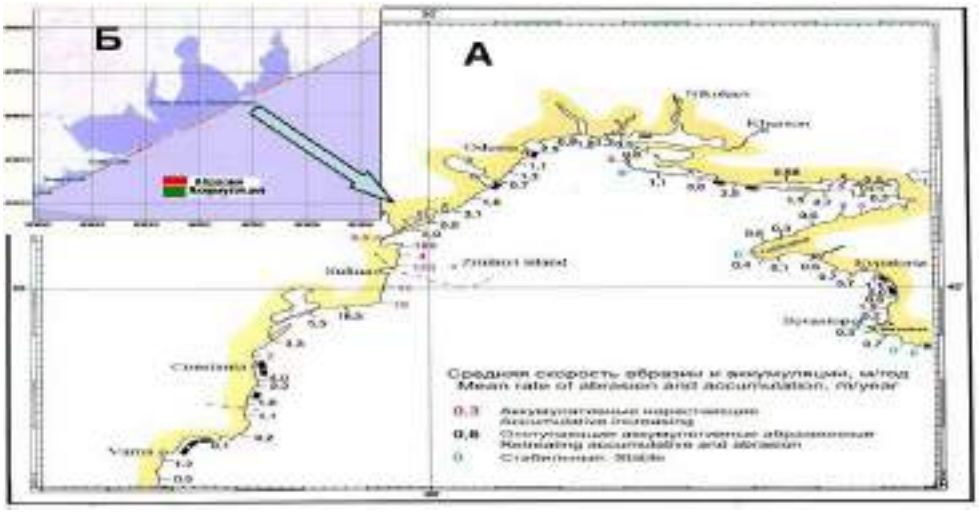

Fig. 2.2. A – average rate of abrasion and accumulation in the northwestern Black Sea coast for the period 1960 - 1994 [Shuiskiy Yu.D, Vykhovanets G.V., 2009]. B – schematic map of the coastline dynamics between the Sasyk Estuary and the Budakskyi Estuary for 1983 – 2013 [Cherkez et al, 2013, 2020].

Long-term changes in the shoreline of different scales are effectively registered using a set of instrumental and space observation methods [Cherkez et al, 2013, 2020], which allow not only to assess the intensity of abrasion and accumulation, but also to proceed further to quantitative estimates of reduction or increase in coastal areas. Thus, it was established based on the Landsat space images processing (of 1983, 1993, 2003 and 2013) that the change in abrasion-accumulation areas at ten-year intervals on the segment between the Sasyk Estuary and the Budakskui Estuary (Fig. 2.2B) made -1.257 km^2 (1983-1993), -0.514 km^2 (1993-2003), +0.137 km^2 (2003-2013). These data indicate the decrease in land area by 1.634 km^2 for many years period due to abrasion (1983-2013) [Cherkez et al, 2013, 2020].

Coastline retreat rates as the result of abrasion, even in local plots, are characterised by spatial unevenness. For example, according to the website Long-Term Shoreline Changes (http://aqua-monitor.appspot.com/=shoreline) the average rate of abrasion-landslide slope retreat in the area of Lebedivka village for the period 1984 - 2016 was 1 - 2 m/year (Fig. 2.3).

Fig. 2-3. Average speed of coastline displacement in the area between the Burnas Estuary and Lebedivka village (http://aqua-monitor.appspot.com/=shoreline).

Accumulation processes prevail in the adjacent section of the sandbar separating the Burnas Estuary from the sea, but the displacement of the shoreline towards the sea is spatially uneven. The average speed of displacement of the shoreline towards the sea is 1-2 m/year. However, in some areas coastline retreat at the speed of 1-3 m/year is observed (Fig. 2.3).

These data indicate spatial and temporal changes in the development of abrasion and accumulation and the position of the coastline.

2.4. Processes Influencing Destruction and Dynamics of the Coasts

The main factors determining the intensity of coastal destruction and underwater erosion, as well as sediments accumulation and coastline dynamics, are:

- hydrological - wind and wave regime, level regime, tides, wind-driven up and down surges, features of wave influence, wave energy, direction of currents, characteristics of sediments movement along the coastal and transverse, depth of a water-body etc.;
- geological structure of the surface and underwater parts of a coastal slope - structural and geological features of the coastal massif, type and lithology of rocks, the ability to lose strength due to moisture, fractures etc.;
- geomorphological conditions of a shore and an underwater slope - shape of the coastal ledge, geomorphological type of the shore, height and steepness of the slope, shape of the shoreline on the ground plan etc.

It is important to emphasize that the northwestern Black Sea coast suffers intensive anthropogenic impact. Here industrial, civil and hydrotechnical construction works are done, dredging is performed, minerals are extracted, tourism and recreation are developing; all that produces negative effects on the coastal zone stability. Therefore, study of the coastline dynamics, along with the issue of preventing from undesirable consequences of human activities, is the key point in development of the coastal zone and the coastline. The dynamics of shores and the development of abrasion processes are indirectly influenced by wind regime, which has a well-defined seasonal variability due to changes in hydrological conditions in the coastal zone. The winds of the northern rhumbs prevail throughout the year, their frequency increases especially in the cold season. Predominance of southern winds is typical of spring period (March - May). In summer, almost equal probability of winds of all rhumbs is obsrved with slight predominance of northwestern direction. Average annual wind speed is 3.5-4.5 m/s, near the coast it increases to 4-6 m/s and on the Zmiinyi Island it reaches 6-7 m/s. Strong winds (15 m/sec and over) prevail in the cold season. Their maximum speed can annually reach 20-24 m/s.

The northwestern part of the Black Sea is shallow and has small slopes of the bottom. The depths 100 m far from the shore rarely exceed 3-4 m. The distance of 150 km from the north shore corresponds to the 50-m isobath. Therefore, the process of sea wave destruction begins at a considerable distance from the coast. Southeastern and southern exposure of the coast contribute to the development of wind waves from the south, southeast, east and partly from the northeast. Northeast and northwest winds, the frequency of which is quite high, are the alongshore ones and cause no surge. Therefore, wind waves of 0.75 m height and 10% probability are considered big [Shuiskiy, 2013]. The 1.5 m high waves are monthly observed on Odesa coast. The following segments are characterised by the highest waves: Zhebryianska Bay - Dniester Estuary (maximum height 3.5 m) and Odesa - Ochakiv (maximum height 3.5 m). The highest waves are usually observed with the winds from east and southeast; they contribute to the wind-driven water inflow to the northwestern Black Sea and the sealevel rise near the shore. Raising of the level during surge contributes to active destruction of the coastal ledge. When the sea level drops during the surge, which occurs with long westerly winds, active erosion of the coastal shoal takes place. There are many factors influencing the sea level: wind, currents, water exchange with the World Ocean, atmospheric pressure and even tectonic processes. Sea level is an important factor determining the nature and level of wave impact on the coast.

Information about the level should characterise its average and predominant regimes, as well as the distribution over time and even its extreme values under specific physical and geographical conditions.

Transition from dropping to rising of the Black Sea level, which occurred in the 20s of last century, became a characteristic feature of changes in its average annual values over a long period.

According to the data from the "Odesa" Station, the level was decreasing at the rate of 0.14 - 0.16 cm/year in 1876-1921, while from 1921 to 1995 the rate of increase made 0.30 - 0.37 cm/year [Konikov et al, 2010; Andriyanova, 2017]. In recent decades, there has been a decrease in growth intensity and stabilization of the level. Analysis of the data on the century-long Black Sea level in Odesa region shows that the abrasion processes taking place actively now are the direct consequence of modern transgression.

The surface of the Black Sea is affected by various factors that cause different dynamic phenomena and influence the position of the level. One of those are short-term wind-caused fluctuations of the water level (Fig. 2.4), reaching 2-3 m within the north-western coast.

Fig. 2.4. Wind-driven water recession in town Chornomorsk, November 12, 2015 (left-side picture) and in Odesa, October 27, 2018 (right-side picture). http://trassae95.com/images/64/big/64205-anomaljnyj-otliv-nablyudaetsya-na-poberezhje-pod-odessoj-foto-big.jpg

Coastline transformation processes are closely related to movement of sediments in the coastal zone of the sea, which entails the necessity to study marine coastal currents. The system of surface currents in the northwestern Black Sea depends on the total magnitude of all sea disturbances within the coastal area for a long time. At long and strong winds steady currents were observed down to the depth of 40-60 m. With strong winds the speed of current can reach 100-150 cm/s. The main Black Sea stream passes mainly by the mainland slope, which separates the shelf and the deep-water zone. Along with the main Black Sea current, there is an intensive current along the coast at the speed of 80-120 cm/s due to the flow of the rivers Dnipro, Dniester, Danube etc. [Zelinskiy et al, 1993]. Currents in the coastal zone, from water edge to of 10-15 m depths, differ in a number of features. Powerful and complex systems of gradient, energy and drift currents develop here. During storms, the currents have the form of channel flow (with the speed of 100-150 cm/s) within the strip between water edge and 2-3 m depth. At depths up to 7-8 m during storms of moderate force, the maximum flow velocities make 80-90 cm/s. Further, towards the sea, the coastal currents interact with the drift currents of the open sea.

High-speed currents can move huge masses of debris, sand and silt material resulting from the abrasion of cliffs, bottom, river runoff, as well as from the grinding of mollusc shells. As the result of coastline abrasion and currents impact, sediment flow is formed and the sediments accumulate in the coastal zone (for example, the Danube Delta, the southern side of the cutoff wall in the navigable canal to Chornomorsk Port).

The variety of factors and the differences in the degree of their manifestation have influenced the activeness and spatial distribution of abrasion and accumulation processes on the coast between the Danube and Karkinitskyi Bay.

Abrasion and sediment accumulation, despite their opposite effects on the shore, are closely related and are therefore considered together. These processes are developed along the northwestern coast of the Black Sea and its estuaries. Abrasion develops mainly near the shores having significant inclination of the underwater slope, while accumulation is characteristic of shores with shoals.

Abrasion is the process of destroying the rocks, which make up the coast, as the result of surf waves. Abrasive erosion depends on geological structure of the coastal zone, lithological composition of rocks, relief and height of surface and underwater slope, hydrodynamic characteristics (sea level, wave regime, direction and saturation of sediment flow along the coast) [Longinov V.V., 1963]. Different rates of abrasion processes are also due to the block nature of modern negative neotectonic movements. Coastline geometry and general layout of hydrographic network with full certainty confirm extensive participation of the inherited neotectonic movements in the formation of coastal morphology and dynamics [Rotar, 1975]. In addition, the current stage is characterised by sea transgression being the consequence of eustatic rise in level of the World Ocean, to which the Black Sea is connected. The intensity of neotectonic movements and sea level control the size of waves' specific energy and the intensity of bottom abrasion, as well as abrasion and abrasion-landslide processes of the coastal slope. Coastal abrasion is one of the main processes on the Black Sea coast, resulting in its destruction, formation of landslides, avalanches and loss of valuable land. As the result of abrasion, large volumes of suspended material enter the underwater extension of the slope and are moved by sea currents. In ecological terms, the negative consequences of this process are reduction of water transparency, siltation of the bottom and oppression of underwater biocenoses. That is why coastal abrasion is one of indicators of impact on marine ecosystems under the EU Marine Strategy Framework Directive.

Costal abrasion and sediment accumulation processes cause alternation of the corresponding landforms and a high degree of dynamism of different modern coastal zone parts. The problem of shore abrasion in its shallow northwestern part is especially relevant for the Black Sea. The intensity of shore destruction in different parts of the coast and different observation periods varies within broad limits. In turn, the abrasive cutting up of the shore by waves creates conditions for coastal slopes destruction in the form of avalanches and landslides. Besides, the process of erosion of accumulative coastal landforms - sandbars, spits and beaches – is widespread. Coastline movement towards the sea is observed only on some sandbars and in some areas. The coastline forming processes and coastal dynamics in different northwestern Black Sea areas depend on lithological composition of the coastal cliffs rocks, their height, beach width (Fig. 2.5), sea level, direction and intensity of waves, as well as composition, direction and intensity of sediment flow and economic activities.

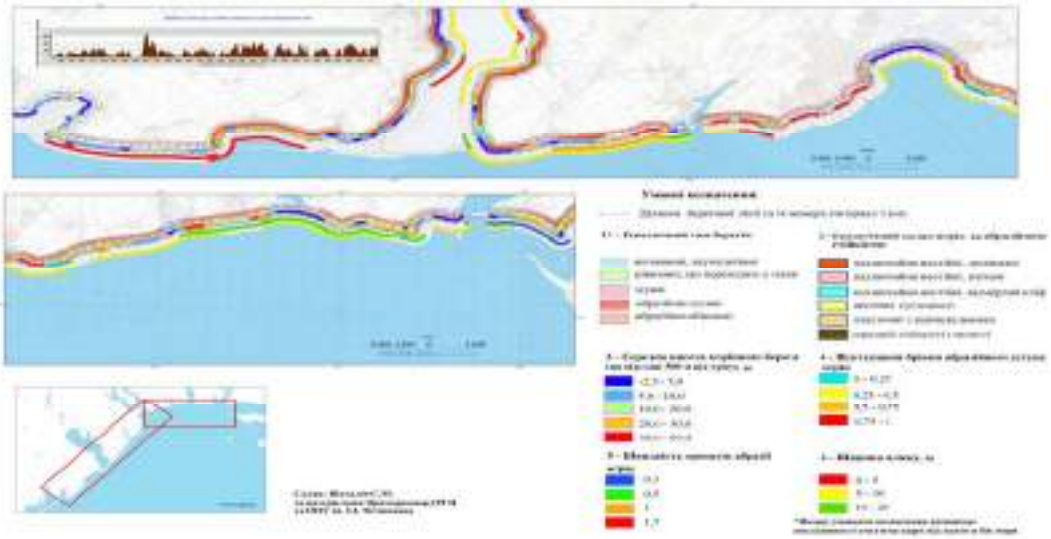

Fig. 2.5. Schematic map of conditions under which abrasion is developing on the segment of the Black Sea coast between the Burnas Estuary and the Dnipro Estuary

The shores of the northern Black Sea are more abraded, with active cliffs, mainly of loess rocks (Fig. 2.6); the lowest level in many areas are composed of red-brown clays (Danube - Dniester) and terrigenous-carbonate rocks (Odesa area). In the section from the Sukhyi Estuary to the Dnipo-Bug Estuary, abrasion is interconnected with landslide processes developed in this area (Fig. 2.6).

Fig. 2.6. Abrasion-avalanche type of coast (left-side picture) and Abrasion-landslide type of coast (right-side picture)..

Abrasive cutting up of the shore by waves, despite its crucial role in damaging the coastal slopes' stability, is only creating the preconditions for the slopes destruction. The mechanisms and ways of coastal slope destruction depend mainly on the properties of the rocks represented in the coastal slope, as well as on the slope's morphometric characteristics - height, inclination and shape of the profile.

The rate of abrasion is influenced by the beaches, namely their composition, size and dynamics. Due to the fact that the Black Sea northwestern coast is composed mainly of loose, easily eroded rocks, more than 75% of the sedimentary mass is carried outside the coastal zone into the open sea under the influence of differentiation processes [Shuiskiy Yu.D., Rotar M.F. 1975]. This causes shortage of the sediments that form beaches. Under these conditions, the excess of wave energy maintains high abrasion rates. It is known that under the modern hydrodynamics a 35-40 m wide Black Sea beach is able to completely protect the coast from erosion; when the width is smaller, the coasts destroy with different intensity.

The beaches located southwest of Odessa differ from the north-eastern areas in the main parameters: width, height and volume of sediments. The first area is characterised mainly by sandy beaches stretching in a continuous strip (Fig. 2.6). Their long-term average annual width is ca. 16 m, maximum up to 26 m. The north-eastern region is represented by pocket-type beaches (Fig. 2.6), which are not continuous and composed of carbonate gravel-sand material with an admixture of boulder fraction of limestone-shellstone rock. Average annual width of the beaches there makes ca. 8 m, i.e. twice less than in the first area. Long-term average annual volume of beach sediments on the southwestern coast is 3 times higher than in the northeastern area - 22 m^3/RM and 6.0 m^3/RM respectively. Thus, beach width and sediments in the studied area are quite low, which leads to abrasion and abrasion-landslide processes development. The transformation of the coastal zone development regime from abrasive to dynamically stable could be achieved by means of artificial increase in the morphometric parameters of the beach area. In addition, the process of accumulative coastal landforms erosion (sandbars, bay bars, spits and beaches) is widespread here (Fig. 2.7). There are only two sandbars where, in some segments, coastline movement towards the sea is observed. Those are Kuyalnyk-Khadzhibey Sandbar (0.3-0.5 m per year) and Zhebryianska Bay (from 1.5 m per year) (Fig. 2.7).

Fig. 2.7. Accumulated and eroded coast (sandy spit separating the group of Tuzla estuaries) (left-side picture) and Accumulative out-building coast (the Danube Delta, town Vylkove) (right-hand picture)..

In Mykolaiv Region, 50 km of the Black Sea coast and the right slope of the Dnipro Estuary (about 10 km) have been damaged by abrasion processes, of which 60% of the slopes are characterised by weak abrasion - less than 0.5 m/year. To the east of the Tiligul Estuary, rather high rate of plateau edge retreat (up to 1.0 m per year; a maximum value - 2.4 m per year) is explained by the presence of Pliocene sands, whose abrasion resistance is much lower than that of loam, clay and limestone. The areas to the east of town Ochakiv are being washed away most intensively (1.5 m/year). Accumulation of sediments is observed on the Tiligul Estuary sandbar, which is accompanied by the coastline movement towards the sea up to 2.4 m per year in some areas.

The eastern part of the studied area is administratively located within the Kherson Region and characterised by low shores, which are periodically flooded and dried up as the result of wind surge of seawater. The strip of wind-dried shores composed of silt and clay is several hundred meters wide, up to a maximum of 2000 m. Their abrasion rate is 0.2-0.4 m per year, maximum 1.8 m/year. The shores of Dzharylgach Bay are characterised by average abrasion rate of 0.1-0.4 m/year. As the result of exogenous geological processes monitoring on the Zmiinyi Island in its southern and southwestern parts, which are composed of uncemented relocated and redeposited rocks, the development of coastal strip abrasion is observed. The rate of the coastline retreat does not exceed a few dozens of centimetres a year. The most dangerous process is the erosion of the base of the pier in the northwestern part of the island, which can lead to its partial destruction and separation from the main body of the island. Differences in abrasion rates, as well as types of coasts and the processes observed in the abrasion-avalanche and abrasion-landslide areas of the northwestern Black Sea are associated with the peculiarities of the coastal slopes' geological structure (Fig. 2.8).

Fig. 2.8. *The area of the northwestern Black Sea coast with abrasion-landslide shore type, where mainly landslide processes prevail (A) and the corresponding alongshore geological & lithological section (B)* [Cherkez et al, 2021].

As an example, let us consider the part of the coast between the Budak and Burnas accumulative sandbars, where the State Regional Geological Enterprise "Prichernomorgeologiya" has established the abrasion monitoring station "Lebedivka" in the late 70s to observe the dynamics of coastal slope erosion and destruction (Fig. 2.9). The Budak - Burnas abrasion area starts with relatively low (8.7 m) Cape Burnas (Lebedivka village) and extends gradually rising (up to 26 m) to the northeast to Cape Budaki (village Kurortne). The length of this section of the coast is 1800 m, the exposure of the slopes is N-E 45°. The shore belongs to abrasive-landslide type. The cliff almost everywhere looks like a steep wall. Its upper and lower parts are close to vertical (70-90°), and the middle is inclined at an angle of 30-40°. The upper part of the cliff is in places cut by short narrow ravines. The coastal cliff is composed by Pleistocene loess rocks, which are prone to destruction by abrasion. The beach in the area is sandy, in the eastern part of the site it is 12-15 m wide, in the western part it narrows to 1-3 m; in some places there is no beach at all. There are landwash niches and landslides of moist loess rocks at the base of the coastal cliff. As the cliff is formed by a series of loess rocks, shore destruction occurs cyclically: first the formation of a landwash niche takes place, than an avalanche of loess rocks happens; this creates a temporary protection of the ledge from abrasion, then the accumulated masses are eroded and a new niche is formed.

Fig. 2.9. Abrasion monitoring Station “Lebedivka” at the Black Sea coast between the Burnas Lake (Lebedivka village) and the Budak Estuary (Kurortne village). On top – scheme of the monitoring station (the triangles show the benchmarks and their numbers) and a photo of the coastal slope; at the bottom – the average for the site cliff edge retreat rate (m/year).

The rate of cliff edge retreat, which is varying along the shore and over time, is the indicator of abrasion processes intensity. It depends on the geological structure and composition of the cliff rocks, hydrological factors (wave energy, sea level fluctuations, wind surges), sediment flow volumes, strength characteristics of rocks etc. According to observations, the generalized value of the cliff edge retreat in some periods (1978-1980, 1990, 2004-2005) could reach 2-3 m/year, with average cliff edge retreat value of 1.01 m/year and the foot retreat value of 0.88 m/year (Fig. 2.8). In the period from 2011 to 2016, the retreat rate was as follows: 2011 - 2.0 m/year; in 2012 - 0.37 m/year; in 2013-2014 - 0.2 m/year and in 2016 - 2.0 m/year. The alternation of years with activation and fading away of the abrasion process is explained by the gradual erosion of a large amount of collapsed material at the foot of the slope. The processing of this material takes some time, in our case from 2 to 5 years. This reduces the speed of the cliff erosion in certain periods of time. In general, all the variety of abrasion manifestations and the range abrasion rates within the "Lebedivka" monitoring station is mainly due to the combination and ratio of three basic factors, namely: geological structure and lithological composition of rocks, quantity and composition of sediments in the coastal zone and hydrological regime of the sea

The northwestern Black Sea coast is composed of sedimentary rocks of low strength, which contributes to intensive development of abrasion, landslides and avalanches. However, the types of landslides, their mechanism, morphometric characteristics and position of the displacement surface are largely determined by the peculiarities of the geological structure: the absolute value and ratio of strength properties of the rock layers, as well as their height relative to the slope [Cherkez et al, 2012, 2021]. The layer of Pontic limestone is the most significant reason of heterogeneity in the properties of soils, as it differs in strength characteristics from the host clay rocks by one or two orders of magnitude (strong layer) (Fig. 2.8). In cases the limestone subface is located above the sea level (most part of the coast) or its superface is below sea level, the average abrasion rates differ very little. If the subface of limestone is located at sea level (Rybakivka village), the average abrasion rate of reduces by 2-4 times (Fig. 2.10) [Zelinskiy et al, 1993].

The intensity of abrasion processes also depends on the lithological composition of landslide accumulations that peel off from the coastal ledge. If clay soils predominate there, the erosion of rocks is maximal and averages to 1.10 - 1.21 m/year. In the areas where shifted blocks of limestone are located at the base of the slope protecting coast from erosion, the rate of shoreline retreat decreases to 0.38 - 0.50 m/year [Zelinskiy et al, 1993].

Fig. 2.10. Abrasion-landslide slope in the area of Rybakivka village.

Lithological factor plays an important role in the development of coastal zone. The main prerequisites for its influence are the composition of the crop rocks, their different erodibility and the mode of their occurrence.

3. Materials and Methods

3.1. Methodological Framework Description

The herein-defined methodology (Figure 3.1) was developed by DUTH PONTOS partner (DUTH Report, 2022. Deliverable D.T1.2.1. PONTOS-GR (Greece) Nestos River, its Delta, and the coastal zone close to the Delta) and will be eventually applied to Ukrainian PONTOS pilot area UA1.

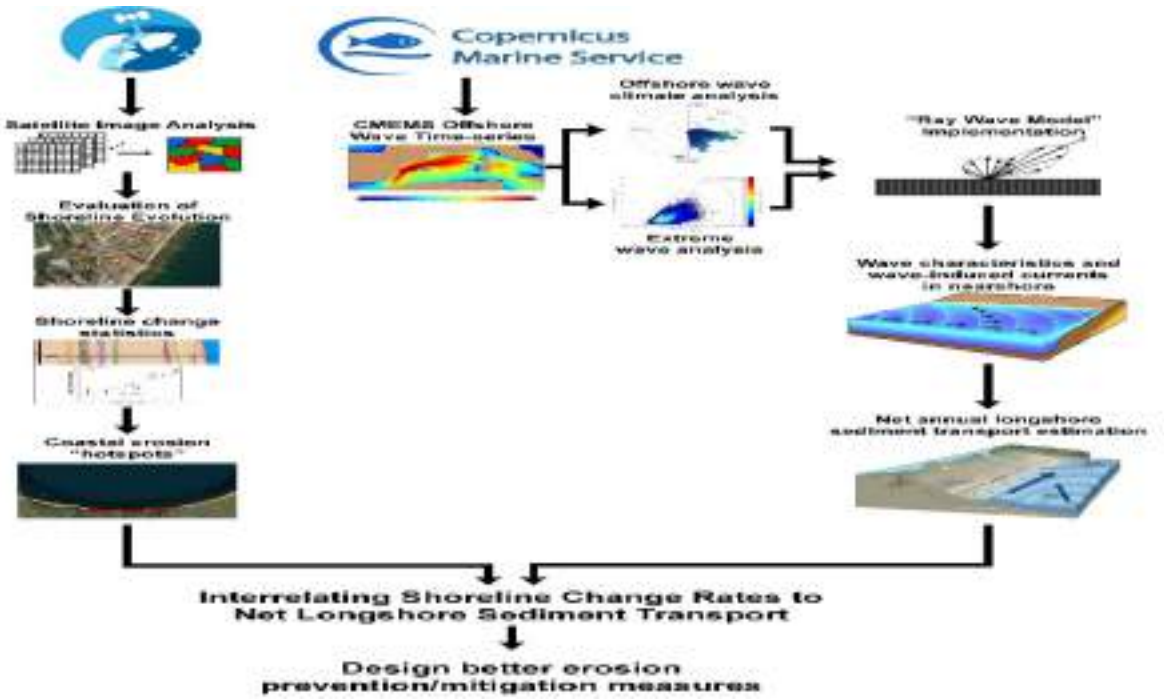

Figure 3.1. Conceptual framework to assess coastal erosion and accretion and to identify the processes responsible for coastline changes and ultimately to design better prevention/mitigation measures [DUTH Report, 2022].

This methodology entails the procedure of shoreline delineation using a semi-automatic image classification technique. All historical shorelines at UA1 PONTOS pilot area will be extracted by processing satellite images from Landsat 3,5,7 and Sentinel 2 satellite sensors. Image selection will be based on the correct geo-reference and the image clarity from the cloud cover. Then, these historic satellite images will be classified in terms of land and water and the historical shorelines will be eventually extracted. The shoreline evolution evaluation will be performed using the Digital Shoreline Analysis System (DSAS) [Thieler et al, 2009] provided by the United States Geological Survey (USGS), capable to produce auto-generated transects. In situ data, retrieved using a highly accurate GPS will further validate the satellite analysis method applied.

In parallel, PONTOS partners will develop in future a series of algorithms to easily download and access existing meteorological (wind speed and direction) and oceanographic data (currents and waves hindcasted and forecasted) from external platforms and systems (e.g., from CMEMS, NOAA, ECMWF). These data will be further used for future analysis to assess extreme waves (e.g., POT, EVA), to perform circular wave statistics, to apply ray wave models from the open sea to nearshore, to compute the wave-induced nearshore current, the wave breaker zone characteristics and the wave-induced theoretical sediment transport, etc.

3.2. Data collection

3.2.1. Topographic/bathymertic data

Topographic/bathymetric data were retrieved from the European Marine Observation and Data Network (EMODnet) Bathymetry portal (http://www.emodnet-bathymetry.eu). The 2020 version of the EMODnet digital terrain model (DTM) has been created at a grid resolution of 1/16 × 1/16 arc-minutes (115 × 115 meters) using available bathymetry data sets from a number of providers, included data from plummets, single beam, multi beam, and LIDAR observations, from composite DTMs and Satellite Derived Bathymetry (via the Sextant Catalogue service). To prevent gaps in the EMODnet DTM layer, the areas without information have been filled with the GEBCO 2020 data (15 arc-second30" gridded data; approximately 320 meters).

Topographic/bathymetric data from the adjacent to the examined shoreline catchment will be retrieved from the Advanced Land Observation Satellite (ALOS) Global Digital Surface Model. This dataset is a global digital surface model (DSM), with horizontal resolution 30 m, produced by the Panchromatic Remote-sensing Instrument for Stereo Mapping (PRISM), which is an optical sensor on board the "ALOS" platform (Takaku et al., 2014).

Bottom slopes in the North-Western part of the Black Sea were calculated in ONU on the EMODnet digital terrain model (DTM) retrieved from the portal http://www.emodnet-bathymetry.eu. DTM is a quantitative model of a topographic surface in digital form. And slope is one of the characteristic' of this surface. In this study there are used the slope calculation algorithms available in GIS. Slope, or other terrain variable value, is calculated for each raster pixel in turn using a ARCGIS computation algorithm. The Slope tool in ARCGIS calculates the maximum rate of change between each cell and its neighbors. The output slope raster calculated as degree of slope (Dolan, 2012).

3.2.2. Seabed substrates data

EMODnet Seabed substrate data (Table 3.1 in part 3.2.7) comprise of multiple datasets at different scales, compiled in EMODnet Geology projects running since 2009. The national datasets are harmonised into a shared schema. The maps illustrate seabed properties at different scales covering all European maritime areas. Seabed substrate data products are in scales: 1:1500 – 1:70 000); 1:100 000; 1:250 000; 1:1 000 000.

Bottom slopes in the North-Western part of the Black Sea were calculated in ONU on the EMODnet digital terrain model (DTM) retrieved from the portal http://www.emodnet-bathymetry.eu (Table 3.1.). DTM is a quantitative model of a topographic surface in digital form. And slope is one of the characteristic' of this surface. In this study there are used the slope calculation algorithms available in GIS. Slope, or other terrain variable value, is calculated for each raster pixel in turn using a ARCGIS computation algorithm. The Slope tool in ARCGIS calculates the maximum rate of change between each cell and its neighbors. The output slope raster calculated as degree of slope (Dolan, 2012).

3.2.3. Land cover data

The 300 m Climate Change Initiative Land Cover (CCI-LC) Maps (22 LCCS classes) were obtained from the processing of the full archives of 300 m MERIS, 1 km SPOT-VEGETATION, 1 km PROBA-V and 1 km AVHRR (Table 1.). 28 yearly classifications from 1992 to 2019 are provided. The typology was defined using the Land Cover Classification System (LCCS) developed by the United Nations Food and Agriculture Organization (Gregorio & Jansen, 2000). The Coordinate Reference System used for the global LC products is a geographic coordinate system based on the World Geodetic System 84 (WGS84) reference ellipsoid and using a Plate Carrée projection. The LC maps are delivered in NetCDF-4 format.

3.2.4 Hydrological data

Historical hydrological data will be retrieved from the Swedish Hydrometeorological Institute (SMHI), and more specifically from the database developed entitled "Hydrological Predictions for the Environment" (HYPE). HYPE model is a dynamic, semi-distributed, and process-based hydrological and nutrient transport model (Lindström et al., 2010) that can be used to assess water quantity and quality on a small and large scale. The HYPEweb, created by regulating HYPE model for pan-European basins, calculates water balance, hydrological processes (snow, glaciers, soil moisture, flow path, the contribution of groundwater and lakes) and sea discharges for the area from the British Isles to the Ural Mountains, Norway to the Mediterranean (9.6 million km^2). The e-HYPE is an operational high-resolution model that generates data with a daily time step. The internal model components are checked and calibrated with observational data in different areas. The e-HYPE system models the flow and provides topographical, precipitation, temperature, evapotranspiration, land cover, soil type, lake, river network-basins and flow data used in modeling from global/continental databases and satellite products. The HYPEweb is an open-access web service, allowing any user to download daily flow rates (m^3/s) for any sub-basin across Europe. The model which is being used to study the effects of climate and land-use change on water resources can also be considered in operational runoff forecasting studies for the early warning service and the hydropower sector. Using reliable quality input data, the model undergoes calibration and verification processes according to sound scientific principles (Arheimer et al., 2011).

3.2.5 Oceanographic Data

Sea level rise is a key indicator of climate change and helps to assess coastal erosion. Currents and waves play a crucial role in the determination of the impact of water circulation in coastal erosion. Therefore, the retrieval of these datasets appears to be necessary to understand the underlying processes in a cost-effective manner. The retrieval of most of these datasets will be carried out through the Copernicus Marine Environment Monitoring Service (CMEMS). The program aimed at developing a set of European information services based on satellite Earth Observation and in-situ (non-space) data.

The Copernicus Marine Environment Monitoring Service provides regular and systematic information about the physical state and dynamics of the ocean and marine ecosystems for the global ocean and the European regional seas. This data covers the analysis of the current condition, short-term forecasts of the conditions a few days in advance, and the provision of retrospective data records (re-analysis datasets).

The CMEMS **Significant Wave Height** extreme variability indicator is aimed at monitoring the extremes of annual significant wave height and evaluate the spatio-temporal variability. The use of percentiles instead of annual maxima, makes these extremes study less affected by individual data. The sea state and its related spatio-temporal variability affect dramatically maritime activities and the physical connectivity between offshore waters and coastal ecosystems, impacting therefore on the biodiversity of marine protected areas. Over the last decades, significant attention has been devoted to extreme wave height events since their destructive effects in both the shoreline environment and human infrastructures have prompted a wide range of adaptation strategies to deal with natural hazards in coastal areas (Hansom et al., 2015). Significant Wave Height mean 99th percentile in the Black Sea region shows an east / west dependence, i.e. highest values of the average of annual 99th percentiles prevail in those areas where high winds and long fetch are simultaneously present. The largest values of the mean 99th percentile in the southwestern Black Sea are around 3.5 m, while in the eastern part of the basin they can amount to around 2.5 m (Staneva et al., 2019a and 2019b). Significant Wave Height mean 99th percentile in the Black Sea region shows the typical east / west dependence with largest values in the southwestern Black Sea ranging up to 3.5 m, while the 99th percentile values in the eastern part of the basin are around 2.5 m. The 99th mean percentile for 2002-2017 shows a similar pattern demonstrating that the highest values of the mean annual 99th percentile are in the western part of the basin (Akpınar et al., 2016 and Akpinar and Van Vledder, 2016). The anomaly of the 99th percentile in 2018 is mostly negative with values down to ~-45 cm.

Seasonal, interannual, and mesoscale variability of the Black Sea **upper layer circulation** derived from altimeter data (Korotaev et al., 2003) comprising the period from May 1992 to May 1999 were assimilated into a shallow water model for providing a dynamically consistent interpretation of the sea surface height variations and estimation of the temporal and spatial characteristics of the upper layer circulation in the Black Sea. The circulation possesses a distinct seasonal cycle whose major characteristic features repeat every year with some year-to-year variability.

Understanding of the Black Sea circulation has significantly increased during the last decade through realization of several international programs. Analyzing all the available data, Oguz et al. [1993] specified the building blocks of the upper layer circulation as the Rim Current system around the periphery, an interior cell composed by two or more cyclonic gyres, and a series of quasi-stable/recurrent anticyclonic eddies on the coastal side of the Rim Current. Construction of optimally interpolated and gridded (in both space and time) dynamical sea level data from altimetry (Korotaev et al., 2001) recently provided a new resource for increasing our present level of knowledge on variability of the Black Sea circulation. They described the methodology for reconstruction of the dynamical sea level data base for the period from May 1992 to November 1996, its validation by the available hydrographic survey data, and interpretation of the results by means of a simple two-layer analytical model of the wind-driven circulation in a rectangular basin. The flow system within the northwestern shelf (NWS) is governed by both intrusions of the Rim Current and discharges from the Danube, Dnieper and Dniester Rivers; the discharge from the former is almost four times stronger than the sum of other two. The typical regional flow regime within the inner shelf is a southward coastal current system. The outer shelf, on the other hand, is characterized by highly dynamic and complicated interactions between the inner shelf and the Rim Current flow systems. The coastal fresh water-induced flow system includes some mesoscale anticyclonic eddies, one of which is located just outside the discharge zone of the Danube. We refer to this feature as the Danube anticyclonic eddy. The other eddy is located slightly south near Cape Kaliakra, in the narrowest part of the northwestern shelf. The Kaliakra anticyclonic eddy also emerges during the late summer and autumn months, whereas it is embedded within the coastal current system during high-discharge periods. Another small anticyclonic eddy (the Constantsa eddy) is often present between the Danube and Kaliakra anticyclones. **Time series of mean sea level trends** over Black sea are derived from the DUACS delayed-time altimeter gridded maps of sea level anomalies based on a stable number of altimeters (two) in the satellite constellation. These products are distributed by the Copernicus Climate Change Service. The mean sea level evolution estimated in the Black Sea is derived from the average of the gridded sea level maps weighted by the cosine of the latitude. The annual and semi-annual periodic signals are adjusted and the time series is low-pass filtered. Mean sea level evolution has a direct impact on coastal areas and is a crucial index of climate change since it reflects both the amount of heat added in the ocean and the mass loss due to land ice melt (Dieng et al., 2017). Long-term and inter-annual variations of the sea level are observed at global and regional scales. They are strongly related to the internal variability observed at basin scale and these variations can strongly affect population living in coastal areas. Using the latest reprocessed altimeter sea level products, it is possible to estimate the sea level rise in the Black Sea since 01/1993. The Black Sea is a relatively small semi-enclosed basin with shallow bathymetry, which explains the high level of inter annual variability observed in the sea level record compared to large, deeper and open ocean areas.

3.2.6 Geological and coastline data

The geological map of the North-Western part of the Black Sea was prepared on the base of the 1:5 M International Geological Map of Europe and Adjacent Areas (IGME 5000) on the pre-Quaternary geology of Europe (Table 3.1.). This map was managed and implemented by the Federal Institute for Geosciences and Natural Resources (BGR) under the aegis of the CGMW (Commission of the Geological Map of the World). In preparation of the map were involved over 48 European and adjacent countries, more than 20 scientific institutes and the area covered reaches from the Caspian Sea in the east, to the Mid-Ocean Ridge in the west, and from Svalbard to the southern shore of the Mediterranean Sea (Asch, 2003).

Additionally we used the EMODNET resources included data for Seabed Substrate, Sea-floor Geology, Coastal Behavior, Submerged Landscapes etc [https://www.emodnet-geology.eu/ https://data.geus.dk/egdi/?mapname=egdi_emodnet_geology&showCustomLayers=true#baslay=null&extent=5224820,2200070,5976780,2550610&layers=emodnet_coastal_migration_satellite and https://www.emodnet-geology.eu/map-viewer/?p=coastal_behavior].

3.2.7 Data collection lists appropriate for the Ukrainian UA1 pilot site

A list of the data products their characteristics and their source, used for the coastal erosion assessment, was created (Table 3.1).

Table 3.1. List of the data products their characteristics used for the coastal erosion assessment in the Ukrainian Black Sea coast UA1 pilot site.

No	Data Products	Description	Number of items	Resolution	Period cover	Type of file / Format	Source	link
1	Landsat 3-4 TM	Historical Satellite images	2	30,5 m	1980 to 2015	Raster	Earth Explorer	https://earthexplorer.usgs.gov/
2	Landsat 5	Historical Satellite image	12	30,5 m	2015-2020	Raster	Earth Explorer	https://earthexplorer.usgs.gov/
3	Landsat 7	Historical Satellite image	2	30 m	2000	Raster	Earth Explorer	https://earthexplorer.usgs.gov/
4	Sentinel 2	Historical Satellite images	4	10 m	2015 to 2020	Raster	Copernicus Open Access hub	https://scihub.copernicus.eu/
5	Geology	The 1:5 M International Geological Map of Europe and Adjacent Areas	1	1:5 M	2005	Vector (.shp)	Bundesanstalt für Geowissenschaften und Rohstoffe	https://www.bgr.bund.de
6	Topography/Bathimetry	ALOS Global Digital Surface Model "ALOS World 3D - 30m", version of 2021,	1	1/16 minutes	2020	Raster (geotiff)		https://www.eorc.jaxa.jp/ALOS/en/aw3d30/data/index.htm and
7	Bathymetry	EMODnet Digital Terrain Model (DTM)	1	1/16 minutes	2020	Raster (geotiff)	EMODnet+GEBCO	https://portal.emodnet-bathymetry.eu/#
8	Seabed Slope	EMODnet Digital Terrain Model (DTM)	1	1/16 minutes	2020	Raster (geotiff)	EMODnet+GEBCO	https://portal.emodnet-bathymetry.eu/#
9	Land cover	Land Cover CCI Climate Research Data Package	1	300	1992 to 2019	netCDF	Copernicus Climate Change Service	http://maps.elie.ucl.ac.be/CCI/viewer/index.php
10	Seabed Substrates	Seabed Substrates Multiscale Data Products	1	1:1 M; 1:250 k; 1:100 k	2009 to 2019	Vector (.shp)	The EMODnet Geology Portal	https://www.emodnet-geology.eu
11	River Discharges	River Discharge data	4	Daily step time series (simulated	1981 to 2010	Excel (.xls)	SMHI HYPEWeb	https://hypeweb.smhi.se
12	Significant Wave Height extreme variability	Significant Wave Height extreme variability	1	undefined (the computation)	2002-2017	*.png	Copernicus Climate Change Service (BLKSEA_OMI_SEASTATE_extreme_var_swh_mean_and_anomaly)	https://resources.marine.copernicus.eu/product-detail/BLKSEA_OMI_SEASTATE_extreme_var_swh_mean_and_anomaly
13	The mean sea level trends over the Black sea	Mean sea level daily evolution since January 1993 from the satellite altimeter observations estimated in the Black Sea	1	undefined (satellite-observation)	From 1993-01-01 to 2020-06-03	*.png	Copernicus Climate Change Service (BLKSEA_OMI_SL_area_averaged_anomalies)	https://marine.copernicus.eu/access-data/ocean-monitoring-indicators/time-series-mean-sea-level-trends-over-blacksea

14	Geological data	Seabed Substrate Sea-floor Geology Coastal Behavior Events & Probabilities Marine Minerals Submerged Landscapes Entity indexes	5		2019	*.wmf	EMODNET Geology discover Europeas seabed geology	https://www.emodnet-geology.eu/ ; https://data.geus.dk/egdi/?mapname=egdi_emodnet_geology&showCustomLayers=true#baslay=null&extent=5224820,2200070,5976780,2550610&layers=emodnet_coastal_migration_satellite; https://www.emodnet-geology.eu/map-viewer/?p=coastal_behavior

3.2.8 Satellite images retrieved for the Ukrainian UA1 pilot site

3.2.8.1 Earth Explorer (Landsat 3 MSS, Landsat 5 TM and Landsat 7 ETM+)

Landsat 3 was launched into space onboard on March 5, 1978. The satellite was placed in standby mode on March 31, 1983 and decommissioned on September 7, 1983. Landsat 3 orbited the Earth in a sun-synchronous, near-polar orbit (99.2 degrees inclination) at a nominal altitude of 917 km (570 miles), circling the Earth every 103.34 minutes, completing 14 orbits per day. The satellite had a repeat cycle of 18 days and had an equatorial crossing time of 9:30 a.m. mean local time (+/-15 minutes). Landsat 3 MSS sensor was a line-scanning device observing the Earth perpendicular to the orbital track. The cross-track scanning was accomplished by an oscillating mirror; six lines were scanned simultaneously in each of the four spectral bands for each mirror sweep. The MSS sensor on Landsat 3 originally had five spectral bands, but one failed shortly after launch. Landsat 3 MSS image data files consist of four spectral bands. The resolution is 80 meters for bands 4 to 7. The approximate scene size is 170 km north-south by 185 km east-west (106 mi by 115 mi). Ground Sampling Interval is 57 x 79 m (Table 3.2) [USGS 1, 2021].

Table 3.2. Landsat 3 Multispectral Scanner (MSS) band list [USGS 1, 2021].

Landsat 3	Wavelength (micrometres)	Resolution (meters)
Band 4	0.5-0.6	60
Band 5	0.6 -0.7	60
Band 6	0.7-0.8	60
Band 7	0.8-1.1	60

The Landsat Thematic Mapper (TM) sensor was carried onboard Landsat 4 and 5 from July 1982 to May 2012 with a 16-day repeat cycle, referenced to the Worldwide Reference System-2. Very few images were acquired from November 2011 to May 2012. The satellite began decommissioning activities in January 2013. Landsat 4-5 TM image data files consist of seven spectral bands. The resolution is 30 meters for bands 1 to 7. The Thermal infrared band 6 was collected at 120 meters but was resampled to 30 meters. The approximate scene size is 170 km north-south by 183 km east-west (106 mi by 114 mi) (Table 3.3. [USGS 2, 2021].

Table 2. Landsat 4- 5 Thematic Mapper (TM) band list [USGS 3, USGS-4, 2021.].

Landsat 4-5	Wavelength (micrometres)	Resolution (meters)
Band 1	0.45-0.52	30
Band 2	0.52-0.60	30
Band 3	0.63-0.69	30
Band 4	0.76-0.90	30
Band 5	1.55-1.75	30
Band 6	10.40-12.50	120 (30)
Band 7	2.08-2.35	30

Landsat 7 was launched on April 15, 1999 and carries the Enhanced Thematic Mapper (ETM+) sensor. Since June 2003, has acquired and delivered data with data gaps caused by the Scan Line Corrector (SLC) failure. The Landsat 7 satellite orbits the the Earth in a sun-synchronous, near-polar orbit, at an altitude of 705 km (438 mi), inclined at 98.2 degrees, and circles the Earth every 99 minutes. The satellite has a 16-day repeat cycle with an equatorial crossing time: 10:00 a.m. +/- 15 minutes. Landsat 7 data are acquired on the Worldwide Reference System-2 (WRS-2) path/row system, with swath overlap (or sidelap) varying from 7 percent at the Equator to a maximum of approximately 85 percent at extreme latitudes. Landsat 7 products are delivered as 8-bit images with 256 grey levels. Landsat 7 ETM+ image data files consist of eight spectral bands. Ground Sampling Interval is 30 m reflective, 60 m thermal (Table 3.4) [USGS-5 2021].

Table 3.4. Landsat 7 Enhanced Thematic Mapper (ETM+) band list [USGS, 2021].

Landsat 7	Wavelength (micrometres)	Resolution (meters)
Band 1	0.45 - 0.52	30
Band 2	0.52 - 0.60	30
Band 3	0.63 - 0.69	30
Band 4	0.77 - 0.90	30
Band 5	1.55 - 1.75	30
Band 6	10.40 - 12.50	60
Band 7	2.08 - 2.35	30
Band 8	0.52 - 0.90	15

3.2.8.2. Copernicus Open Access Hub (Sentinel 2)

The Copernicus Sentinel-2 mission comprises a constellation of two polar-orbiting satellites placed in the same sun-synchronous orbit, phased at 180° to each other. It aims at monitoring variability in land surface conditions, and its wide swath width (290 km) and high revisit time (10 days at the equator with one satellite, and 5 days with 2 satellites under cloud-free conditions, which results in 2-3 days at mid-latitudes) will support monitoring of Earth's surface changes. Sentinel-2 satellites are on track from 2016 to today and image data files consist of twelve spectral bands with maximum resolution of 10 m (Table 3.5).

Table 3.5. Sentinel 2 band list [**Earth observing system, 2021**].

Sentinel 2	Central wavelength (micrometres)	Resolution (meters)
Band 1 (coastal aerosol)	0.44	60
Band 2 (Blue)	0.49	10
Band 3 (Green)	0.56	10
Band 4 (Red)	0.66	10
Band 5 (Red Edge 1)	0.70	20
Band 6 (Red Edge 2)	0.74	20
Band 7 (Red Edge 3)	0.78	20
Band 8 (NIR)	0.83	10
Band 8A (NIR Vapor)	0.86	20
Band 9 (Water Vapor)	0.94	60
Band 10 (SWIR-Cirrus)	1.37	60
Band 11 (SWIR-1)	1.61	20
Band 12 (SWIR-2)	2.20	20

3.3 Description of coastal erosion analysis methodology using of historical satellite images

3.3.1. Satellite image selection

Historical satellite images were retrieved to cover the period from the early 1980s to 2020 (Table 3.6). The historical satellite images selection was mainly based on correct geo-reference of each image, clarity from cloud cover and seasonality. All images were retrieved during summer months (May to September). Table 6 shows the satellite images selected for coastal erosion assessment. All the images selected were for the summer months. Moreover, the images were chosen according to their clarity from the cloud cover, correct georeference, and orthorectification.

The shoreline movement analysis was carried out for the period from 1980 to 2020 and the following images were used:

a) One satellite image from Landsat 3 MSS of 1980 retrieved from the Earth Explorer database provided by the United States Geological Survey Global Visualizer (USGS - https://earthexplorer.usgs.gov/) [USGS, 2021].

b) One satellite image from Landsat 4 TM of 1983 retrieved from the Earth Explorer database provided by the United States Geological Survey Global Visualizer (USGS - https://earthexplorer.usgs.gov/) [USGS Earth Explorer, 2021].

c) Twelve satellite images from Landsat 5 TM covering almost 25 years' time period (from 1985 to 2010) retrieved from the Earth Explorer database provided by the United States Geological Survey Global Visualizer (USGS - https://earthexplorer.usgs.gov/) [USGS Earth Explorer, 2021].

d) Two satellite images from Landsat 7 ETM+ collection covering the area of interest for 2000. The image was retrieved from the Earth Explorer database provided by the USGS) [USGS Earth Explorer, 2021].

e) Four satellite images from Sentinel 2 sensor covering 5 years period (from 2015 to 2020) retrieved from the Copernicus Open Access Hub provided by the Copernicus and European Space Agency (https://scihub.copernicus.eu/) [Planet Explorer, 2021].

Table 3.6. Data product specifications used for Ukrainian pilot areas assessment [USGS Earth Explorer, 2021; Planet Explorer, 2021].

Data Products	Number of images retrieved	Resolution*	Year of Image Acquisition	Source
Landsat 3 MSS	1	60 m	1980	Earth Explorer, USGS
Landsat 4 TM	1	30 m	1983	
Landsat 5 TM	12	30 m	1985-2010	
Landsat 7	2	30 m	2000	
Sentinel 2	4	10 m	2015 to 2020	Copernicus Hub
GeoEye-1	3	1.64 m (0.41 m)	2019-2020	MAXAR
QuickBird-2	3	2.44 m (0.61 m)	2005, 2007, 2009	
WorldView-2	9	1.84 m (0.46 m)	2013, 2015-2017, 2019, 2021	
WorldView-3	4	1.24 m (0.31 m)	2019-2021	

Note: *Resolution - multyspectral bands (panchromatic band)

Table 3.7 . List of the selected Satellite images processed for the Ukrainian pilot assessment.

No	Date	Data Products	Resolution	Dataset	Format	Index
1	30/08/1980	Landsat 3 MSS	60 m	Landsat Collection 2 Level- 1	.TIF	NDWI
2	20/07/1983	Landsat 4 TM	30 m	Landsat Collection 2 Level- 1	.TIF	NDWI
3	02/08/1985	Landsat 5 TM	30 m	Landsat Collection 2 Level- 1	.TIF	NDWI
4	02/08/1985	Landsat 5 TM	30 m	Landsat Collection 2 Level- 1	.TIF	NDWI
5	16/18/1990	Landsat 5 TM	30 m	Landsat Collection 2 Level- 1	.TIF	NDWI
6	16/18/1990	Landsat 5 TM	30 m	Landsat Collection 2 Level- 1	.TIF	NDWI
7	14/08/1995	Landsat 5 TM	30 m	Landsat Collection 2 Level- 1	.TIF	NDWI
8	14/08/1995	Landsat 5 TM	30 m	Landsat Collection 2 Level- 1	.TIF	NDWI
9	19/08/2000	Landsat 7 ETM+	30 m	Landsat Collection 2 Level- 1	.TIF	NDWI
10	19/08/2000	Landsat 7 ETM+	30 m	Landsat Collection 2 Level- 1	.TIF	NDWI
11	08/07/2005	Landsat 5 TM	30 m	Landsat Collection 2 Level- 1	.TIF	NDWI
12	31/07/2005	Landsat 5 TM	30 m	Landsat Collection 2 Level- 1	.TIF	NDWI
13	25/08/2005	Landsat 5 TM	30 m	Landsat Collection 2 Level- 1	.TIF	NDWI
14	06/06/2005	Landsat 5 TM	30 m	Landsat Collection 2 Level- 1	.TIF	NDWI
15	23/08/2010	Landsat 5 TM	30 m	Landsat Collection 2 Level- 1	.TIF	NDWI
16	14/08/2010	Landsat 5 TM	30 m	Landsat Collection 2 Level- 1	.TIF	NDWI
17	02/08/2015	Sentinel 2	10 m	Sentinel-2 mission	.TIF	NDWI
18	02/08/2015	Sentinel 2	10 m	Sentinel-2 mission	.TIF	NDWI
19	05/08/2020	Sentinel 2	10 m	Sentinel-2 mission	.TIF	NDWI
20	05/08/2020	Sentinel 2	10 m	Sentinel-2 mission	.TIF	NDWI
21	09/01/2019	GeoEye-1	1.64 m (0.41 m)	GeoEye-1, Image ID: 1050010013D61C00	.kml	NDWI

No	Date	Data Products	Resolution	Dataset	Format	Index
22	11/08/2019	GeoEye-1	1.64 m (0.41 m)	GeoEye-1, Image ID: 105005006DDD6F00	.kml	NDWI
23	27/09/2020	GeoEye-1	1.64 m (0.41 m)	GeoEye-1, Image ID: 10500500B6DD8100	.kml	NDWI
24	27/11/2005	QuickBird-2	2.44 m (0.61 m)	QuickBird-2, Image ID: 1010010004AC2800	.kmz	NDWI
25	28/03/2007	QuickBird-2	2.44 m (0.61 m)	QuickBird-2, Image ID: 10100100058C1800	.kmz	NDWI
26	07/10/2009	QuickBird-2	2.44 m (0.61 m)	QuickBird-2, Image ID: 101001000A65ED00	.kmz	NDWI
27	04/05/2013	WorldView-2	1.84 m (0.46 m)	WorldView-2, Image ID: 10300100229E2300	.kml	NDWI
28	03/09/2015	WorldView-2	1.84 m (0.46 m)	WorldView-2, Image ID: 1030010048153900	.kml	NDWI
29	23/08/2016	WorldView-2	1.84 m (0.46 m)	WorldView-2, Image ID: 103001005CA18700	.kml	NDWI
30	02/12/2017	WorldView-2	1.84 m (0.46 m)	WorldView-2, Image ID: 1030010075CD2B00	.kml	NDWI
31	21/06/2019	WorldView-2	1.84 m (0.46 m)	WorldView-2, Image ID: 1030010093982300	.kml	NDWI
32	13/07/2019	WorldView-2	1.84 m (0.46 m)	WorldView-2, Image ID: 1030010096942400	.kml	NDWI
33	23/03/2021	WorldView-2	1.84 m (0.46 m)	WorldView-2, Image ID: 10300100BB4F8000	.kml	NDWI
34	18/06/2021	WorldView-2	1.84 m (0.46 m)	WorldView-2, Image ID: 10300100C02BD300	.kml	NDWI
35	20/07/2021	WorldView-2	1.84 m (0.46 m)	WorldView-2, Image ID: 10300100C23A7300	.kml	NDWI
36	30/06/2019	WorldView-3	1.24 m (0.31 m)	WorldView-3, Image ID: 1040050016DBF300	.kml	NDWI
37	08/03/2020	WorldView-3	1.24 m (0.31 m)	WorldView-3, Image ID: 104005001FDCC300	.kml	NDWI
38	20/04/2020	WorldView-3	1.24 m (0.31 m)	WorldView-3, Image ID: 1040050022DBF500	.kml	NDWI
39	15/08/2021	WorldView-3	1.24 m (0.31 m)	WorldView-3, Image ID: 104001006D0E9700	.kml	NDWI

3.3.2 Coastline extraction from satellite images

The methodology applied in all PONTOS study areas entails the semi-automatic shoreline delineation procedure [Zachopoulos K., 2020]. Historic satellite images processed and their historical shorelines were extracted by applying the semi-automatic classification process allowing identification of land and sea in an image according to their spectral signature.

1. For the classification process, the Normalized Difference Water Index (NDWI) by McFeeters (1996) was estimated [McFeeters, S. K., 1996]. The NDWI value is used to produce a binary classification of water vs. non-water areas. As water bodies strongly absorb light in the visible to the infrared electromagnetic spectrum, the NDWI uses green and near-infrared bands to highlight water bodies. NDWI was calculated according to [McFeeters, S. K., 1996] formula:

$$NDWI = \frac{(\text{Band Green} - \text{Band NIR})}{(\text{Band Green} + \text{Band NIR})}$$

2. The produced NDWI image was imported to the Semi-Automatic Classification Plugin (SCP) for QGIS [Condego L., 2018] and around 30 Regions of Interest (ROI's) were manually identified on each historical image by training the algorithm in two main macro-classes: *Land* and *Water*. The new raster file was further classified into two bands (*Land* and *Water*) by applying the minimum distance classification algorithm.

3. The shoreline was extracted by vectorizing the classified raster image and applying a Gaussian filtering algorithm to smooth the produced polyline and receive a better fit to the coast [Zachopoulos K., 2020].

4. The same process was applied for every historical satellite image and historical shorelines were extracted.

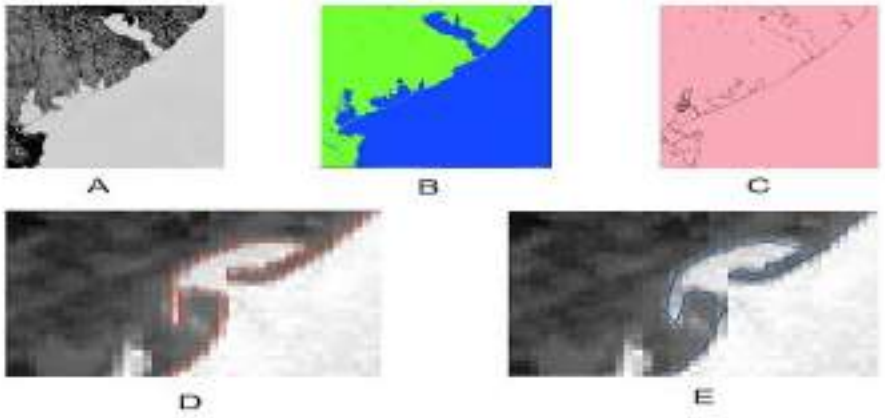

Figure 3.2. Coastline extraction methodology in steps. A - Satellite image – NDWI, B - Classified image (Land-Sea), C- Raster to Vector, D- Shoreline Extraction, E - Smoothed Shoreline.

Validation of the semi-automatic classification method and error assessment were performed comparing the shoreline polyline extracted by the semi-automatic technique with polyline obtained by the Odesa National University using manual GIS method.

Landsat space images retrieved from the site https://earthexplorer.usgs.gov/ [USGS Earth Explorer, 2021] were also used to define the coastline position according to the ONU methodology [Cherkez et al., 2013; Cherkez et al., 2014, Cherkez et al., 2020].

Vextractor 4.91 [11] and ArcMap 9.2 [12] software was used to process the satellite images.

The raster picture was produces from the space images downloaded using the ArcMap package. It was further processed with Vextractor 4.91 [Vextractor. Raster to vector conversion tool, 2021] and converted into a vector file. The results of processing were stored in shape format [Cherkez et al., 2013]. The file received was further processed with ArcMap package, where final correction was done using editing toolbar. As the result, we received the file with shoreline smoothened with the Smooth function. This final polygonal shape-file with the shoreline fixed using Trace instrument (from editing toolbar) and the shoreline dynamics polygons created was used for quantitative assessment of land area increase/decrease for the studied period. For those calculation we used the function from Analysis Tools – Erase package. Using this function, 2 shape-files were received: one containing polygons with land area increase, the other – with information on decrease (shrinking) of land (increase of water area). In each file we calculate the area of the polygons received using the Calculate Geometry instrument.

To effectively compare the results of calculation of differences in the position of coastline received using two methods, we made polygonal shape-files of the polylines built using the DUTH method for each selected area and calculated the respective changes in land and water areas.

The results are set out in the papers [Cherkez et al., 2013; Cherkez et al., 2014, Cherkez et al., 2020], where the shoreline changes in 1983-2013 were analysed for the following areas:

1. the Danube Delta, from 29°45′42″ E 45°10′38″N to 29°37′33″ E 45°30′20″N;
2. the Sasyk Estuary, from 29°37′33″ E 45°30′20″N to 29°42′20″ E 45°34′27″N;

2A. the Sasyk Estuary, from 29°42′20″ E 45°34′27″N to 29°43′47″ E 45°35′19″N;

3. from the Sasyk Estuary to Budakskyi Estuary, from 29°43′47″ E 45°35′19″N to 30°16′36″ E 45°54′43″N;

3A. the Budakskyi Estuary, from 30°16′36″ E 45°54′43″N to 30°25′30″ E 46°2′30″N;

4. the Dniester Estuary, from 30°25′30″ E 46°2′30″N to 30°36′24″ E 46°13′19″N;

4A. from the Dniester Estuary to the Sukhyi Estuary, from 30°36′24″ E 46°13′19″N to 30°38′34″ E 46°16′6″N;

5. city Odesa (from the Sukhyi Estuary to the Great Adzhalyk estuary), from 30°38′34″ E 46°16′6″N to 30°54′35″ E 46°34′24″N;

6. from the Great Adzhalyk estuary to the Berezanskyi Estuary, from 30°54′35″ E 46°34′24″N to 31°30′19″ E 46°37′21″N;

7. Dniprovskyi Estuary, from 31°30′19″ E 46°37′21″N to 31°30′19″ E 46°34′40″N.

To compare the two method we used only part of our previous studies, the area of which we divided into 8 sub-areas (Fig. 3.3.); the comparison was done for the sub-areas 1 to 5. Fig. 3.4 show the shoreline schematic maps for 1983-2013, calculated using the DUTH methodology [Democritus University of Thrace. 2021] and the ONU methodology [Cherkez et al., 2013; Cherkez et al., 2014, Cherkez et al., 2020].

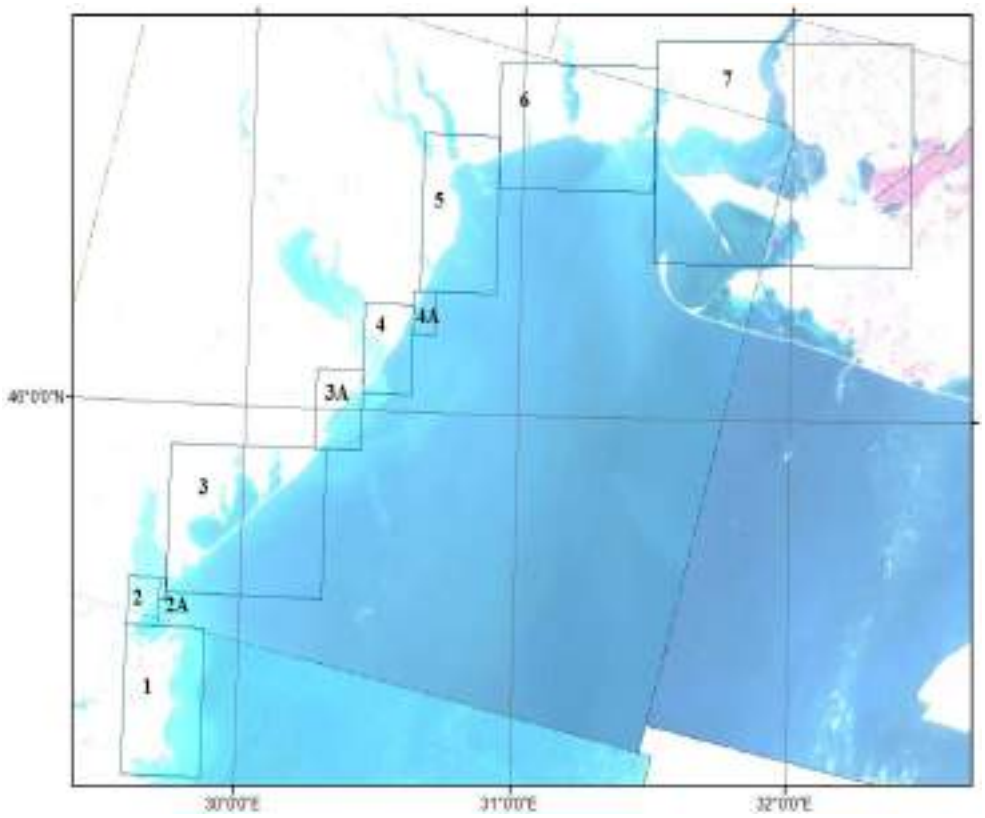

Fig. 3.3. Schematic map of the NWBS sub-areas

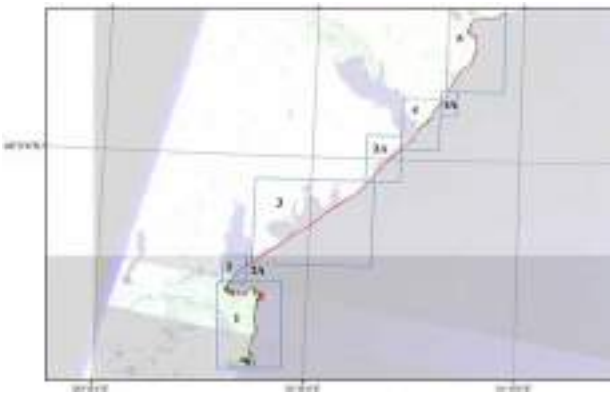

Fig. 3.4. General schematic map of shoreline changes for 1983-2013 calculated using the DUTH methodology [Democritus University of Thrace, 2021]

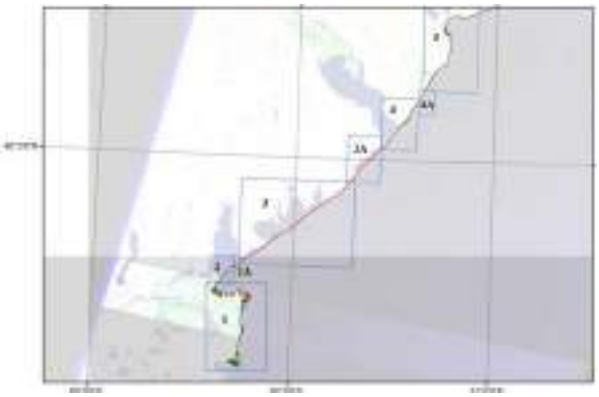

Fig. 3.5. General schematic map of shoreline changes for 1983-2013 calculated using the ONU methodology [Cherkez et al., 2013; Cherkez et al., 2014, Cherkez et al., 2020].

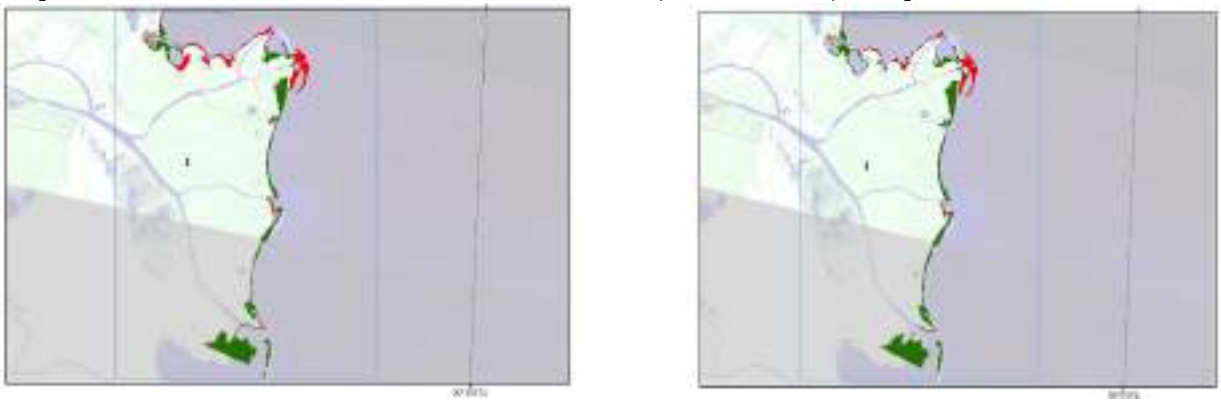

A **B**

Fig. 3.6. Schematic map of shoreline changes for 1983-2013 calculated using the DUTH methodology (A) and the ONU methodology (B) for the Danube Delta (sub-area 1)

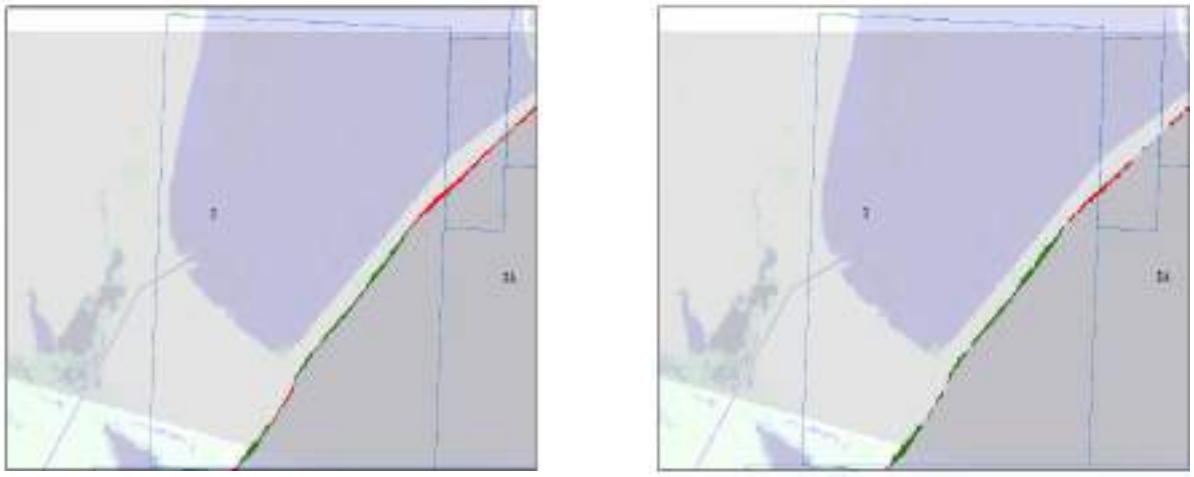

A B

Fig. 3.7. Schematic map of shoreline changes for 1983-2013 calculated using the DUTH methodology (A) and the ONU methodology (B) for the Sasyk Estuary area (sub-areas 2, 2A)

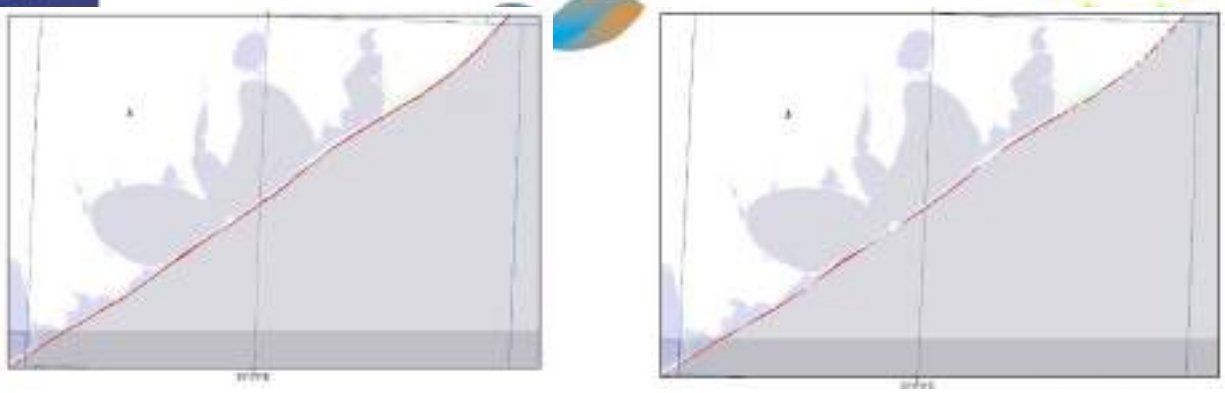

A **B**

Fig. 3.8. Schematic map of shoreline changes for 1983-2013 calculated using the DUTH methodology (A) and the ONU methodology (B) for the area from the Sasyk Estuary to Budakskyi Estuary (sub-area 3)

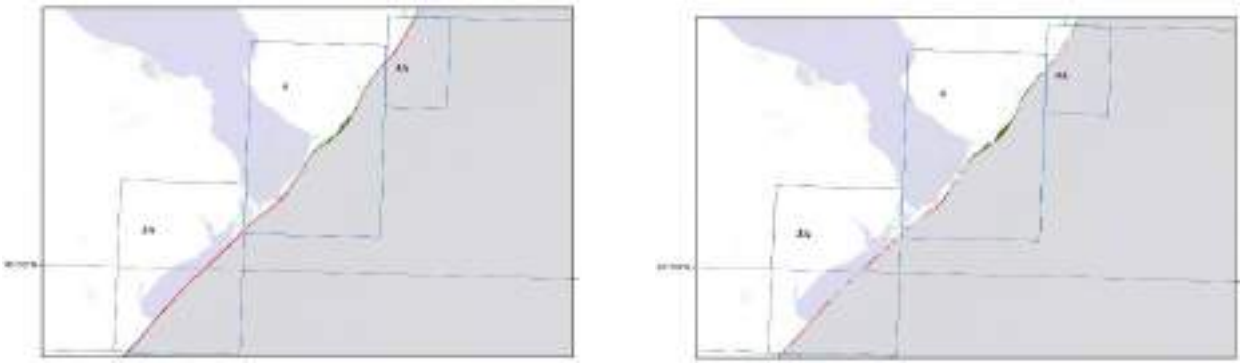

A **B**

Fig. 3.9. Schematic map of shoreline changes for 1983-2013 calculated using the DUTH methodology (A) and the ONU methodology (B) from the Dniester Estuary to the Sukhyi Estuary (sub-areas 3A, 4, 4A)

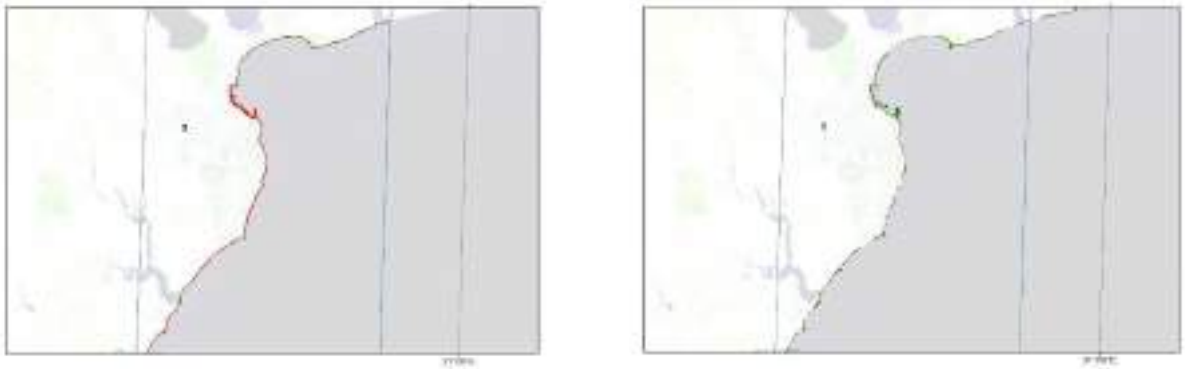

A **B**

Fig. 3.10. Schematic map of shoreline changes for 1983-2013 calculated using the DUTH methodology (A) and the ONU methodology (B) in Odesa area (from the Sukhyi Estuary to the Great Adzhalyk estuary) (sub-area 5)

The results of comparison of shoreline area changes received by the DUTH method and the ONU method are presented in Table 3.8.

Table 3.8. Changes in shoreline area in 1983-2013 by sub-areas (DUTH method and ONU method)

Sub-area No.	Calculated using DUTH method, km^2	Calculated using ONU method, km^2[Cherkez et al., 2020]	Difference between the methods, km^2
1	+10.968	+14.617	-3.649
2	+0.164	+0.455	-0.291
2a	-0.08	-0.105	+0.025
3	-3.27	-1.634	-1.636
3a	-1.053	-0.413	-0.64
4	+0.491	+1.053	-0.562
4a	-0.225	-0.008	-0.217
5	-1.339	+1.698	-3.037
Total	+5.656	+15.663	-10.007

The results of comparison of land and water areas changes received using two methods for the period 1983-2013 enable us to make the following conclusions:

Maximal difference between the values were found for the Danube Delta and Odesa coast. In this case. Using the DUTH method, we have to add the manual method and field measurements to receive more precise results, i. e. there are much sediments from rivers and reed-beds in the Danube deltaic area, so when calculating the NDWI index, the automatic method could result at an error distinquishing between water and land. There is a port on Odesa coast with many berths, which also requires manual processing.

If we take the image of 1983 with resolution 60 m, i.e. length of one side of pixel is 60 m and pixel area is 120 m^2 , the tolerable error in comparison of both methods makes 120 m^2 (0.00012 km^2). Using the DUTH method we receive more precise results with the NDWI index that can better distinguish between land and water due to the combination of the spectra, which can not be seen by human eye.

In the OUN method we used images in combination that is the closest to seen by human eye (red, green blue) but for deltaic areas hand corrections are obligatory.

In general, both methods show similar results in land increasing/ decreasing except for the area near Odesa (sub-area 5) from the Sukhyi Estuary to the Great Adzhalyk estuary.

Among the benefits of the new method is better precision due to use of reflection in the near IR area for the NDWI index calculation and the possibility to calculate the additional statistical characteristics of the shoreline changes.

3.3.3. Evaluation of the shoreline evolution

The shoreline analysis was performed for time periods 1980 – 2020 every 5 years. To evaluate the shoreline evolution, an analysis was carried out by the Digital Shoreline Analysis System (DSAS), provided by the USGS [Thieler et al., 2009]. The DSAS procedure used transects positioned along the shoreline at distances of 60 m. The reference baseline required by the DSAS procedure will be manually digitized and positioned onshore. A series of statistical indices will be produced, such as the Net Shoreline Movement index (NSM, meters), reporting the distance between the oldest and the latest shorelines for each transect, the End Point Rate (EPR, m/y) calculated by dividing the distance of Net Shoreline Movement by the time elapsed between the oldest and the latest shoreline, and finally, the Weighted Linear Regression (WLR, m/y), in which the weight w is a function of the variance of the measurement uncertainty (Genz et al., 2007):

$$w = 1/e^2$$

where *e* is the shoreline uncertainty value [USGS Digital Shoreline Analysis System (Dsas), 2021].

Using the data produced by the DSAS transects, a statistical analysis of the shoreline evolution along the study years will be applied and various statistical parameters will be calculated and analyzed (Table 3.9).

The shoreline change envelope (SCE) reports a distance (in meters), not a rate. The SCE value represents the greatest distance among all the shorelines that intersect a given transect. As total distance between two shorelines has no sign, the value for SCE is always positive [USGS DSAS, 2021].

Table 3.9. Table of standardized field headings provided by Digital Shoreline Analysis System (DSAS) for change calculations [USGS Digital Shoreline Analysis System (DSAS), 2021].

NSM	Net Shoreline Movement
SCE	Shoreline Change Envelope
EPR	End Point Rate
LRR	Linear Regression Rate
LSE	Standard Error of Linear Regression
LCI	Confidence Interval of Linear Regression
LR2	R-squared of Linear Regression
WLR	Weighted Linear Regression Rate
WSE	Standard Error of Weighted Linear Regression
WCI	Confidence of Weighted Linear Regression
WR2	R-squared of Linear Regression
LMS	Least Median of Squares

A linear regression rate-of-change statistic (LRR) can be determined by fitting a least-squares regression line to all shoreline points for a transect.

The regression line is placed so that the sum of the squared residuals (determined by squaring the offset distance of each data point from the regression line and adding the squared residuals together) is minimized.

The linear regression rate is the slope of the line [USGS Digital Shoreline Analysis System (DSAS), 2021].

The end point rate (EPR) includes a computation of the uncertainty associated with the calculation. The standard error, correlation coefficient, and confidence interval are computed for the two linear regression methods (LRR and WLR). These additional statistics provide information that is helpful in assessing the robustness of the computed regression rates.

LSE - The standard error of the estimate assesses the accuracy of the best-fit regression line in predicting the position of a shoreline for a given point in time [USGS Digital Shoreline Analysis System (DSAS), 2021].

The standard error of the slope with confidence interval (LCI for ordinary linear regression and WCI for weighted linear regression) describes the uncertainty of the reported rate.

The R-squared statistic (R2), or coefficient of determination, is the percentage of variance in the data that is explained [USGS Digital Shoreline Analysis System (DSAS), 2021] by a regression. It is a dimensionless index that ranges from 1.0 to 0.0 and measures how successfully the best-fit line accounts for variation in the data, where 1.0 is a perfect fit. In other words, it reflects the linear relationship between shoreline points along a given DSAS transect. For the linear regression rate (LRR) the statistic is defined as LR2, whereas for the weighted linear regression it is WR2 [USGS Digital Shoreline Analysis System (DSAS), 2021].

For 1980-2020 period we used the main statistical indicators NSM, SCE and WLR in our analysis.

Processing and analysing the data received using the DSAS we found out that there were some peculiarities in processing of images of some local areas, which were characterised by spatiotemporal irregularity and led to significant mistakes in determination of the NSM (Net Shoreline Movement - represents the distance between the oldest and the youngest shorelines for each transect), the SCE (Shoreline Change Envelope - represents the greatest distance among all the shorelines that intersect a given transect) and the WLR (Weighted Linear Regression). Getting the reliable values of the parameters calculated using the DSAS requires editing and discarding of the wrong values of coastline position which appear due to the following:

1. Relatively low resolution of the Landsat 3 MSS satellite images (60 m) for 1980.

2. Presence of deltaic lakes, river arms and big areas overgrown with reeds in the Danube Delta – those are masking the real coastline position in some years (Fig. 3.11).

3. Changes in river and sea waters' level regime, as well as floods and up and down surges (Fig. 3.12).

4. Avalanchine-landslide processes which result at coastline shifting seawards (Fig. 3.13).

5. Availability of the areas where coastal protection hydro-engineering and port's berthing facilities of complex configuration (cities Odessa and Chornomorsk) (Fig. 3*.07-3*.08); anti-landslide and coastal protection works – quay piers, spurs, breakwaters, counterdams, embankments, rubbleworks, man-made cape landforms (Fig. 3.14).

Fig. 3.11 Wrong positionы of coastlines in the UA1-1 subarea from 0.0 km to 3.18 km (left) and from 31.56 km to 31.82 km (right).

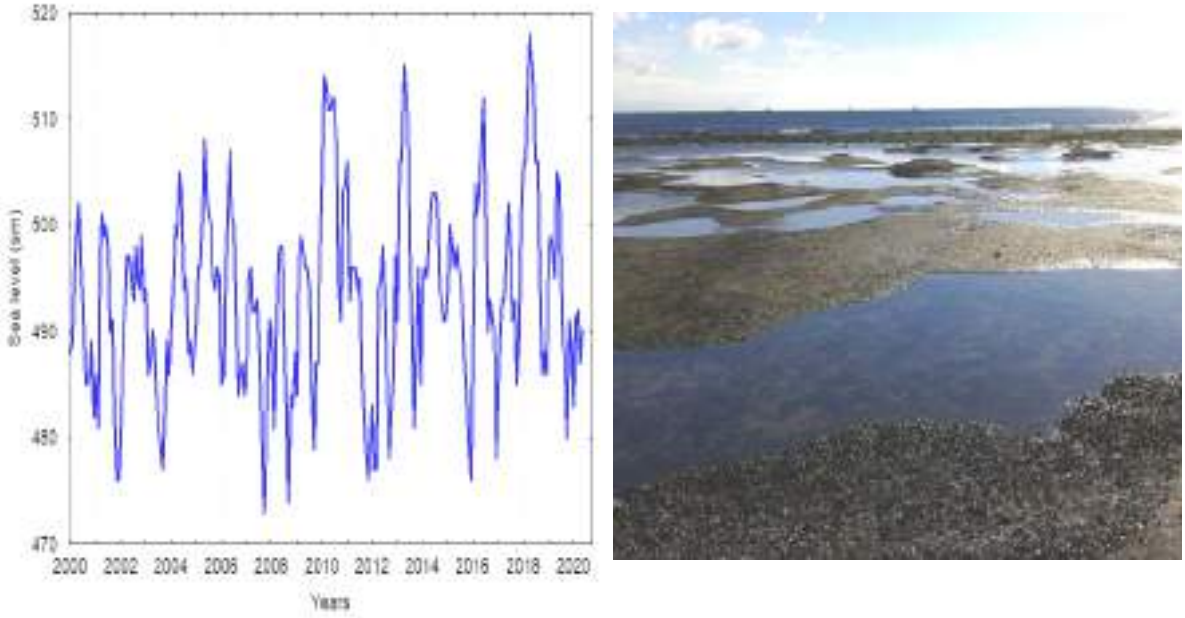

Рис. 3.12.Average monthy values of sea level in Maliy Adzgalyr estuary in 2000-2020 (left) and example of displacement of the shoreline as a result of wind preesing to sea waters level near Chornomorsk city (right).

Fig. 3.13. Coastline displacement as the result of avalanches (village Lebedivka) (left) and as the result of a landslide (village Hrygorivka) (right).

Fig. 3.14. Odessa Port's berthing facilities. Light-blue polygon outlines show the sites for which wrong result was obtained in the previous calculations of coastline displacement.

Fig. 3.15. Hydro-engineering structures of the marina in Chornomorsk. Light-blue polygon outlines show the sites for which wrong result was obtained in the previous calculations of coastline displacement (left) and man-made cape landforms of landslide prevention works in village Fontanka. Light-blue polygon outlines show the sites for which wrong result was obtained in the previous calculations of coastline displacement (right).

To eliminate the identified inaccuracies and correct the unrepresentative values of statistical characteristics we edited the initial data, namely we withdrew from the database the shoreline segments for 1980 (according to the Landsat 3 MSS image, resolution 60 m) along the entire coast where berthing facilities were built before 1980, as well as the segments where coastal protection and landslide prevention works were built (for the period after the works were built). Within the abrasion-avalanchine and abrasion-landslide types of coast we were excluding the segments of the coastline after the date of destruction processes manifestation.

This enabled us to improve the precision and reliability of the coastline dynamics' main characteristics calculation and thereby of the results of coastline dynamics analysis based on the data from the Landsat space images (1985-2020).

To create an objective picture, Chapter 5 contains the results for the period 1980-2020 presented both without the above mentioned corrections and with the corrections described and partially changed sequence of calculations, namely: after editing of the coastline in accordance with the conditions identified the automatic assessment of coastline movement was carried out for the second time using the digital shoreline analysis system (DSAS). Satellite images from the collections Landsat 3 MSS, Landsat 4-5 TM, Landsat 7 ETM+ with spatial resolution of 30 m and Sentinel 2 – 10 m were used for this analysis (Table 3*.1). In accordance with the DSAS methodology, the transects situated along the coastline at the set distance of 60 m were used. For two segments of the coast we used the high-resolution (0.31 – 0.61 m) images GeoEye-1, QuickBird-2, WorldView-2, WorldView-3 (Table 3.6-3.7) with transects situated at the 10 m distance. The selected segments of the coastline, for which the high-resolution space images were used, belong to different types of shores and are characterised by different combinations of natural and technogenic conditions. Lebedivka village (pilot sub-area UA1-3) is a section of accumulative-erosion and abrasion-avalanchine types of shores and the city Chornomorsk (pilot sub-area UA1-5) is a section belonging to the abrasion-landslide type of shore.

4. Study site Description

4.1. Ukrainian PONTOS UA1 pilot area in north-western part of the Black Sea

The Ukrainian PONTOS UA1 pilot area is located in one of the most important north-western part of the Black Sea (NWBS) which occupies vast area is the most productive Black Sea region is presented in the NWBS topographic/bathimentric map - (Figure 4.1) which we created using GEBCO 2020 data [GEBCO_2020 Grid map, 2020].

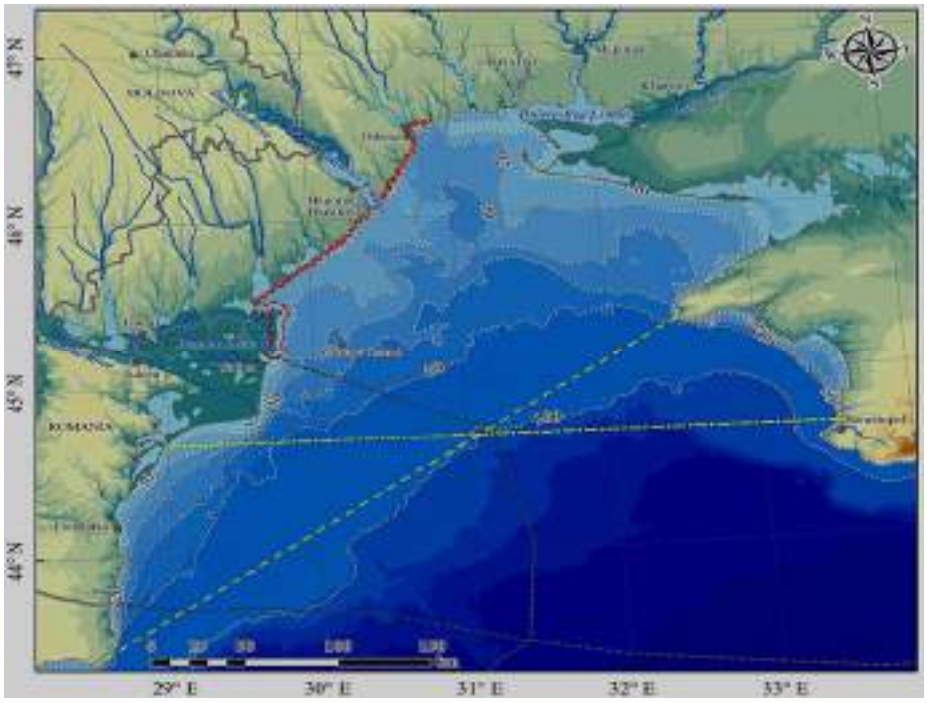

Figure 4.1. Topographic/Bathymetric map of the North-Western part of the Black Sea. Source: the EMODnet Digital Terrain Model (DTM), version of 2020 [GEBCO_2020 Grid map, 2020].

World Maritime Boundaries

PONTOS-UA_1 area

The NWBS south boundary by (Biology of the North-Western …, 1967)

The NWBS south boundary by (Zaitsev et al., 2006)

The heights (m) legend

-2 225 - -2 200	-99 - -50	0 - 10	401 - 600
-2 199 - -2 000	-49 - -40	11 - 20	601 - 800
-1 999 - -1 500	-39 - -30	21 - 50	801 - 1 000
-1 499 - -1 000	-29 - -20	51 - 100	1 001 - 1 200
-999 - -500	-19 - -10	101 - 200	1 201 - 1 400
-499 - -100	-9 – 0	201 - 400	1 401 - 1 600

In past (till 2006) as it is shown in monograph (Vinogradov et al, 1967) the north-western Black Sea part was defined as the vastest shallow-water zone of the Black Sea stretching to the west of the line connecting the Tarkhankut Peninsula (Ukraine) with Cape Kaliakra (Bulgaria). After the years that followed the boundaries of the NWBS area were specified more precisely (Zaitsev et al., 2006): the NWBS is located to the north from 44° 40'; total area is 49900 km2; volume of water is 2700 km3; average depths makes 54.1 m.

Very important water bodies of NWBS are estuaries and river basins which are important constituents of the Ukrainian Black Sea coastline (Zaitsev, 2006).

4.2. Topograpy and Bathymetry

The Ukrainian pilot area UA1 (Figure 4.1) is located in the north-western part of the Black Sea at the border with the Black Sea Lowland, which is a part of the East European Plain. The total length of the UA1 pilot area coastline is about 270 km from the Limba Arm (in the Danube Delta; 45.2022 N; 29.6897 E) to the Velykyi Adzhalyk Estuary (46.5721 N; 30.9 E). The Black Sea Lowland is a plain crossed by wide valleys of numerous rivers, the largest of which are the Danube, Dniester, Dnipro and Southern Bug. The river discharge into the northwestern part of the Black Sea is about 270 sq. km. (80% of the total river flow into the Black Sea) [The state of the Black Sea]. There are 14 estuaries in the Danube-Dnipro interfluve. Their combined area makes 1952 sq. km. and water salinity is from 0.3 to 296 ‰. There are 20 wetlands with the total area of 635000 hectares adjacent to the NWBS, having great nature conservation value and included both into the national wildlife sanctuaries and reserves, and into the list of the sites protected under the Ramsar Convention.

The elevation marks of the relief on the Black Sea Lowland adjacent to the sea vary from 5 m below sea level (region of the Kuyalnyk Estuary) to 90-150 m above sea level. The Black Sea Lowland is composed of Paleogene and Neogene sediments (limestones, sands, clays) overlain by loesses and loesslike loams. Its territory is dominated by steppe landscapes with southern Chernozems and dark chestnut soils. Most of the NWBS basin is ploughed up and used as agricultural land. The coastal zone of the NWBS is characterized by steep banks, often with landslides, as well as by many bays, estuaries, lagoons and lakes deeply cut into the land. There are also numerous sandy spits and peninsulas protruding into the sea. The NWBS shelf is the direct continuation of the land, which in the course of time turned out to be under water; it occupies a significant area of the shelf northwestern part. In the NWBS, the shelf width down to 100 m depth varies from 8 km off the Crimean coast to 210 km along the line from Odesa to the southern border of the continental slope (Figure 4.2).

Figure 4.2. Bottom slopes in the north-western part of the Black Sea. Source: the EMODnet Digital Terrain Model (DTM), version of 2020, https://portal.emodnet-bathymetry.eu/

Analysis of the real NWBS bottom relief (down to the edge of depth drop-off) using the Black Sea bottom relief map (Figure 4.3) presented in the paper (Ignatov et al., 2008) is shown as follows.

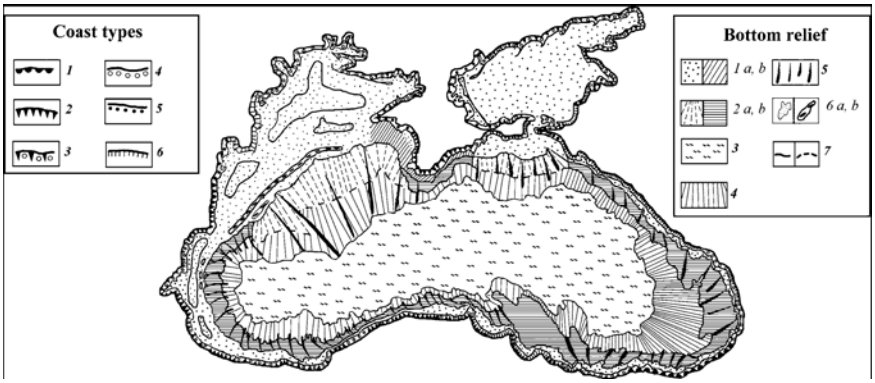

Figure 4.3. Topography of the coasts and floor of the Black Sea [gnatov et al., 2008].

Bottom relief : *1* shelf *a* accumulative, *b* abrasive; *2* continental slope *a* accumulative, *b* stepwise; *3* floor of the basin; *4* continental footstep; *5* underwater canyons; *6* bars *a* sandy, *b* marginal; *7* morphological boundaries *a* distinct, *b* fuzzy. *Coast types*: *1* landslide; *2* abrasive; *3* abrasive–accumulative; *4* accumulative; *5* lagoonal; *6* deltaic

The NWBS shelf zone has a slight slope and plane accumulating & erosional relief, which is significantly complicated by underwater valleys and slopes. Mainly those are underwater continuations of river valleys of the adjacent mainland. In the NWBS ancient valleys of the rivers Danube, Dniester, Dnipro and Southern Bug can be traced. Emerging, development and existence of this or that bottom landscape type depend significantly on its geological and structural situation, as well as on geo-morphological processes of Holocene and present time (Fesyunov, 1996). Also, the NWBS bottom relief determines the nature of bottom landscapes and together with physicochemical properties of marine environment form the main factor of biotopes distribution in the northwestern part of the sea. Scheme of the Black Sea northwestern shelf bottom relief is presented in Figure 4.4.

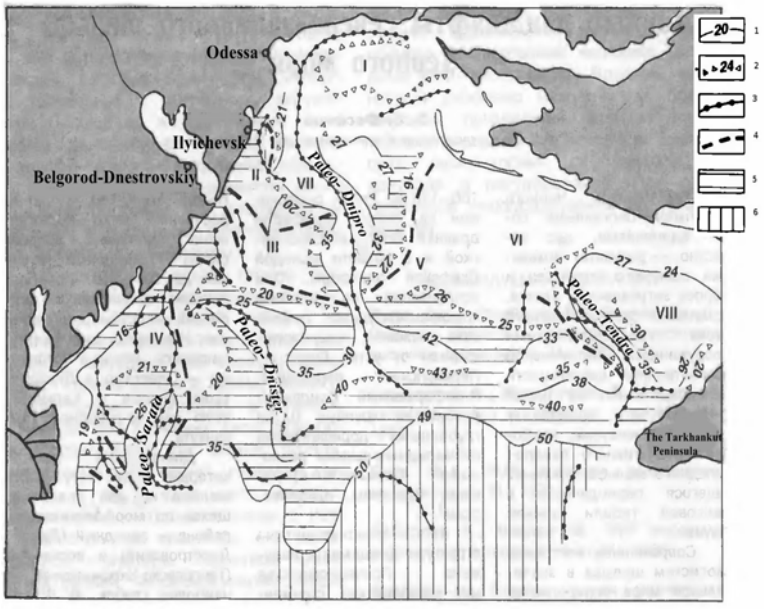

Figure 4.4. Scheme of the Black Sea northwestern shelf bottom relief (Fesyunov, 1996). 1– foot of slope, 2. - edge of the shelf, 3. – axes of depressions, 4. – axes of elevations, 5 – slope, 6 – flat. Elevations marked with Roman numbers: I — Odesa, II — Chornomorsk, III —Dniester, IV — Budak, V — Western—Tendra, VI — Tendra slope. Depressions marked with Roman numbers: VII — Odesa, VTII — Karkinitskyi. Arabic numerals stand for depth of the foot and edge of the shelf.

Current surface of the bottom is a gently inclined to the south (2-3^0) flat dissected by linear submeridional depressions (trenches). Along the whole length of the slope there are two pronounced scarps of sublatitudinal extension. First one corresponds to the current coastal underwater slope, its drop of depth makes 10-15 m and incline of relief is up to 20^0. The second one is located within the 30-40 m interval of depth and incline of relief is 6-7^0. To the south the scrap passes into flat-lying indiscrete plain (Fesyunov, 1996; Suchkov, 1999). The flat trenches of sublatitudinal extension showing up within the shelf correspond to valleys of paleo-rivers separated by underwater flats. Width of the trenches varies from 2 to 20 and over kilometers. Bottoms of the trenches are flat and concave. The biggest trenches are Paleo-Dnipro and Paleo-Dniester. The Paleo-Dnipro trench is the deepest and it divides the internal part of the shelf into two sub-regions of different morphology — western (Danube-Dniester) and eastern (Tendrovsko-Karkinitskyi). Paleo-Dnipro trench stretches in latitudinal direction, changes its orientation into longitudinal to the south from Odesa bank, widens and forms the Odesa basin.

We have to point out that in the pre-Holocene relief elevation difference reached 20-30 m. Further on, with sea transgression and sediments accumulation the relief flattened out due to much sediments accumulation in the trenches. The current difference between the trenches and flat surfaces of underwater elevations is 10-15 m. (Suchkov, 1999). The map of the NWBS bottom landscapes is presented in Figure 4.5. Characteristics of landscapes of the Black Sea northwestern shelf are given using the papers by O.E. Fesyunov (Fesyunov, 1996; Fesyunov, 2000).

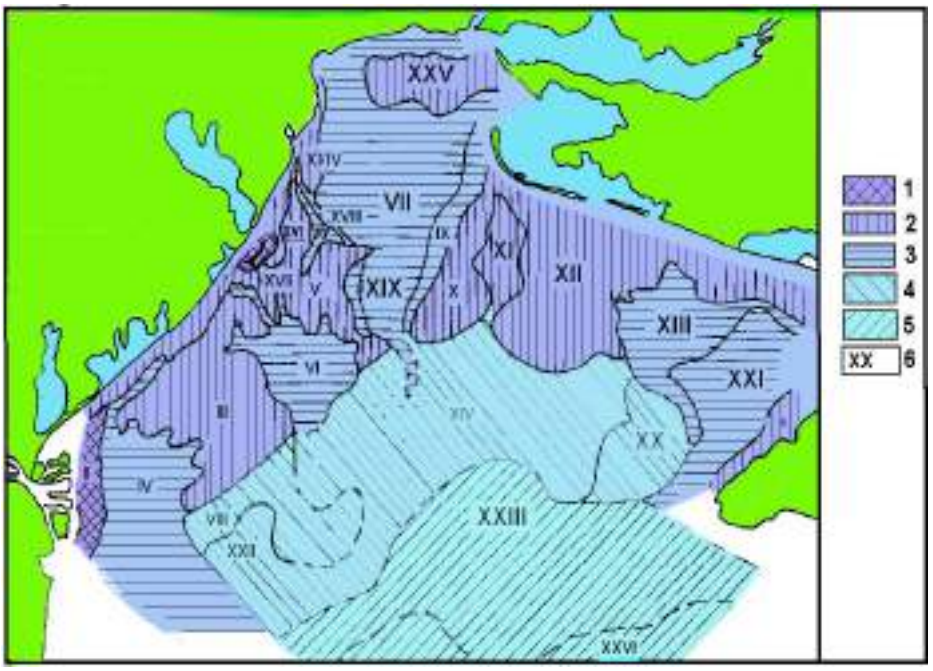

Figure 4.5. Scheme of landscape zoning of the Black Sea northwestern shelf (Fesyunov, 2000).

Types of bottom landscapes: 1. – offshore outflow areas, 2. – coastal underwater slopes and underwater elevations, 3. – paleovalleys, 4. – outer scrap of coastal part of the shelf, 5. – flats in the central par of the shelf, 6. – numbers of landscape areas. Landscape areas: I—landscapes of the coastal slope, II— the Danube Prodelta, III—Budakskyi Rise, IV—Paleo-Sarata, V — Dniester Rise, VI — Paleo-Dniester, VII — Dnipro Trench, VIII—Area of shell stones of the outer scrap, IX— eastern slope of the Dnipro Trench, X—Western-Tendra Rise, XI— eastern slope of the Western-Tendra Rise, XII— Tendra Slope, XIII— slopes of the Karkinitskyi Basin, XIV—area of silty shell stones of outer scrap, XV— northern slop of the Dniester Rise, XУ1-XУII— areas of mud and clay mud in the Dniester offshore outflow area, XVIII—southern slope of Odesa Basin, XIX — western slope of the Dnipro Trench, XX — area of shelly muds on the outer slope, XXI— Karkinitskyi Basin, XXII —area of muddy shell stone, XXIII — northern area of the central part of the shelf, XXIV— Chornomorsk Elevation, XXV— Odesa bank, XXVI— southern area of the central part of the shelf.

At present, the flat relief of the NWBS shelf has a number of morphological features due to the presence of banks (shoals). First of all, these are the Odessa (from the mouth of the Dnipro-Bug Estuary to the west) and the Dniester (near the Dniester River mouth) banks, which have a significant impact on water circulation in the NWBS (Dotsenko & Tuchkovenko, 2006). A relatively large elevation of the bottom is adjacent to the Tendra Spit. There is also a small group of bottom uplands along the line from Cape Tarkhankut to the Danube Delta. These bottom uplands are separated from the bottom elevation near the Tendra Spit by a significant depression. The stratigraphy of recent sediments in the NWBS (Shcherbakov & Morgunov, 1975) shows that the identified relief elements are closely related to the geological structure of continental sediments underlying the modern sediments.

So, the most ancient deposits, represented by the Pliocene dense speckle clays (similar to the deposits of the Kuyalnyk Estuary) are forming the base of the chain of Tarkhankut-Danube 'belt' uplands. Most of the territory is covered by the Upper Pleistocene rocks represented by various continental facies. The main extensive depressions in the NWBS and trough-shaped relief depressions located to the south of the Dniester and Dnipro-Bug Estuaries are filled with alluvial, lacustrine-alluvial and estuary facies. Most of the positive relief elements (elevations) are composed of loesslike loams of the Upper Pleistocene.

4.3 Geomorphology and Geology

We substantiate the real NWBS boundaries taking into account bottom relief (down to the edge of depth drop-off) using the Black Sea bottom relief map (Figure 4.3) presented in the paper (Ignatov et al., 2008) see part 4.2. Thus, we could make a point that the northwestern shelf occupies the area limited by the coastline in the north and by the shelf edge in the south; the latter is located at sea depths of 130–200 m and runs from Cape Kaliakra in the west to Cape Khersones in the east.

The maximum width of the shelf is 210 km. The present-day morphology of the shelf is defined by the major rivers that fall into the northwestern part of the sea. Their near-mouth features were formed in the Quaternary over the paleo-relief flooded during regressive stages of the sea level history. The present-day surface of the shelf retains fragments of relic topographic features in the form of paleo-deltas and ancient coastlines. Overall, the shelf represents a stepwise alluvial–marine plain with superimposed underwater bars, relics of river valleys, and abrasive escarpments. In the south, it is rimmed by marginal bars extended along the shelf edge at depths of 100–130 m. The inner zone of the northwestern shelf consists of the underwater coastal slope with signs of intensive wave action extending down to depths of 30–40m. The width of this zone sharply changes from 10 km in the west to 110 km at the meridian of the Berezan Lagoon. Here, the manifestation of the sediment-forming activity of the rivers is especially strong.

The central zone of the shelf is dominated by accumulation processes, which results in smoothing and burying of relic topographic features. This zone is 35–90 km wide and occupies areas with sea depths from 40 to 60 m. The outer shelf zone is located at depths greater than 60 m; its marginal part is characterized by steeper slopes than those in the inner and central zones. The greatest depths here reach 60–100 m; its smallest width (down to 10 km) is observed in the east, while in the west, off the Danube River mouth, it reaches 60 km. Here, the shelf edge is confined to 130–150 m depth contours.

The portion of the shelf between Cape Tarkhankut and Cape Khersones represents a slightly inclined abrasive–accumulative plain with traces of relic coastal topographic features down to sea depths of 40–50 m. As in previous years different authors determined the NWBS boundaries and the main morphological characteristics differently, there is quite a wide scatter, which requires analysis and revision of the previously used data, as well as specification of morphological characteristics.

To achieve this goal, we recalculated all the morphometric characteristics of the NWBS using GEBCO bathymetric map [GEBCO, 2020]. As far as we know, these bathymetric maps have been never used for such assessments before. In this connection we carried out new calculations of area, average depth and other NWBS morphometric characteristics using GIS (Table 4.1).

Table 4.1. The main NWBS Geomorphological Characteristics

Characteristics	units	Value	% of total Black Sea	% of NWBS
Total shoreline of NWBS	km	1812	38.8	100
Bulgaria	km	56	1.2	3.1
Romania	km	266	5.7	14.7
Ukraine	km	1490	31.9	82.2
Area of Water Surface (200 m) of NWBS	km^2	69442	61.5	100
Bulgaria		2296	2.0	3.3
Romania		22429	19.9	32.3
Ukraine		44718	39.6	64.4
Area of Water Surface (150 m) of NWBS	km^2	68379	62.7	100
Bulgaria		2167	2.0	3.2
Romania		22017	20.2	32.2
Ukraine		44196	40.6	64.6
Area of Water Surface (100 m) of NWBS	km^2	63646	64.3	100
Bulgaria		1997	2.0	3.1
Romania		19793	20.0	31.1
Ukraine		41857	42.3	65.8
Water volume of NWBS	km^3	4530	0.80	100
Bulgaria		181	0.03	4.0
Romania		1673	0.30	36.9
Ukraine		2663	0.47	58.8
Average depth of NWBS	m	65.24		
Bulgaria		78.85		
Romania		74.59		
Ukraine		59.55		

To analyse the NWBS geological structure we should take in account **t**he following tectonic elements of different age in the structure of the Northwestern Black Sea shelf: Eastern-European Archaean Proterozoic Platform, Scythian epi-Hercynian Platform and the Black Sea Cretaceous-Cainozoic Superimposed Depression [Moroz et al., 1995]. Formation of the current NWBS shelf took place under conditions of transgressing sea in Holocene [Dolukhanov et al., 2009; Suchkov et al., 2001] and caused by relief of inundated valley and character of transgression (series of glaciological and eustatic transgressions and regressions) [Tuleneva and Suchkov, 2011], as well as inseparably connected with tectonic and neo-tectonic development of the Black Sea depression [Scherbakov and Morgunov, 1975; Morgunov et al., 1976]. Neo-tectonic and current geodynamic processes significantly determined character and intensity of the current exogenous geological processes, which had been depicted in the formation of the main morphological structures of the north-western shelf in the Black Sea basin [Shnyukov, 1982]. In general, the Holocene transgression within the Black Sea northwestern shelf had character of ingression [Tuleneva and Suchkov, 2011]. The scheme of the surface inundated during the Black Sea transgression [Shnyukov et al., 1999] is shown in Figure 4.6.

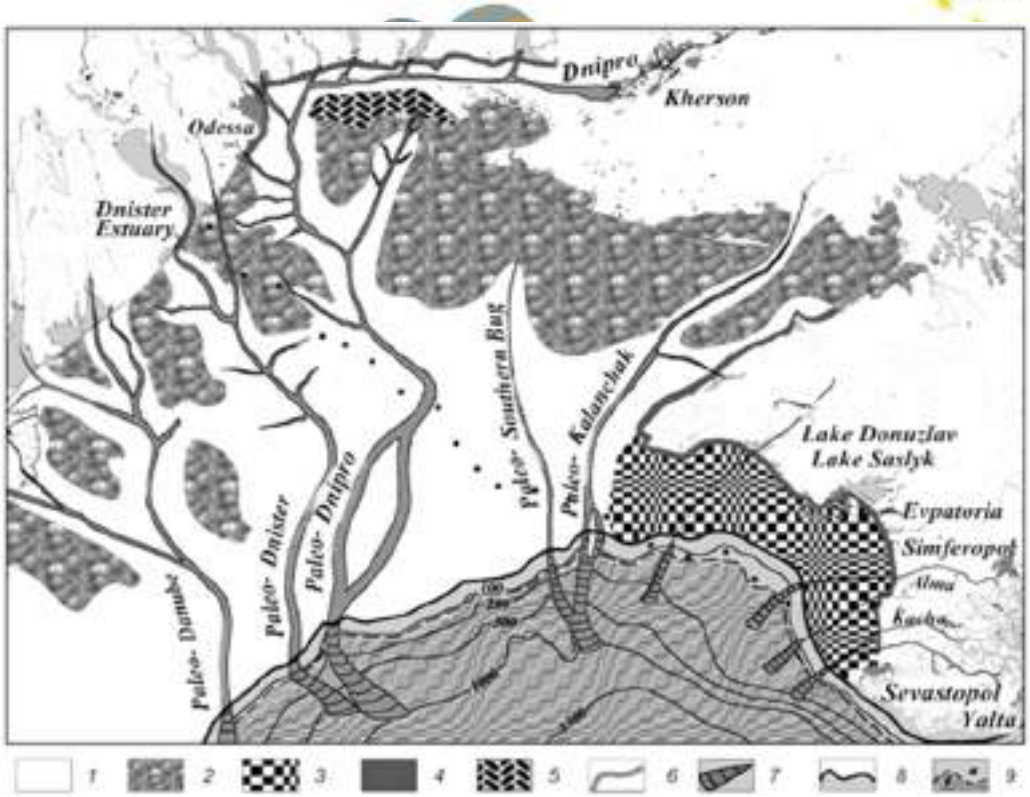

Figure 4.6. Schematic map of pre-Holocene surface of the Northwestern Black Sea [Shnyukov et al., 1999]. Legend: 1 – paleovalleys of rivers and alluvial valleys of dissected relief, 2 - gentle elevations formed by late Pleistocene marine and continental depositions, 3 - gently-inclined submontane elevations, 4 – cliffed shores and segments of sea bottom formed by bedding rocks, 5 – big relict accumulative sand bodies, 6 – paleo-rivers courses, 7 – underwater alluvial cone, 8 – coastline location in the period of the Black Sea level maximal recession ca. 18 thousand years ago, 9 – sea basin in the period of maximal Quaternary regression

In the structure of the Black Sea bottom we single out shelf, continental slope and deep-sea through. The shelf or continental terrace is an immediate continuation of land, which happened to be under sea water and occupied a significant area of the north-western part of the sea. Here the shelf width exceeds 200 km, depth makes 0-100 m, sometimes down to 160 m. Marine depositions of Holocene age within the Black Sea northwestern shelf cover blanketlike accumulative-erosion surface after Pleistocene subaerial relief of coastal lowland dissected by valleys of paleo-rivers, formed by pre-Holocene buildups, represented by middle to upper Pleistocene continental marine and estuarine & marine depositions [Suchkov, 1999]. The largest height of Holocene depositions have been found in the offshore outflow areas of estuaries (10 to 13 m) and to the east of meridian of city Mykolaiv (15 to 24.5 m). The smallest heights are connected with elevations on the shelf, which correspond to embedded interstream areas [Tyuleneva, 2010]. Distribution of bottom sediment types is presented in Figure 4.7 [Shnyukov, 1985; Fedoronchuk et al., 2001]. Bottom sediments of the northwestern Black Sea shelf are represented by sand, shell stone with different level of saturation with aleuritic and pelitic material, aleuritic & pelitic and pelitic mud [Shnyukov, 2001]. Sands superpose within coastal underwater slope down to the depth of 10 m. Shell stones and shelly aleuritic mud dominate and cover the surfaces of underwater elevations. Aleuritic & pelitic and pelitic muds are widespread within the Danube delta front and also compose bottom surface of underwater depressions corresponding to paleo-river valleys (Odesa Depression).

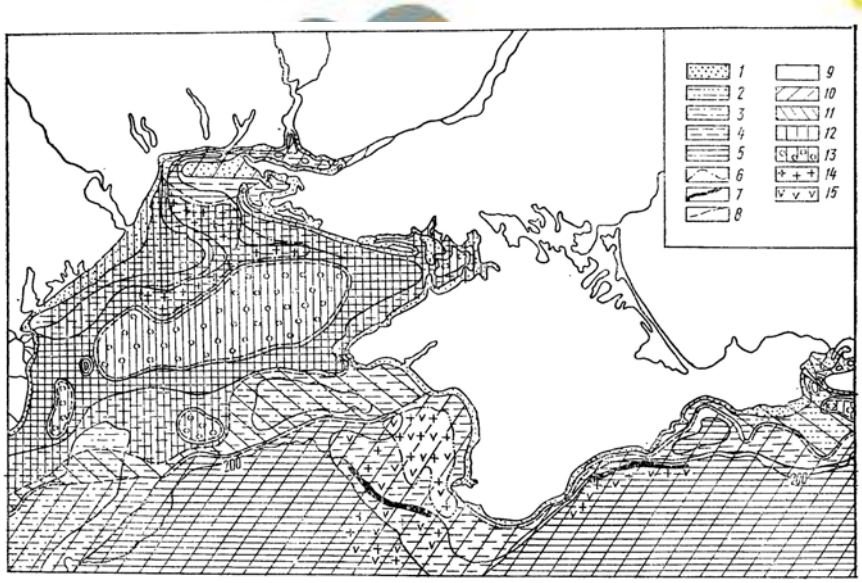

Figure 4.7. Scheme of distribution of compositional and genetic types of the Black Sea shelf current sediments [Shnyukov, 1985; Fedoronchuk et al., 2001]. Grain size: 1—sand; 2—coarse aleurite; 3 — fine aleuritic mud; *4* — aleuritic and peltic mud; 5—peltic mud. Material composition: 6—field of manganese and box stones; 7 —Pre-Holocene depositions; *8*— boundaries of compositional and genetic types; *9* — terrigenous, fragmental; *10* — low carbonate, shelly; *11* — carbonate, shelly; 12 — high carbonate, shelly; *13* —shell stone; *14* — low ferruginous; *15* low manganiferous

Estuarine landscape areas are located at the depth under 25 m and cover relatively small space. There composition of bottom sediments is more diverse than in landscapes of other types, low carbonate clayey muds dominate. Biocoenoses are also diverse with usual domination of polychaete, however biomass is small.

Landscapes of abrasion coastal slope are located in the narrow stripe along the coast, from water edge to 10-15 m depth. Bottom sediments are represented here by detrital shell stone, sometimes by muddy shell stone on which Mytilus biocoenoses are developed, often having high productivity. Those landscapes are characterized by active hydrodynamic regime.

Landscapes of underwater elevations are connected with areas of relative non-tectonic elevations. They are located at the depth under 30 m. Dominating types of bottom sediments are shell stone and detrital shell sand with carbonate content exceeding 70—60% and containing small quantity (0.3—0.7%) of organic carbon. Hydrodynamic activity here in general is also significant which determines carrying of fine-grain material outside summit plain of elevations where just nutrient sedimentation takes place. Mytilus and Cerastoderma & Mytilus biocoenoses here have different productivity. Total biomass varies from 0 to 1000 g/m^2 and over.

Landscapes of paleovalleys are connected with topographic lows. Depth of these landscapes is bigger than in other areas of coastal shelf, from 23-25 m in the upper edges of the valleys to 40—42 m as they go offshore. Hydrodynamic influence on the bottom decreases, share of pelitic material in sediments increases. Bottom sediments on the slopes of depressions are represented by muddy shell stones changing with depth into shelly muds and in the deepest areas into muds (Odesa and Karkinitskyi basins). Correspondingly, decreases carbonate content of sediments (to 30—50%). Content of organic matter ($C_{org.}$) in sediments grows to 1.8-2.4%. Biocoenoses there are all Mytilus, sub-dominating species are polychaeta (mainly Melinna). In good years total biomass on slopes of depressions reaches 500 g/m^2, in paleovalleys 300—400 g/m^2, in basins — not more than 100 g/m^2.

Landscapes of outer slope of the coastal part of the shelf are located at the depth 25 to 50 m, dominating depth is 35—45 m. Prevailing types of bottom sediments are shell stones and muddy shell stones with carbonate content about 70%, changing in the east into medium-carbonate shelly muds. Organic carbon content also grows from west to east: from 0.5 to 2%. On the upper slope, as well as on the underwater elevations, biocoenoses are Mythilus and Cerastoderma & Mytilus with different polychaete species. Total biomass here reaches 300-600 g/m^2, however, in some areas and in bad years decreases to 30—40 g/m^2.

Landscapes of the flat in the centre of shelf are located at the depth from 45—50 m to 60 m and over. As a rule, bottom sediments are represented by muddy shell stones with carbonate content 50—70% and $C_{org.}$ 1.6—2.3%. This part of the shelf is located in the zone of the main Black Sea current and is characterized by free hydrodynamic connection with open sea. Its relief is monotonous. According to hydrobiological data, two landscape areas are singled out within the plane — the northern area, situated at the depth under 60 m and the more offshore area — southern, which is deeper. Biocoenoses of the first area are Mytilus and Modiolus phaseolinus, at that both species are dominant. This biocoenosis is transitional from Mytilus only, which is characteristic of coastal part of the shelf, to Modiolus phaseolinus, which are characteristic of deep areas. Apart from dominating molluscs, crustacean (Theneidae), Ophiuroidea and Polychaeta can be found here in significant quantities. In south landscape region Modiolus phaseolinus biotic community is developed, dominating species in it is Modiolus phaseolinus, sub-dominating -Theneidae and Terebellidae. Total biomass in both areas in not high – it averages to about 50 g/m^2. In places there are sites with biomass exceeding 200 g/m^2 in the first area and up to 100—200 g/m^2 in the second.

Digital geological map of the Northwestern Black Sea part, which we can use for PONTOS (Figure 4.8) was built based on the 1:5 M International Geological Map of Europe and Adjacent Areas (IGME 5000) with the data on the pre-Quaternary geology of Europe (Table 4.2).

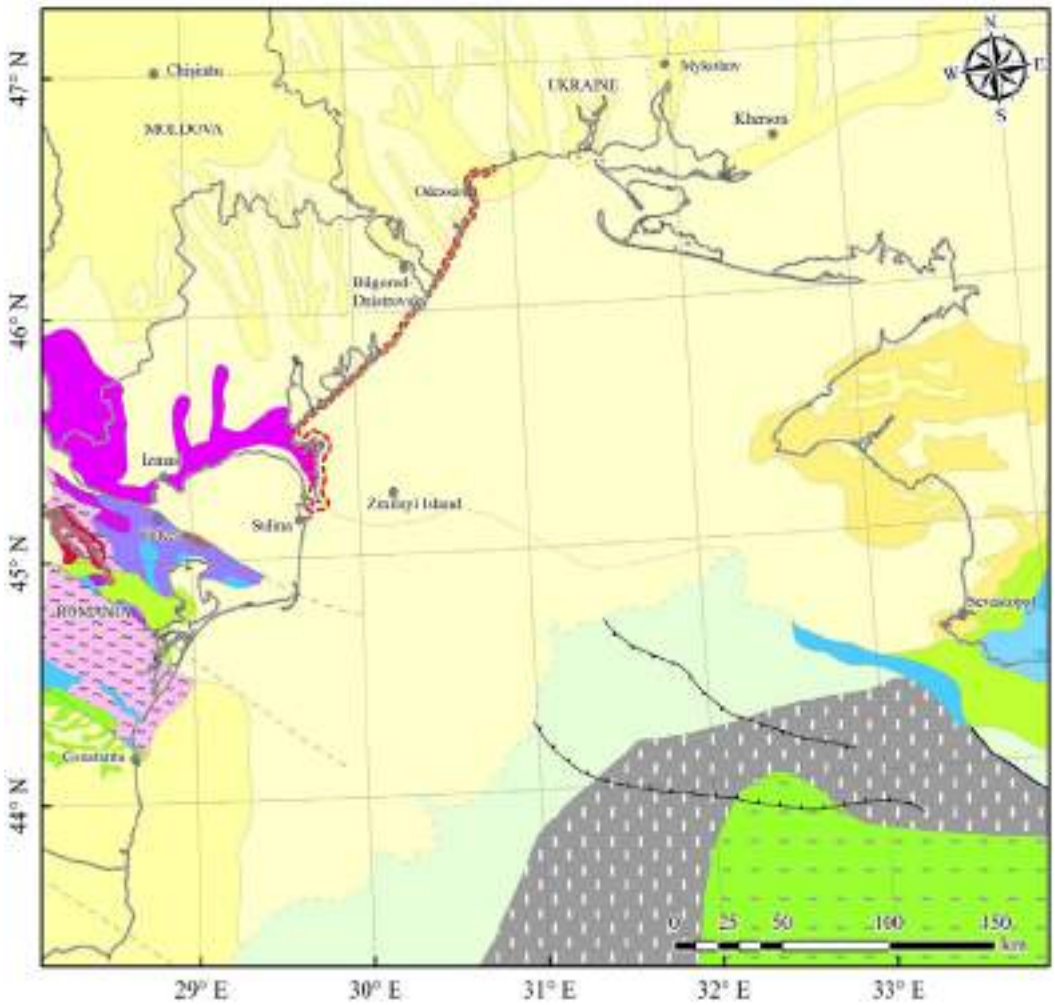

Figure 4.8. Geological map of the Northwestern part of the Black Sea **Source:** The 1:5 M International Geological Map of Europe and Adjacent Areas, version of 2005, https://www.bgr.bund.de

Table 4.2. Geological map legend (BGR classification)

Geological features		Symbol/Color
Boundaries or structure lines	fault	
	fault, inferred	
	geological boundary	
	geological boundary, inferred	
	strike/slip fault	
	thrust	
Metamorphic rocks	low grade	
	medium grade	
Igneous rocks	plutonite Palaeozoic	
	plutonite Precambrian	
	volcanite Cenozoic	
	volcanite Mesozoic	
Crust-related units	oceanic crust, older	
	rifted thinned continental crust of various ages	
Rocks age names	Cadomian	
	Cretaceous	
	Jurassic	
	Late Cretaceous	
	Middle Jurassic - Late Jurassic	
	Miocene	
	Neogene	
	Oligocene	
	Palaeozoic	
	Pliocene	
	Proterozoic	
	Proterozoic III - Cambrian	
	Triassic	
	Variscan	
	undifferentiated	

This map was managed and implemented by the Federal Institute for Geosciences and Natural Resources (BGR) under the aegis of the CGMW (Commission of the Geological Map of the World). Over 48 European and adjacent countries and more than 20 scientific institutes were involved in preparation of the map and the area covered reaches from the Caspian Sea in the east, to the Mid-Ocean Ridge in the west, and from Svalbard to the southern shore of the Mediterranean Sea [Asch, 2003].

Seabed substrates map of the Northwestern part of the Black Sea (Fugure 4.9 and Table 4.3) was created using map from the EMODnet Geology Portal, version of 2019 [https://www.emodnet-geology.eu], which summarized the national datasets and harmonised them into a shared schema. EMODnet Seabed substrate data (Table 4.3) comprise multiple datasets at different scales, compiled in EMODnet Geology projects running since 2009. The national datasets are harmonised into a shared schema.

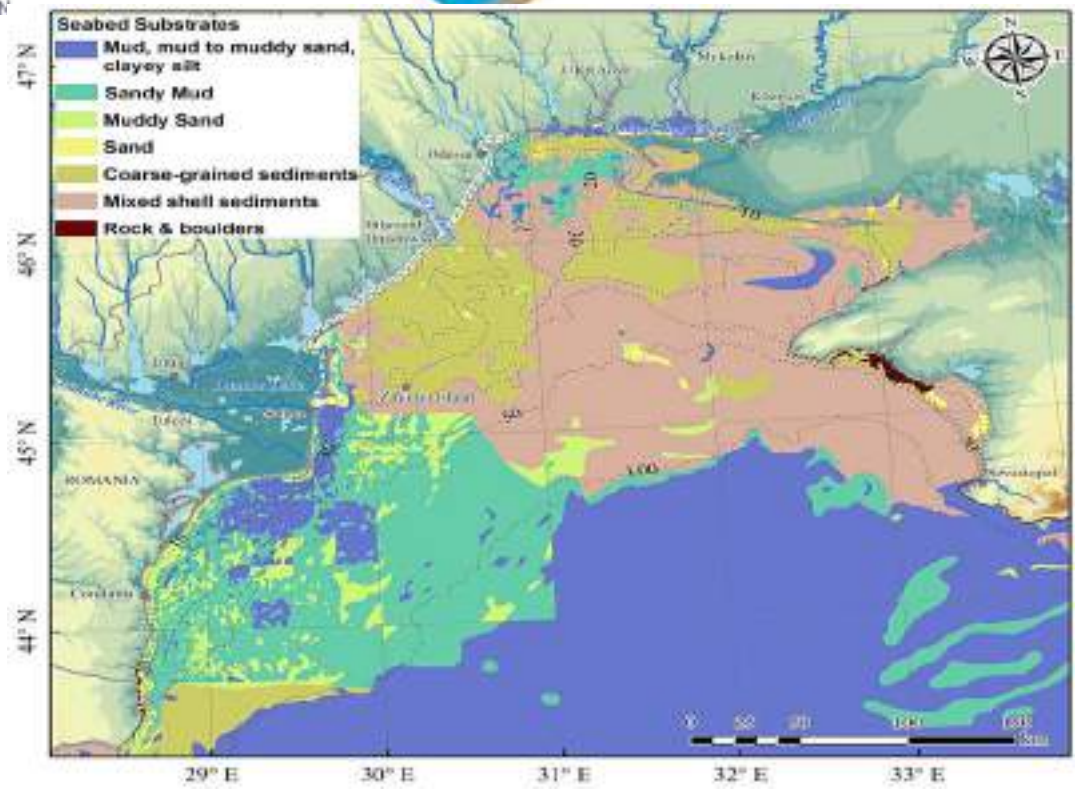

Figure 4.9. Seabed substrates map of the Northwestern part of the Black Sea
Source: The EMODnet Geology Portal, version of 2019, https://www.emodnet-geology.eu

Table 4.3. Types and areas of seabed substrates in the Northwestern part of the Black Sea and in the PONTOS-UA_1 pilot site

Seabed substrates type	Substrate area in the NWBS, km^2	Share of the substrate area in the NWBS area, %	Substrate area in the PONTOS-UA-1 area, km^2	Share of the substrate area in the PONTOS-UA-1 area, %
Mud, mud to muddy sand, clayey silt	4602.6	8.5	9.9	3.0
Sandy mud	13221.9	24.5	59.1	17.6
Muddy sand	4303.6	8.0	70.6	21.0
Sand	822.1	1.5	113.3	33.7
Coarse-grained sediments	11660.1	21.6	48.8	14.5
Mixed shell sediments	19200.2	35.6	33.5	10.0
Rock & boulders	92.1	0.2	0.6	0.2

The presented compiled map of bottom substrates (Figure 4.11) describes separate areas of the NWBS and the pilot site with different degree of detail.

For almost the entire PONTOS-UA_1 pilot site the scale of this map is 1:50 000 with the exception of the Danube River delta, where the scale is 1: 1 000 000 [Rokitskiy V.E. et al., 2020].

Assessment of each of the seabed substrate area (Table 2.) showed the prevalence in the NWBS of mixed shell sediments - 35.6%, sandy mud - 24.5% and coarse-grained sediments - 21.6%. In the PONTOS-UA_1 pilot area the relative share of bottom substrates changes as follows: sand (33.7%) and muddy sand (21.0%) prevail with still relatively high percentages of sandy mud (17.6%) and coarse-grained sediments (14.5%).

Thus, more than 75% of the bottom area in the pilot site is covered mainly with mixtures of sand and silt.

According to the map presented in Fig. 4.9 , mud, sandy mud, shelly clayey silt bottom substrates dominate in the water areas adjacent to the deltas of the Danube and the Dnipro Rivers (mud, sandy mud, shelly clayey silt, (clayey) sandy shell deposits, fine aleuritic silt, sandy shell deposits, (shelly) aleuritic clayey silt, fine sand, shelly fine sand). This is especially typical of the Danube, which influences significantly the mosaic of sea bottom substrates up to the transition from the shelf to continental slope due to huge volumes of suspended particles and silt the river brings (Figure 4.2. Bottom slopes). The sea bottom in the interfluve between the Danube and the Dniester down to 40 m depth is covered with coarse-grained sediments: shelly medium sand, aleurite, sandy shell deposits, silty shell deposits [Rokitskiy V.E. et al., 2020]. Bottom substrates in the water areas adjacent to the Tendra Spit down to 20-30 m depth are similar: sandy shell deposits, shelly fine sand, shelly medium sand, (clayey) shell deposits. Substrates in Karkinitskyi Bay are partly the same: shelly fine sand, shelly medium sand [Avramets et al., 2007]. Most of the bottom substrates in the NWBS are mixed shell sediments: silty (sandy) shell deposits, shelly aleurite silt, shelly clayey silt [Sibirchenko et al., 1983]. In the relatively small water area bottom substrates are represented by rock & boulders, most of which are concentrated off the western coast of the Crimean Peninsula. Continental slope and continental footstep are covered with clayey silt, mud, silty [sandy] shell deposits and shelly aleurite silt and are outside the NWBS zone.

4.4. Land cover

The 300 m Climate Change Initiative Land Cover (CCI-LC) Maps (22 LCCS classes) obtained from processing of the full archives of 300 m MERIS, 1 km SPOT-VEGETATION, 1 km PROBA-V and 1 km AVHRR were used to assess land cover types in the northwestern Black Sea area (Figure 4.7). The typology was defined using the Land Cover Classification System (LCCS) developed by the United Nations Food and Agriculture Organization (Gregorio & Jansen, 2000) (Table 4.4). The coordinate system is a system based on the World Geodetic System 84 (WGS84) reference ellipsoid and using a Plate Carrée projection.

Analysis of the **Land cover map of the northwestern part of the Black Sea** (Figure 4.10) has shown that the following land cover types prevail in the 100 km wide zone of the sea coast belonging to the NWBS (Table 4.5): Rainfed cropland land cover – 63.8%, Herbaceous cover – 11.4%, Water bodies – 6.9% and Mosaic cropland / natural vegetation – 4.2%, forest, plantation forest, sparse forest and shrubs – 6.7%, urban areas – 2.8%. The area of other land cover types does not exceed 4 %. Water bodies (6.9%) are represented by rivers and lakes with fresh water, as well as numerous marine estuaries and lagoons.

Intensive economic activities in the northwestern Black Sea area (crop growing and livestock breeding) are the reason of intensive anthropogenic pressure on soils and inland aquatic ecosystems, as well as on the marine coastal zone.

Located in the coastal zone of the northwestern Black Sea, the PONTOS-UA_1 pilot site comprises mainly long sandy beaches with shrub and herbaceous vegetation and many fresh and saline water bodies. Significant part of the territory is under agriculture (up to 24%) and urban areas (up to 23%). The urban areas include all the cities/towns and villages (Odesa, Chornomorsk, Zatoka), major ports and many seaside resorts (Odesa, Koblevo, Fontanka, Grybovka, Zatoka, Lebedivka, Kurortne, Prymorske), whose intensive growth in recent years was accompanied by development of infrastructure, changes in natural landscapes and pollution of riparian land and coastal water.

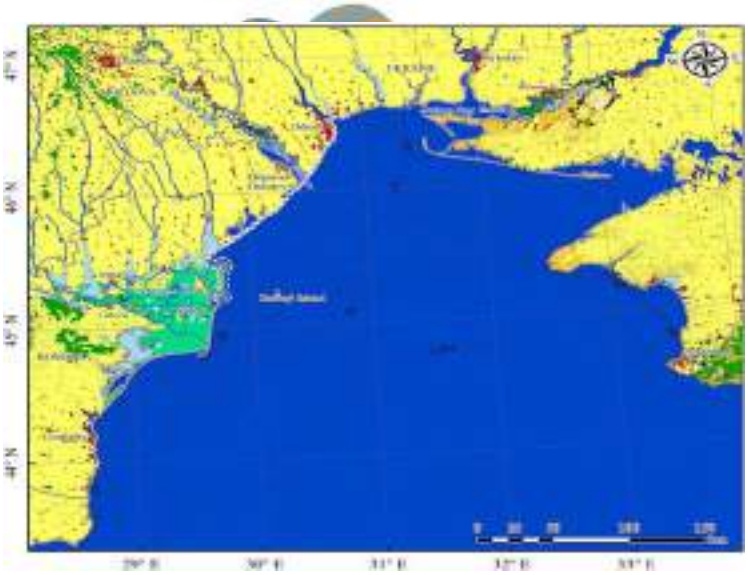

Figure 4.10. Land cover map of the northwestern part of the Black Sea. **Source:** Land Cover CCI Climate Research Data Package, version of 2019, http://maps.elie.ucl.ac.be/CCI/viewer/index.php

Table 4.4. Land cover map legend based on Land Cover Classification System (LCCS)

Cover type	Color
Cropland, rainfed	
Herbaceous cover	
Tree or shrub cover	
Cropland, irrigated or post - flooding	
Mosaic cropland (>50%) / natural vegetation (tree, shrub, herbaceous cover) (<50%)	
Mosaic natural vegetation (tree, shrub, herbaceous cover) (>50%) / cropland (<50%)	
Tree cover, broadleaved, deciduous, closed to open (>15%)	
Tree cover, broadleaved, deciduous, closed (>40%)	
Tree cover, needle leaved, evergreen, closed to open (>15%)	
Tree cover, needle leaved, evergreen, closed (>40%)	
Tree cover, needle leaved, deciduous, closed to open (>15%)	
Tree cover, mixed leaf type (broadleaved and needle leaved)	
Mosaic tree and shrub (>50%) / herbaceous cover (<50%)	
Mosaic herbaceous cover (>50%) / tree and shrub (<50%)	
Grassland	
Sparse vegetation (tree, shrub, herbaceous cover) (<15%)	
Tree cover, flooded, fresh or brackish water	
Shrub or herbaceous cover, flooded, fresh/saline/brackish water	
Urban areas	
Bare areas	
Consolidated bare areas	
Unconsolidated bare areas	
Water bodies	

Table 4.5. Types of land cover in the territories adjacent to the Black Sea northwestern part

Type of land cover	Square, km^2	Input, %
Cropland, rainfed	61407,4	63,804
Herbaceous cover	10985,8	11,415
Water bodies	6633,2	6,892
Mosaic cropland (>50%) / natural vegetation (tree, shrub, herbaceous cover) (<50%)	4061,5	4,220
Grassland	3642,8	3,785
Shrub or herbaceous cover, flooded, fresh/saline/brackish water	3190,7	3,315
Urban areas	2680,1	2,785
Tree cover, broadleaved, deciduous, closed to open (>15%)	1825,9	1,897
Tree cover, needleleaved, evergreen, closed to open (>15%)	626,0	0,650
Cropland, irrigated or post‐flooding	268,8	0,279
Sparse vegetation (tree, shrub, herbaceous cover) (<15%)	232,8	0,242
Tree or shrub cover	165,5	0,172
Mosaic tree and shrub (>50%) / herbaceous cover (<50%)	153,9	0,160
Bare areas	116,2	0,121
Mosaic natural vegetation (tree, shrub, herbaceous cover) (>50%) / cropland (<50%)	102,8	0,107
Tree cover, mixed leaf type (broadleaved and needleleaved)	76,0	0,079
Mosaic herbaceous cover (>50%) / tree and shrub (<50%)	27,9	0,029
Tree cover, flooded, fresh or brackish water	21,1	0,022
Tree cover, broadleaved, deciduous, closed (>40%)	10,4	0,011
Unconsolidated bare areas	7,0	0,007
Consolidated bare areas	6,8	0,007
Tree cover, needleleaved, deciduous, closed to open (>15%)	1,3	0,001
Tree cover, needleleaved, evergreen, closed (>40%)	0,5	0,001

4.5. Hydrology of estuaries and rivers in northwestern part of the Black Sea

4.5.1 . Estuaries of the NWBS

Estuaries of the Black Sea northwestern coast are situated in southern and middle part of the Black Sea Plain. There are in total 25 estuaries on the NWBS coast, 21 of them are on the segment between the Danube and Dnipro deltas and their water table area exceeds 5 km^2 (Figure 4.11). According to their geographical position and some morphometric characteristics, they are divided into two groups: Danube-Dniester and Dniester-Dnipro.

Figure 4.11. Schematic map of estuaries of the NWBS coast

All the estuaries are separated from the sea with sand and shell stone bars or spits. They could be completely (closed type of estuaries) or partially isolated from sea. In first case an estuary is cut off from the sea by a solid bar, in the second it is either separated by spits or there are artificial breaches in a bar. Gravitational morphostructure of banks of estuaries is represented by landslips, falls and taluses. Aeolian forms of relief are developed on the bars and spits of the estuaries: sand-dunes, deflation basins etc.

Estuaries of the northwestern Black Sea area differ in their origin and conditions of development. Dniester, Bug and Dnipro Estuaries are the estuarine areas of big rivers (Table 4.6), the Sukhyi, Khadzhybei, Kuyalnyk, Velykyi Adzhalyk (Dofinivskyi), Malyi Adzhalyk (Hrygorivskyi), Tiligul and solonetz Tuzly are the flooded by sea estuarine areas of rivers, at the moment not functioning as full-fledged river systems.

The estuaries between the rivers Danube and Dniester: Dzhanshteiskyi, Malyi Sasyk, Tuzly Group (Shagany, Karachaus, Alibey, Khadzhyder, Kurudiol, Burnas) and Budak are sea gulfs separated from the sea by bars with regulated canals connecting the estuaries with the sea; only the Sasyk Estuary was formed in the estuarine part of the sea-flooded valley common for two rivers, the Kogylnyk and the Sarata (Estuarine Complexes..., 1988). This group of water-bodies are referred to as estuarine–lagoon type. Their longitudinal axes are mainly orientated in parallel to the coast and sand bars. Total length of the bars is 66 km and their widths vary from 50 to 400 m. On the 20 km long segment between the Burnas Estuary and the Budakskyi Estuary bars are broken by a stretch of abrasion bedrock coast.

Table 4.6. Morphological Characteristics of the NWBS estuaries

	Name	Area, km²	Coastline Length, km	Maximal Depth, m	Additional Information
R1	Sinoe	136-171	118	1.6	
R2	Golovita	119-130	86		
R3	Razelm	386-415	124		
U1	Sasyk	204-210	104	2.7	Length 29 km, Width 3-12 km
U2	Dzhanshteiskyi	8.8	28	?	
U3	Malyi Sasyk	2	10		
U4	Shagany	70-72	42	2.4	Length 9 km, Width 8 km
U5	Karachaus	76	22	?	
U6	Alibey	72 -87	44	2.5	Length 15 km, Width 11 km Area 72 km², Salinity 30‰
U7	Khadzhyder	80	?	?	Length 4 km, Width 2.5 km Catchment area — 80.3 km²
U8	Kurudiol	4	11	?	
U9	Burnas	21	31	?	Length 7 km, Width 1-3 km Salinity 30%
U10	Budakskyi	31	?	2.2 (average 1.05)	Length 17 km, Width 2,5 km Volume 31 mln m³ Salinity ~14 ‰
U11	Dniester	360 - 408	139	2.7 (average 1.8)	Length 42.5 km, Width 12 km Volume 387.4 mln m³ Salinity 0.5-3 ‰
U12	Sukhyi	3	13	14.0 (average 1.5)	Elevation over sea level = -1 to 5 m Length 13.3 km, Width 0.17-1.78 km Type of mineralization saline Inflowing river: Dalnyk
U13	Khadzhybei	70	?	15	Length 31–33 km, Width 0.5-3.5 km, Maximal depth 15 m Salinity 5–6 ‰
U14	Kuyalnyk	58-60	?	Average 3	Length 28 km, Width 3 km Salinity 29-269 ‰ Inflowing river: Velykyi Kuyalnyk
U15	Dofinivskyi	50	?	1.2 (average 0.5)	Length 8 km, Width 1 km Average depth 0,5 m

	Name	Area, km²	Coastline Length, km	Maximal Depth, m	Additional Information
U16	Hrygorivskyi	5.8-6.0	10	14 (average 1.8)	Length 12 km, Width 1.5 km Volume 44 mln m³
U17	Tiligulskyi	170	?	19	Length 80 km, Width 2.5 km Inflowing river: Tiligul
U18	Tuzly estuaries	206	-	3	Comprised estuaries: Shagany, Alibey and Burnas, Solone, Khadzhyder, Karachaus,Kurudiol, Budury, Martaza, Magala, Malyi Sasyk, Dzhanshteiskyi.
U19	Berezanskyi	59-60	105	15 (average 3.3)	Length 20-25 km, Average width 2-3 km, Water volume 200 mln m³
U20	Butskyi	105	78	-	Length 47 km, Width up to 11 km.
U 21	Dnipro	715	240	Average 5	Length 55 km, Width 7.4-16.7 km,
U22	Donuzlav	39-48	73-104	27	Length 30 km, Width 8.5 km Mineralization type - saline and fresh (utmost north) Salinity 7.06. Catchment area 1288 km² Inflowing rivers: Staryi Donuzlav, Donuzlav, Burnuk, Chernushka. Outflowing rivers - none

Notes to the table. Data for R1-R3 - http://www.aboutromania.com/geography.html

Northern bank of the Sasyk, where the rivers Kogylnyk and Sarata enter the estuary, is a marshy reed-bed system. Eastern and western banks of the Sasyk are cliffy, up to 12 m high, descending towards the sea. The estuary is cut off from the sea by barrier beach up to 400 m wide embanked with concrete on the estuarine side. The banks of the other estuaries of this group are 2-4 m higher than the current sea level. Only the Burns Estuary and the Budakskyi Estuary banks have cliffy segments up to 18-20 m high. All the estuaries-lagoons are shallow; their maximal depth makes 0.6—3.0 m.

Axes perpendicular to the sea shore line is characteristic of the estuaries located between the Dniester and the Dnipro rivers, as well as: crooked bank lines; length 10 and more times exceeding width; many sand spits, river mouths, small flat bottom-valleys and ravines in the bank zone. Maximal depth of the Khadzhybey and Tiligul Estuaries is 18 and 21 m respectively, the depth of the Kuyalnyk, Velykyi Adzhalyk and Tuzly Solonetz Estuaries does not exceed 1.5—2.5 m. Land-locked character of the estuaries, periodicity of surface run-off and big volume of evaporation cause significant seasonal variations of water level and concentration of salts in water. The Sukhyi and Malyi Adzhalyk Estuaries had been converted into sea gulfs due to building of navigable channels through their barrier beaches. The Berezanskyi Estuary having no significant inflow of river water is connected to the sea through the 400 m wide strait having average depth of 2.5 m.

Group of open estuaries stays separately. They are formed in the mouths of big rivers whose discharge is quite significant now and largely determine the NWBS's water regime. The biggest coastal water-body in the area is the Dnipro Estuary. It is 63 km long with minimal width of 4 km and maximal width of 15 km. In the medium part of the estuary depth is 4—6 m, maximal depth is up to 12 m. The estuary is connected to the sea with the Kinburn Strait (width – 4 km, medium depth – 5 m, maximal depth -18 m).

The Kinburn sand-spit is a very dynamic formation: its shifting towards the estuary makes about 0.5 m a year, lengthening of distal ending is 5 m a year (Liman and estuarine complexes..., 1988).

The length of the Bug Estuary is about 82 km, width — 2 to 6 km. In some cases in the low water period, saline water goes up the Southern Bug River 10—12 km (Dnipro-Bug Estuary system, 1989). Relatively wide meandering fairway channel goes along the Bug Estuary, shallow zone is less pronounced than in the Dnipro Estuary. There are intensive landslide processes on the right banks of the Dnipro and the Bug Estuaries.

Mean discharge of the rivers Southern Bug and Dnipro flowing into these estuaries makes respectively 3 and 48 km3 • year^{-1}. Second big estuary is the Dniester - the widened valley of the Dniester River, elongated from north-west to southeast. The estuary is 44 km long; its maximal width is 12 km, mean depth – from 1.5 to 2.0, maximal depth – 2.6 m. The estuary is naturally connected with the sea with the Dnistrovsko-Tsaregradske Arm, which is about 300 m long and up to 16 m wide.

There is a man-made canal 5-6 m deep and 14.5 km wide connecting the entrance to the estuary with Bilgorod-Dnistrovskyi port. The estuary is separated from the sea by sand and shell-stone Bugaz Spit, which is 60 to 500 m wide and 11 km long (Liman and estuarine complexes..., 1988). Hydrographic network of the areas between the Danube and the Dniester rivers and between the Dniester and the Dnipro is represented by small rivers: Nerushai, Kogilnyk, Sarata, Khadzhyder, Alkalyia, Velykyi Kuyalnyk, Malyi Kuyalnik, Velykyi Adzhalyk, Malyi Adzhalyk, Tiligul, Sasyk and Berezan. Those rivers are low, fed mainly by snow. Most part of their discharge (up to 80%) falls on spring period (Polischuk et al., 1990). During dry months, most of the small rivers dry up. Many of them are regulated, ponds have been built in their valleys and a significant portion of the rivers discharge is caught by the ponds.

Depth of runoff in the estuary basins between the rivers Danube and Dniester is 6 to 15 mm • year-1, depth of precipitation — 350—400 mm • year-1, climatic difference between evaporation and precipitation — 550—600 mm • year-1. Depth of runoff in the estuary basins between the rivers Dniester and Dnipro is 20 to 30 mm • year-1, depth of precipitation — 400—450 mm • year-1, climatic difference between evaporation and precipitation — about 600 mm • year-1 (Atlas..., 2002). In some years, the values of the last quantity deviate significantly from the climatic ones mainly as the result of excision of evaporation volumes. Under these circumstances, processes of closed estuaries drying strengthen and water salinity increases.

In summer period, water in the shallow estuaries could warm up to 32 °C and in winter cool down to negative temperatures. On the most of estuaries, ice forms every year, but periods of freezing up are different. Exceptions are the Kuyalnyk Estuary and the Tuzly Solonetz, which freeze up very seldom due to very high water salinity (see Table 3). The longest ice periods are in the Dniester, Bug and Dnipro Estuaries. In cold winters, ice stays for 100 days, its thickness reaches 0.5—0.6 m. Hydrodynamic activeness of water in the Dniester, Bug and Dnipro Estuaries depends on river discharge, wind and water exchange with the sea; in the Sukhyi, Malyi Adzhalyk and Berezan Estuaries – on wind and water exchange with the sea, in the enclosed estuaries – mainly on wind.

4.5.2. NWBS river and estuaries basins

The basins of the biggest Ukrainian rivers Danube, Dniester, Dnipro and Southern Bug (Fig. 4.12) in the northwestern Black Sea area are the main source of suspended matter, pollution and nutrients to the NWBS, which is practically completely enters the marine economic zone of Ukraine.

Fig. 4.12– River basins in the northwestern Black Sea are

Besides, there are 18 unique water bodies, the estuaries, part of which are the deltaic areas of the biggest Ukrainian rivers Dniester, Southern Bug and Dnipro (Fig. 4.13).

Fig. 4.13 – Catchments of the Dnipro-Bug and Dniester Estuaries (including the catchments of the rivers entering the estuaries)

Other estuaries (Fig. 4.14) are less dependent on river discharge and their water exchange with the sea is restricted, which causes high salinity of their water. However, they anyway influence the quality and state of coasts of the adjacent Black Sea areas.

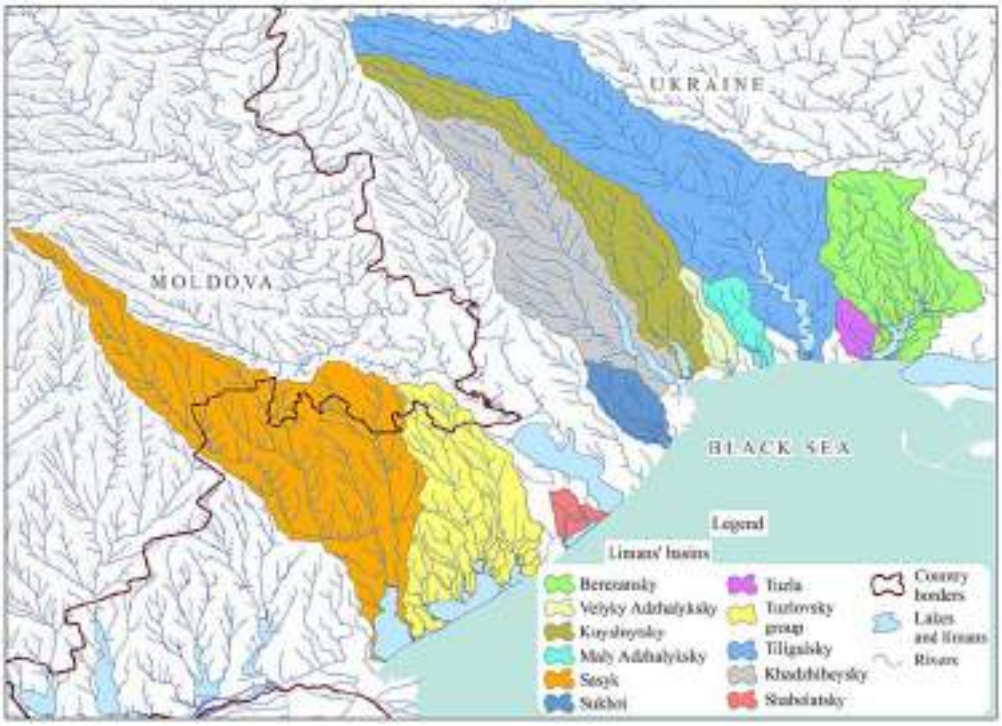

Fig. 4.14 – Catchments of the Barezan, Velykyi Adzhalyk, Kuyalnyk, Malyi Adzhalyk, Sasyk Sukhyi, Tuzla, Tuzlovsky Group, Tiligul, Khadzhibey and Shabolatskyi Eatuaries

As is known, about 80 % of the total river flow into the Black Sea enters the NWBS (Dovgiy et al., 2010).

River discharge is the factor, which determines the main environmental problems forming in the shallow NWBS (tables 4.8-4.12). The main sources of water discharge into the NWBS are the rivers Danube, Dnipro, Dniester, Southern Bug and a numerous small rivers. The discharge of the four main rivers into the Black Sea Basin equals to 270 cubic meters a year. Catchment of those rivers makes 1.46 mln. square km and covers the area where 160 mln. people live.

Table 4.8. Characteristics of the main rivers in the NWBS catchment (Mikhailova, 2009)

River	Catchment area, thousand sq.km	Length, km	Average many years' discharge, sq.km/year	Area of river delta, sq.km
Danube	817	2857	204	5912
Dnipro	504	2201	53	500
Dniester	72.1	1362	10.2	240
Southern Bug	63.7	806	2.8	0
Total:	1456.8		270	6652

Table 4.9. Types of the major river mouths in the Black Sea area (Mikhailova, 2009)

River mouth	Country	Type of the river mouth	Type of the delta	Type of the semi enclosed coastal water body	Type of the open near shore zone
Danube	Romania Ukraine	Open deltaic	Protruding, multi-branch	Semi enclosed coastal water body is absent	Deep
Dniester	Ukraine	Semi enclosed deltaic	Filling (bayhead), with few branches	Estuary	Deep
Dnipro and Southern Bug	Ukraine	Semi enclosed deltaic, complex	Filling (bayhead), multibranch	Estuary	Deep

Table 4.10. Morphometrical characteristics of the major river mouths in the Black Sea area (dash stands for lack of data) (Mikhailova, 2009)

River mouth	Delta area, km^2	Number of the delta branch mouths	Length of the main delta branch, km	Length of the delta coastline, km	Area of the semi-enclosed coastal water body,	Area of the open near-shore zone, km^2	References
Danube	4200	16	116	190	Semi enclosed coastal water body is absent	1360	Dzhaoshvili, 1999; Mikhailov, 1998
Dniester	49	2	13	22	360	-	Mikhailov, 1997
Dnipro and Southern Bug	350	12	47	15	1000	-	Mikhailov, 1997

Table4.11. Average water runoff and suspended sediment load of the rivers entering the Black Sea along the northwestern coast within Romania and Ukraine (Mikhailova, 2009)

River	Drainage area, 10^3 km	Annual water discharge, m^3s^{-1}	Specific water discharge, L s^{-1} km^{-2}	Water runoff, km^3 $year^{-1}$	Suspended sediment load, 10^6 t $year^{-1}$	References
Danube	817	6590 6320*	8.1 7.7*	208 199*	36.3 52.4*	GEOS, 2004
Dniester	72.1	288 320*	4.0 4.4*	9.1 10.1*	4.1 5.5*	Hydrological Regime…, 1992; Mikhailov, 1997
Southern Bug	73.4	87.5	3.0	2.76	0.326	Mikhailov, 1997

Dnipro	503	1375 1683*	2.7 3.3*	43.4 53.1*	0.80 2.10*	Dzhaoshvili, 1999; Jaoshvili, 2002; Mikhailov, 1997
Total	1465	8340 8410*	5.69 5.74*	263.2 265.0*	41.5 60.3*	

Table 4.12. Present-day average water runoff and suspended sediment load of the rivers flowing into the Black Sea (Mikhailova, 2009)

Sector of the coast	Drainage area, 10^3 km^2	Annual water discharge, m^{3}s^{-1}	Water runoff, km^3 year^{-1}	Suspended sediment load, 10^6 t year^{-1}
Northeastern (Russia)	5.1	201	6.4	1.6
Eastern (Georgia)	50.3	1450	45.7	18.6
Southern (Turkey)	229	1190	37.7	13.6
Southwestern (Bulgaria)	8.7	37.3	1.2	0.75
Northwestern (Romania and Ukraine)	1465	8340	263.2	41.5
Crimea (Ukraine)	2.2	8.8	0.28	0.13
Total	1760	11230	354.5	76.2

Danube River Basin

As it was shown in (Second Assessment, 2011), the Danube River Basin (DRB) (Figure 4.15) is the "most international" river basin in the world, covering territories of 19 countries. Of these 19 countries, Albania, Italy, Poland, Switzerland and the former Yugoslav Republic of Macedonia usually do not appear in compilations of the relative share of the 19 countries in the basin due to their very small areas that belong to the DRB. This also applies to the tables in this assessment report; however, the total area of the basin includes the areas of these countries as referenced in relevant footnotes. The Danube River itself has a length of 2,587 km[4] and an approximate discharge of 6,500 m^3/s at the river mouth.

Organic pollution is mainly caused by the emission of partially treated or untreated wastewater from agglomerations, industry and agriculture. Many agglomerations in the DRB have no, or insufficient, wastewater treatment and are therefore key contributors to organic pollution. Very often industrial wastewaters are insufficiently treated or are not treated at all before being discharged into surface waters (direct emission) or public sewer systems (indirect emission).

Figure 4.15. Danube basin map

A total of 6,224 agglomerations with a p.e. ≥2,000 (population equivalent) are located in the DRBD. Out of those, 4,969 agglomerations (21 million p.e.) are in the class of 2,000–10,000 p.e. and 1,255 agglomerations can be classified with a p.e. >10,000 (73.6 million p.e.). The updated assessment of the Danube River Basin District Management Plan (DRBMP) shows that COD and BOD5 emissions from large agglomerations (>10,000 p.e.) in the DRB are respectively 922 kt/year and 412 kt/year. The assessments have been improved by calculating emissions from agglomerations ≥2,000 p.e. The total emission contribution from these sources is 1,511 kt/year for COD and 737 kt/year for BOD5.

Concerning nutrient pollution, the Danube, as one of the major rivers discharging into the Black Sea, was estimated to introduce on average about 35,000 tones of phosphorus (P) and 400,000 tones of inorganic nitrogen (N) into the Black Sea each year in the period 1988-2005. The present level of the total P load that would be discharged to the Black Sea (including the P storage that occurs today in the Iron Gate impoundments) would be about 20% higher than in the early 1960s (based on modelling results). The Iron Gate Dams are a significant factor in reducing the amount of P from countries upstream on the Danube River, as the large amounts of sediment containing attached P settle out in the reservoir.

Pollution by hazardous substances can seriously damage riverine ecology, and consequently impact upon water status, affecting the health of the human population. Information provided by the EU member States in the European. Pollutant Emission Register (EPER) reporting shows an increase of the reported load values of arsenic, cadmium, chromium, copper, mercury, nickel, lead and zinc in 2004 (compared with 2001 values). In 2004, the amount of lead directly discharged was 138 t/year, and for zinc, 171 t/year.

Another major source of hazardous substances is pesticides used in agriculture. Information on pesticides' use within the Danube countries prepared for the DBA10 showed that 29 relevant active ingredients were used in pesticide products. Of these, only three pesticides are authorized for use in all of the DRB countries, while seven are not authorized in any of the countries, despite the fact that they have been found when testing water and sediments.

Compared with Western Europe, and including the upstream Danube countries, the level of pesticide use in central and lower DRB countries is still relatively low.

Three key hydromorphological pressure components of basin-wide importance have been identified: (1) interruption of river and habitat continuity; (2) disconnection of adjacent wetlands/floodplains; and (3) hydrological alterations.

The pressure analysis in the DRBMP showed that the key driving forces causing eventual river and habitat continuity interruptions in the DRBD are mainly flood protection (45%), hydropower generation (45%) and water supply (10%). Some 600 of the 1,688 continuity interruptions are dams/weirs, 729 are ramps/sills and 359 are classed as other types of interruptions. 756 are currently indicated to be equipped with functional fish migration aids. Thus, as of 2009, 932 continuity interruptions (55%) remain a hindrance for fish migration and are currently classified as significant pressures.

Connected wetlands/floodplains play a significant role when it comes to retention areas during flood events, and may also have positive effects on the reduction of nutrients. To date, 95 wetlands/floodplains (covering 612,745 ha) have been identified as having the potential to be re-connected to the Danube River and its tributaries. The absolute length of water bodies with restoration potential in relation to disconnected wetlands/ floodplains is 2,171 km (9% of the total river network). The main types of pressure in the DRBD causing hydrological alterations are in numbers: 449 impoundments, 140 cases of water abstractions and 89 cases of hydropeaking (rapid changes of flow). The pressure analysis concludes that 697 hydrological alterations are located in the DRBD, 62 of them in the Danube River.

Altogether 112 future infrastructure projects at different stages of planning and preparation have been reported in the DRBD, 70 in the Danube River itself. Some 64 (57%) are related to navigation; 31 (28%) to flood protection; 4 (4%) to water supply; 3 (3%) to hydropower generation and 10 (9%) projects to other purposes. Out of the 112 future infrastructure projects, 22 are at an implementation stage.

The Danube countries committed themselves to implement the Memorandum of Understanding adopted by the International Commission for the Protection of the Black Sea (ICPBS) and the ICPDR in 2001, and agreed that “the long-term goal is to take measures to reduce the loads of nutrients discharged to such levels necessary to permit Black Sea ecosystems to recover to conditions similar to those observed in the 1960s”. In 2004 the Danube countries adopted the Danube Declaration in the framework of the ICPDR Ministerial Meeting, and agreed that in the coming years they would aspire “to reduce the total amount of nutrients entering the Danube and its tributaries to levels consistent with the achievement of good ecological status in the Danube River and to contribute to the restoration of an environmentally sustainable nutrient balance in the Black Sea”.

The effects of measures to reduce nutrient pollution by 2015 have been assessed applying the MONERIS model, which takes into account both emissions from point sources and from diffuse sources. MONERIS compares the calculated nutrient input (scenario 2015) with the observed nutrient loads (reference situation average 2001-2005) in the rivers of the DRB, and allows conclusions to be drawn for implementing appropriate measures. On the basin-wide level, basic measures (fulfilling the UWWTD and EU Nitrates Directive) for EU member States and the implementation of the ICPDR Best Agricultural Practices Recommendation for non-EU countries are the main measures contributing to nutrient reduction. An overall Baseline Scenario-Nutrients (BS-Nut-2015), which combines the agreed most likely developments in different sectors (urban wastewater, agriculture and atmospheric deposition), has been compared to the expected emissions of nutrients based upon application of the management objectives for the basin-wide scale. Comparison between the Baseline Scenario-Nutrients 2015 and the Reference Situation-Nutrients shows a reduction of N and P pollution in the DRB. However, it can be concluded that the measures taken by 2015 on the basin-wide scale to reduce nitrogen and phosphorus pollution will not be sufficient to achieve the respective management objective and the WFD environmental objectives 2015.

A ban of P containing laundry detergents by 2012 and dishwasher detergents by 2015 (Phosphate Ban Scenario-Nutrients) is seen as a cost-effective and necessary measure to complement the efforts of implementing urban wastewater treatment. This ban would further reduce the P emissions by approximately 2 kt/year to a level only 5% above the values of the 1960s. Consequently, the 2015 management objective related to the reduction of the nutrient load to the level of the 1960s will be partially achieved for N and P.

The ICPDR's basin-wide vision for hazardous substances pollution is no risk or threat to human health, and the aquatic ecosystem of the waters in the DRBD and Black Sea waters impacted by the Danube River discharges. Reducing hazardous substances emissions is a complex task that requires tailor-made strategies, as the relevance of different input pathways is highly substance-specific and generally shows a high temporal and spatial variability. Although there is insufficient information on the related problems at a basin-wide level, it is clear that continued efforts are required to ensure the reduction and elimination of discharges of these substances. Due to the synergies between measures to address organic, nutrient pollution and hazardous substances, the further implementation of the UWWTD for EU member States contributes to the reduction of hazardous substances pollution from urban wastewater and indirect industrial discharges. Other relevant measures covering substances being released to the environment include chemical management measures.

The Dangerous Substances Directive, the IPPC Directive, and the UWWTD implementation by EU member States, as well as widespread application of Best Available Technique/Best Environmental Practice throughout the DRB, will improve but not solve problems regarding hazardous substances pollution. An overall improvement in the information available on the use of hazardous substances and their emissions into waters is a priority task for the ICPDR in the future. A majority of the surface waters of the DRBD fail to meet the WFD objectives because of hydromorphological alterations, signalling the need for measures to achieve the management objectives and the WFD environmental objectives. Interruption of river and habitat continuity, disconnection of adjacent wetland/floodplains, hydrological alterations and future infrastructure may impact water status and are therefore addressed as part of the JPM. Measures reported by the Danube countries to restore hydromorphological alterations have been screened for their estimated effect on the basin-wide scale.

The ICPDR's basin-wide vision for hydromorphological alterations are the balanced management of past, ongoing and future structural changes of the riverine environment, so that the aquatic ecosystem in the entire DRB functions holistically and includes all native species. This means, in particular, that anthropogenic barriers and habitat deficits should no longer hinder fish migration and spawning; and sturgeon species and specified other migratory species should be able to access the Danube River and relevant tributaries. The latter two species are represented with self-sustaining populations, according to their historical distribution. The focus for measures in the DRBD is on establishing free migration for long and medium distance migrants of the Danube River and the connected lowland rivers. To address the disconnection of adjacent floodplains/wetlands, the ICPDR's basin-wide vision is that floodplains/wetlands in the entire DRBD are to be re-connected and restored. The integrated function of these riverine systems ensures the development of self-sustaining aquatic populations, flood protection and reduction of pollution. The DRBMP reports the area of floodplains/wetlands to be reconnected by 2015 for both the Danube River and its tributaries. The inter-linkage with national River Basin Management Plans (RBMP) is vital for wetland reconnection, as, for example, significant areas are expected to be reconnected to rivers with catchment areas <4,000 km^2. The approach will be further developed during the second RBM cycle. The ICPDR's basin-wide vision for groundwater is that the emissions of polluting substances do not cause any deterioration of groundwater quality in the DRBD. Where groundwater is already polluted, restoring good quality will be the goal. Prevention of deterioration of groundwater quality and any significant and sustained upward trend in concentrations of nitrates in groundwater has to be achieved primarily through the implementation of the Nitrates Directive and the UWWTD. To prevent pollution of groundwater bodies by hazardous substances from point sources, the following measures are needed: an effective regulatory framework ensuring prohibition of direct discharges of pollutants into groundwaters; the setting of all necessary measures required to prevent significant losses of pollutants from technical installations; and the prevention and/or reduction of the impact of accidental pollution incidents.

The ICPDR's basin-wide vision is that groundwater use is appropriately balanced and does not exceed the available groundwater resource in the DRBD, considering the future impacts of climate change.

Appropriate controls regarding abstraction of fresh surface water and groundwater and impoundment of fresh surface waters (including a register or registers of water abstractions) must be put in place, as well as the requirements for prior authorization of such abstraction and impoundment. In line with the WFD, it must be ensured that the available groundwater resource is not exceeded by the long-term annual average rate of abstraction. The concept of registers of groundwater abstractions is well developed throughout the DRBD.

According to model data from the Swedish Hydrometeorological Institute (HYPE database, https://hypeweb.smhi.se), average daily flow of the Danube in the period 1981-2010 was 6390 m^3/sec, minimal daily flow made 1355 m^3/sec (27.08.2003) and maximal – 22306 m^3/sec (24.03.1981) (Figure 4.16).

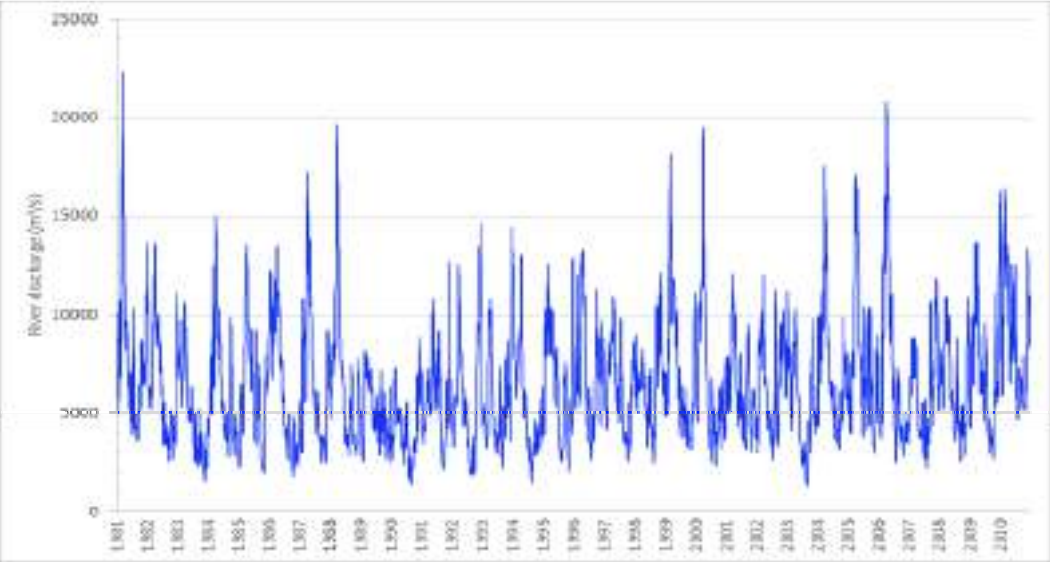

Figure 4.16. Temporal variability of daily discharge of the Danube River (retrieved from HYPE database, 1981-2010, https://hypeweb.smhi.se)

According to the data (HYPE database, https://hypeweb.smhi.se), minimal water discharge of the Danube in 1981-2010 within the seasonal variation was usually observed during summer-autumn period (July-November); maximal – during spring, in March-May (Figure 4.17). According to literature sources (Grychulevych, 2020) there three well-pronounced phases in the Danube water regime – spring high water, summer and autumn floods, autumn and winter low water seasons. Many years' observations show that average annual discharge of the Danube is 198 km^3, however the flow is not steady. In January-March water level sometimes rises reaching the critical point (232 cm BS port station Kiliya), while during summer period it drops down to 10 cm BS (port station Vylkove). High water level is often observed in winter and spring, which is due to significant rainfall all over the catchment area.

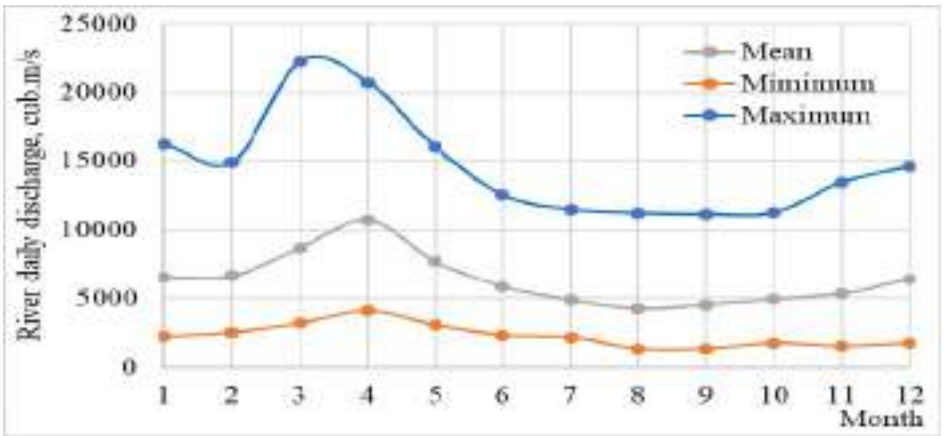

Figure 4.17. Longstanding average monthly minimal and maximal values of the Danube River daily discharges (retrieved from HYPE database, 1981-2010, https://hypeweb.smhi.se) (red line - Gaussian distribution)

Average annual discharge according to the data (HYPE database, https://hypeweb.smhi.se) for the period of 1981-2010 made 202 km^3/year with minimum of 133 (1990) and maximum of 284 (2010) km^3/year (Table 4.13). According to instrumental measurements at hydrological stations in 1950-2010, average annual discharge of the Danube made 210.4 km^3/year with minimum of 132.2 (1990) and maximum of 303.4 (1970) km^3/year (IMB data, 2018). From both sources, the positive linear trend was revealed for the annual discharge value: +0.23 km3/year for 1950-2010 and +1.23 km3/year for 1981-2010 respectively.

Inter-annual fluctuations of the Danube discharge volume for the period 1990-2010, according to the results of spectral analysis (Gazyetov & Dyatlov, 2021), contain 7 harmonic components with the periods: 2.4, 3.6, 4.9, 8.2, 14.0, 19.6 and 32.7 years. Hence, the resulting curve of the Danube River annual discharge for the mentioned years will be composed of superposition of harmonicas with minimum seven mentioned periods.

Table 4.13. Average annual Danube River Discharges

	River Discharge (m^3/s)				
Year	Average	Minimum	Maximum	Standard deviation	Total Runoff (10^6 m^3/y)
1981	7783.526	3544.453	22306.461	2.123	245461.267
1982	6529.830	2548.977	13626.753	1.903	205924.733
1983	5106.524	1551.678	10701.783	1.739	161039.350
1984	6210.860	2804.632	14938.971	1.789	196402.296
1985	6035.574	1928.881	13509.762	1.866	190337.868
1986	6285.087	1778.557	13467.239	2.219	198206.505
1987	6640.286	2419.375	17264.029	2.279	209408.065
1988	6673.803	2874.385	19617.576	2.306	211041.674
1989	4947.307	2501.643	8172.998	1.088	156018.289
1990	4206.633	1424.392	8873.802	1.341	132660.373
1991	5688.073	2095.884	12765.002	1.434	179379.074
1992	5919.800	1848.317	14643.065	2.117	187198.274
1993	5503.593	2167.545	14071.733	1.543	173561.319
1994	5729.424	1477.444	14416.200	2.072	180683.118
1995	6246.640	2004.924	12556.330	1.716	196994.037
1996	7359.320	2645.257	13281.182	1.647	232719.371
1997	6217.118	2591.441	10874.521	1.351	196063.029
1998	6612.077	2411.053	12118.025	1.343	208518.459
1999	6990.592	3106.240	18124.230	2.039	220455.294
2000	6656.432	2321.085	19489.605	2.280	210492.357
2001	6272.676	3054.798	12030.995	1.433	197815.117
2002	6495.851	2663.794	11987.216	1.573	204853.148
2003	5573.635	1355.268	11199.470	1.750	175770.152
2004	7184.611	3172.388	17536.771	1.864	227194.635
2005	7554.741	2978.860	17128.189	2.108	238246.307
2006	7328.419	2489.175	20784.094	2.805	231109.031
2007	5975.054	2170.072	11849.904	1.584	188429.313
2008	6094.664	2605.542	10888.373	1.447	192727.901
2009	6881.100	2692.103	13627.582	1.723	217002.382
2010	8999.148	4637.643	16384.486	1.749	283797.146

Dnipro River Basin

As it was shown in (Second Assessment, 2011), the 2,200-km long basin of the Dnipro River (Figure 4.18) is shared by Ukraine, the Russian Federation and Belarus. The river has its source in the southern part of Valdai Hills in the Russian Federation and discharges into the Dnipro Estuary in the Black Sea.

Figure 4.18. Dnipro basin map (Second Assessment, 2011)

Transboundary tributaries of the Dnipro include the Pripyat, Desna, Sozh, Psel and Vorskla. The 800-km section of the river furthest downstream is a chain of consecutive reservoirs. The Dnipro is connected with the Bug River through a canal. The basin has a pronounced lowland character.

Table 4.14. Basin of the Dnipro River (*Source:* UNDP-GEF Dnipro Basin Environment Programme; Ukraine)

Country	Area in the country (km2)	Country's share (%)
Russian Federation	90 700	18
Ukraine	292 700	58
Belarus	121 000	24
Total	504 400	

Due to insufficient capacity and the poor technical condition of treatment facilities, wastewater discharges from industry and settlements have a significant negative impact on water resources. In Belarus, Orsha, Mogilev, Rechytsa, Love, Borisov, Minsk (especially Svisloch area), Gomel and Bobruisk are among the main sources of industrial wastewaters. Within the Belarusian part of the basin, the most significant pollution load, urban/municipal wastewater, originates from Svisloch, where the Minsk Wastewater Treatment Plant is located, but some load also originates from Mogilev. Nutrients are the most important pollutants. Belarus assesses the impact of municipal wastewaters as widespread but moderate. The Dnipro is among the biggest recipients of pollutants in Ukraine, where until recently (2004) metallurgy was the biggest wastewater producer, followed by the coal industry and the chemical and petrochemical industries. Zaporozhye oblast has a large industrial zone, including metallurgy. Untreated or insufficiently treated wastewaters from these industries typically contain heavy metals, phenols, oil products and other hazardous substances.

Run-off from agricultural areas has a local but severe impact on water resources (Belarusian part). Large-scale development of timberland and draining of waterlogged lands for agriculture, as well as pollution with surface run-off from urban and agricultural areas, has affected the environment in the basin. In recent years, pollution with domestic waste, including waste left by holiday-makers, has increased along the Dnipro River and its tributaries. Belarus ranks the impact related to nuclear power generation as widespread and severe. However, the transboundary transfer of cesium-137 from the radioactively contaminated Belarus-Bryansk area, transported through surface waters of Sozh and its tributaries, has naturally decayed to insignificant levels. The impact of low-active strontium-90 is markedly amplified during flooding. Radioactive elements have been monitored since the Chernobyl catastrophe. Decrease in average annual cesium-137 and strontium-90 concentrations is observed in the reservoirs of the Dnipro cascade.

In Ukraine, measures for water protection are implemented in the framework of the State Programme of the Dnipro Basin ecological rehabilitation and drinking water quality improvement. Both Belarus and Ukraine report on-going efforts to reconstruct and extend wastewater treatment facilities. The Dnipro discharge is mainly (up to 80%) formed in the upper part of the basin. The Middle Dnipro tributaries' input into the renewable water resources of the river makes ca. 15%. Lower Dnipro forms less than 5% of the river discharge. Under the natural conditions, the mouth reach of the Dnipro was receiving in the average 53.0 km³ of water, in a high-water years – up to 73 km³, in a low-water year – up to 24 km³, which corresponded to average annual flow - 1680, 2315 and 760 m³/sec respectively. The Dnipro is fed from a number of sources; the main is the snowmelt (50%). There are also groundwater (27%) and rainfall (23%). The further downstream the role of snowmelt is growing, while the role of rainfall goes down (Plan of management …, 2018). Flow regulation and intensive water have resulted at visible changes of the Dnipro discharge.

According to the model data from the Swedish Hydrometeorological Institute (HYPE database, https://hypeweb.smhi.se), the Dnipro average daily flow for the period 1981-2010 was 1936 m^3/sec, minimal daily flow made 446 m^3/sec (17.08.1990) and maximal 3955 m^3/sec (02.06.1982) (Figure 4.19).

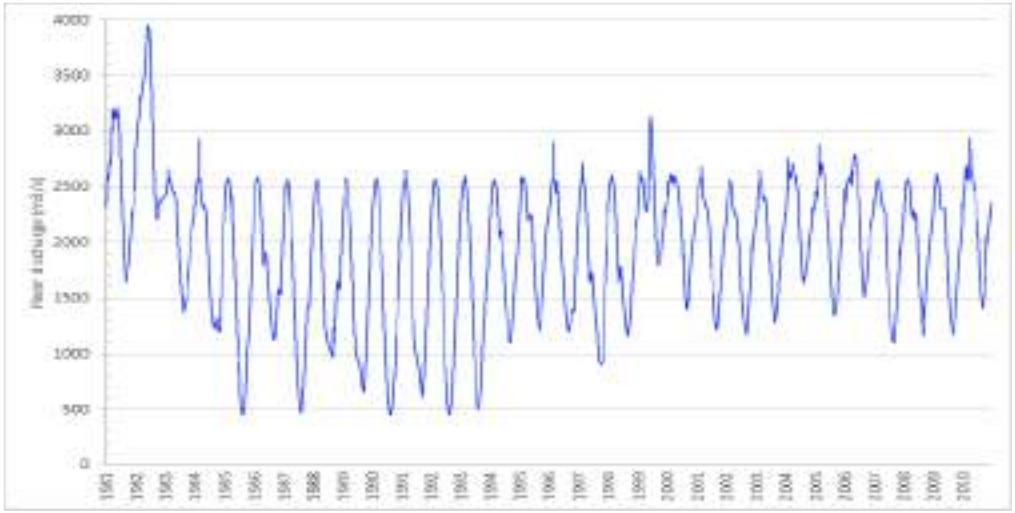

Figure 4.19. Temporal variability of the Dnipro River daily discharge of (retrieved from HYPE database, 1981-2010, **https://hypeweb.smhi.se**)

According to the data (HYPE database, https://hypeweb.smhi.se), minimal water discharge of the Dnipro River in 1981-2010 within the seasonal variation was usually observed in July-October, maximal – in December-April (Figure 4.20). At that, it should be mentioned that several cascades of water reservoirs built on the river have completely changed the natural seasonal fluctuations of the Dnipro discharge. Peak values of the river flow can be observed in the months with low precipitation number – June-July.

According to the literature (Plan of management …, 2018), average annual river flow in the mouth is 1670 m^3/sec. In the upper reaches the total flow changes from year to year insignificantly, growing and exceeding the norm 1.5-2 times in water-rich years or decreasing down to 0.5-0.7 of the normal value in low-water years. Summer and autumn discharge makes 25-35% of the total volume of annual river discharge, while winter discharge - 10-20%. Spring flood usually consists of one wave, starts in the second half of March and lasts 2–2.5 months.

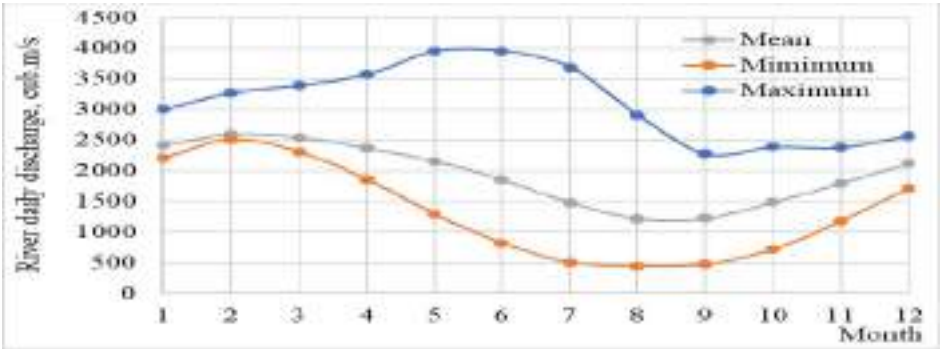

Figure 4.20. Many years' average monthly, minimal and maximal values of the Dnipro River daily discharges (retrieved from HYPE database, 1981-2010, https://hypeweb.smhi.se) (red line - Gaussian distribution)

The Dnipro River average annual discharge according to the data (HYPE database, https://hypeweb.smhi.se) for the period of 1981-2010 made 61 km^3/year with minimum of 48 (1985, 1990, 1992) and maximum of 94 (1982) km^3/year (Table 4.15). According to instrumental measurements at hydrological stations in 1950-2010, average annual discharge of the Dnipro made 42.5 km^3/year with minimum of 22.9 (1960) and maximum of 84.9 (1970) km^3/year (IMB data, 2018). For the period of 1981-2010 positive linear trend was observed in the distribution of river discharge values both for the instrumental (IMB data, 2018) measurements (+ 0.05 km^3/year) and the data from the HYPE model (+ 0.14 km^3/year (HYPE database).

The difference can be explained by the fact that significant volume of water is abstracted from the river for economic purposes and not taken into account in the model. According to the data (IMB data, 2018), linear trend of annual discharge for the period of 1950-2010 was negative and made – 0.04 km^3/year.

Inter-annual fluctuations of the Dnipro discharge volume for 1990-2010 according to spectral analysis results (Gazyetov & Dyatlov, 2021) contain 7 harmonic constituents with the periods of 2.2, 4.7, 5.8, 9.8, 12.3, 24.5 and 32.7 years.

Table 4.15. Average annual Dnipro Rivers Discharges

	River Discharge (m^3/s)				
Year	Average	Minimum	Maximum	Standard deviation	Total Runoff (10^6 m^3/y)
1981	2459.203	1630.189	3215.581	0.538	77553.410
1982	2967.540	2200.400	3954.684	0.560	93584.345
1983	2043.883	1378.335	2656.477	0.469	64455.889
1984	1888.087	1189.978	2922.877	0.610	59705.830
1985	1534.343	451.553	2572.690	0.988	48387.027
1986	1834.126	1119.702	2591.774	0.575	57840.988
1987	1572.869	461.662	2569.393	0.934	49602.005
1988	1717.484	976.963	2566.488	0.690	54310.968
1989	1582.072	651.708	2574.276	0.879	49892.238

	River Discharge (m^3/s)				
Year	Average	Minimum	Maximum	Standard deviation	Total Runoff (10^6 m^3/y)
1990	1510.405	446.230	2573.239	0.999	47632.128
1991	1577.149	608.227	2653.511	0.881	49736.979
1992	1508.692	447.207	2566.538	1.009	47708.455
1993	1568.859	494.922	2598.099	0.932	49475.527
1994	1844.572	1096.460	2561.990	0.585	58170.423
1995	1968.520	1196.964	2589.202	0.520	62079.234
1996	1887.119	1194.386	2904.815	0.607	59675.238
1997	1723.093	895.833	2714.852	0.711	54339.452
1998	1876.081	1154.625	2597.554	0.559	59164.087
1999	2335.689	1803.351	3140.001	0.368	73658.298
2000	2157.011	1393.440	2616.734	0.433	68209.853
2001	1975.480	1223.126	2681.298	0.521	62298.742
2002	1940.973	1164.824	2565.659	0.531	61210.537
2003	2022.937	1274.535	2659.228	0.485	63795.336
2004	2246.880	1631.186	2756.707	0.382	71051.737
2005	2115.353	1336.811	2878.890	0.520	66709.759
2006	2247.969	1516.755	2782.267	0.440	70891.954
2007	1900.209	1094.393	2566.056	0.594	59924.999
2008	1955.438	1156.436	2568.208	0.520	61835.655
2009	1931.366	1164.561	2622.477	0.562	60907.545
2010	2182.356	1411.703	2935.831	0.459	68822.766

Dniester River Basin **(Second Assessment, 2011)**

The basin of the 1,362-km long river Dniester (Figure 4.21) is commonly considered shared by Ukraine and the Republic of Moldova, as the share of Poland is very small. The river has its source in the Ukrainian Carpathians, and discharges into the Black Sea. Major transboundary tributaries include the Kuchurhan and the Yahorlyk. The basin is mountainous in the upper part, and lowlands prevail in the lower part. Valuable wetland systems extend along the Dniester Estuary, including some 100 wetland lakes (10-15 of the lakes are major). They play a vital role in maintaining the water balance and supporting the basin's biological diversity.

Figure 4.21. Dniester basin map

Table 4.16. Basin of the Dniester River (*Source:* Statistical Yearbook Environment of Ukraine, Kyiv 2008; Ministry of Environment, the Republic of Moldova.)

Country Area	in the country (km^2)	Country's share (%)
Ukraine	52 700	72.1
Republic of Moldova	19 400	26.8
Poland	226	0.4
Total	72 326	

Surface water resources in the Ukrainian part of the Dniester basin are estimated at 10.7 km^3/year in an average year (at 6 km^3/year in a dry year) and groundwater resources at 1.87 km^3/year. More than 90% of the total flow of the Dniester is generated in Ukraine. Approximately 40% of the groundwater resources are in Cretaceous formations, less than 20% in Quaternary, and around 12-13% each in Neogene, Devonian and Silurian. The majority of the aquifers are only weakly connected to surface waters. In the Moldovan part, surface water resources are estimated at 9.87 km^3/year (average for the years 1954 to 2008). The Dniester has a highly specific flood regime, featuring up to five flood events annually, during which water levels may increase by 3–4 m or even more.

The significant variability of water levels, especially in the upper Carpathian reach, is attributed to the river channel's low capacity. No significant changes in surface water quality have been registered in Ukraine during the period from 2007 to 2009. At Mogilev-Podolsky and Jampol utilities, in 2008–2009 exceedance in the concentrations of organic matter (as COD) and ammonium nitrogen were observed. The main pollutants are nitrogen, organic matter (BOD), phosphates, suspended solids and synthetic surfactants. At some monitoring points, copper is also a quality defect that occurs. In the Carpathian part of the Dniester, concentrations of metals systematically exceed MACs (e.g. iron and manganese).

Despite improvement of water quality over the last decade, related to a decrease in economic activity, significant water quality problems remain. Trends of salinization and eutrophication of the Dniester estuary are observed.

The main area where the Dniester discharge forms is the Carpathian mountainous segment of the catchment with its developed hydrographic network. Though the share of the Carpathians with the adjacent foothills in the catchment area is less than 9% and the share of the Carpathian tributaries is 17%, more than one-half of the Dniester discharge is formed there (Transboundary diagnostic study …, 2005). In the average, 800 to 1500 mm of precipitation fall out in the mountainous and foothill parts of the basin. High rain load on the north-eastern hillside of the Carpathians causes excessive soil moistening and storm floods, which are the characteristic features of the Dniester regime in general. The central (Podolska) part of the river basin is a hummocky surface with well-developed hydrographic network. Atmospheric precipitation makes in the average 450-700 mm/year and produce less influence on the regime of the river. The soils are more water permeable than in the Carpathians and the conditions for groundwater accumulation are more favourable. The lower part of the basin (from town Dubossary to the mouth) is characterised by low annual precipitation level. It is the dissected plain with gentle slope and poorly developed hydrographic network. Tributaries of this part of the river are mainly small and do not influence the Dniester discharge significantly. Thus, the main area where the Dniester discharge forms is the upper part of the basin (20.4 thousand km^2 or 28% of the catchment area). Flood can happen any month on the watercourses entering the mainstream in this area. The upstream part of the Dniester gives about 2/3 of annual water discharge.

According to model data from the Swedish Hydrometeorological Institute (HYPE database, https://hypeweb.smhi.se), the Dniester daily discharge for the period 1981-2010 made 257 with minimum of 6 (08.-09.1990) and maximum of 17605 (16.03.1999) m^3/sec (Figure 4.22).

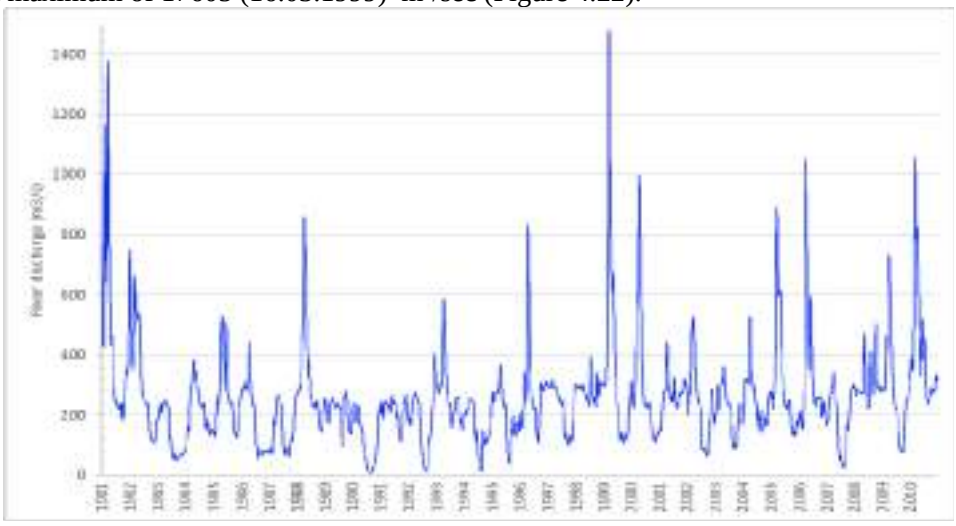

Figure 4.22. Temporal variability of the Dniester River daily discharge (retrieved from HYPE database, 1981-2010, https://hypeweb.smhi.se)

At that, daily discharge of 200-400 m3/sec was registered in ca. 56% of observations (Figure 4.23).

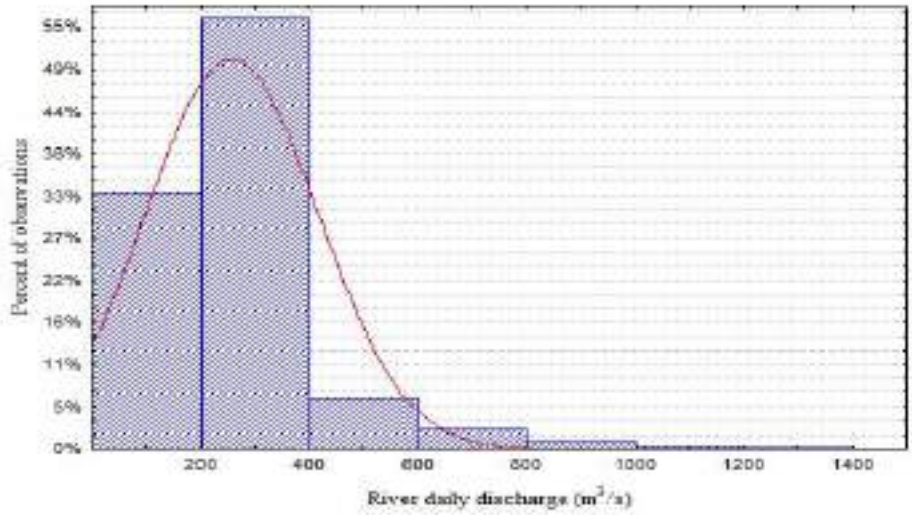

Figure 4.23. Frequencies of the Dniester River daily discharges (retrieved from HYPE database, 1981-2010, https://hypeweb.smhi.se) (red line - Gaussian distribution)

In terms of seasonality, 10-20% of annual precipitation falls out in the Dniester basin in winter, 35-45% in summer, spring and autumn account for 20-25% each (Transboundary diagnostic study …, 2005). Snow cover, apart from the upper basin, is not durable. In Moldova snow cover can form and melt more than once during winter season; in some winters it does not form at all, especially in the estuarine area. Thus, about 60% of annual discharge falls on the summer-autumn period, 25% on the spring period due to snowmelt, the rest 15% is the winter discharge formed mainly due to groundwater feeding the river. It should be mentioned that inter-annual distribution of discharge has slightly changed the recent decades: river flow decreased during spring flood and increased in the low water season. Average long-term flow in the river mouth area is 310 m^3/sec (Ropot et al., 1997). The value of 1% occurrence maximal spring flood flow in the Dniester mouth is 2660 m^3/sec. The flows of spring stormy floods are, respectively, 3010 and 5300 m^3/sec (Aliyev, 1997). Minimal flow is observed during winter low-water period and in September-October. According to the data (HYPE database, https://hypeweb.smhi.se), minimal water discharge of the Dniester in 1981-2010 within the seasonal variation was usually observed in July-November, maximal – in March-May (Figure 4.24).

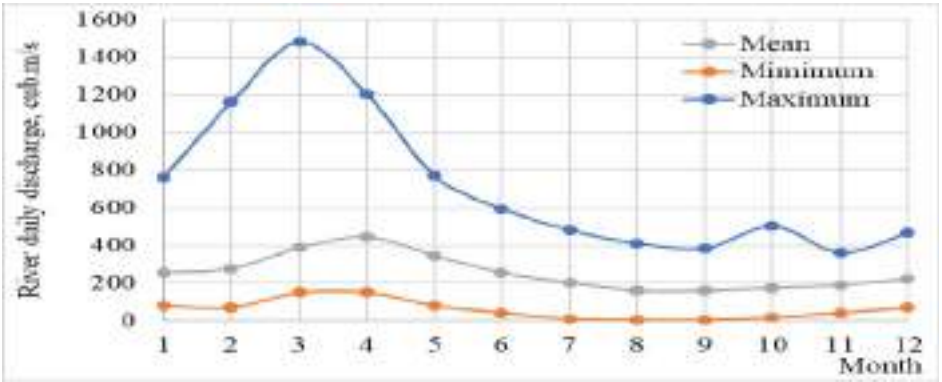

Figure 4.24. Long-term average monthly, minimal and maximal values of the Dniester River daily discharges (retrieved from HYPE database, 1981-2010, https://hypeweb.smhi.se) (red line - Gaussian distribution)

The Dniester water resources near the city Bendery at the catchment area of 66100 km^2 make (Main indicators…, 2000; Main indicators …, 2003): norm – 10.7 km^3; occurrence 50% - 10.4 km^3; occurrence 75% - 8.64 km^3; occurrence 90% - 7.17 km^3; occurrence 95% - 6.56 km^3.

According to the data (HYPE database, https://hypeweb.smhi.se), average value of the Dniester annual discharge for the period 1981-2010 made 8 km^3/year with minimum of 3 (1990) and maximum of 14 (1981) km^3/year (Table XXX.). According to the data of instrumental measurements at hydrological stations in 1950-2010 (IMB data, 2018), average annual Dniester discharge made 9.7 km^3/year with minimum of 4.9 (1990) and maximum of 19.2 (1980) km^3/year.

According to the data (Transboundary diagnostic study …, 2005) for the long-term period, the Dniester River discharge is decreasing (observation since 1881), which is explained, first of all, by climatic changes. The tendency of atmospheric precipitation decrease is observed in the western part of Ukraine, which usually tells upon the flow characteristics. Certain impact on water quantity results from irrevocable water consumption from the river.

However, for the period of 1981-2010, positive linear trend was observed according to the data (IMB data, 2018): + 0.07 km^3/year and the data (HYPE database, https://hypeweb.smhi.se): + 0.08 km^3/year. According to the data (IMB data, 2018), the linear trend of annual discharge value in 1950-2010 was also positive and made + 0.02 km^3/year.

According to spectral analysis(Gazyetov & Dyatlov, 2021), inter-annual fluctuations of the Dniester River discharge volume for the period of 1990-2010 contain 7 harmonic constituents with the periods 2.4, 3.6, 5.5, 10.3, 14.4, 24.0 and 36.0 years.

Table 4.17. Average annual Dniester River Discharges

	River Discharge (m^3/s)				
Year	Average	Minimum	Maximum	Standard deviation	Total Runoff (10^6 m^3/y)
1981	448.931	176.018	1380.449	0.710	14157.503
1982	322.799	105.697	749.381	0.536	10179.795
1983	139.391	50.622	250.988	0.343	4395.829
1984	217.191	85.691	383.904	0.281	6868.096
1985	265.071	124.809	526.407	0.361	8359.270
1986	194.462	57.694	440.519	0.431	6132.542
1987	157.040	65.763	269.938	0.308	4952.413
1988	325.613	145.282	861.913	0.494	10296.677
1989	214.525	93.215	282.888	0.158	6765.259
1990	106.570	5.701	243.708	0.409	3360.807
1991	214.172	110.799	270.584	0.155	6754.133
1992	182.470	10.091	405.981	0.404	5770.147
1993	267.749	150.501	584.183	0.301	8443.721
1994	156.022	14.847	258.175	0.306	4920.321
1995	207.884	39.822	368.481	0.308	6555.829
1996	289.353	107.095	832.217	0.439	9150.047
1997	227.980	101.007	316.723	0.252	7189.589
1998	283.216	225.853	394.948	0.096	8931.492
1999	348.928	108.451	1481.578	0.829	11003.800
2000	305.723	111.016	996.055	0.618	9667.692
2001	268.907	139.136	444.025	0.190	8480.246

	River Discharge (m^3/s)				
Year	Average	Minimum	Maximum	Standard deviation	Total Runoff (10^6 m^3/y)
2002	235.043	65.643	525.492	0.407	7412.328
2003	217.636	90.546	361.284	0.246	6863.367
2004	259.004	145.318	524.096	0.298	8190.341
2005	311.362	128.040	891.118	0.552	9819.106
2006	330.622	155.816	1052.920	0.583	10426.499
2007	192.067	26.752	343.966	0.373	6057.039
2008	308.946	219.062	503.328	0.199	9769.619
2009	287.661	78.292	731.178	0.517	9071.677
2010	411.181	236.212	1056.458	0.488	12966.995

The Southern Bug River

The Southern Bug River (in Ukrainian – Pivdenniy Bug) is the only river whose entire catchment is in Ukraine (Figure 4.25).

It starts from the Volyno-Podolsk Plateau in the village of Kholodets in Khmelnitsk Oblast and enters the Bug Estuary. Total length of the river is 813.6 km. Total area of the Southern Bug basin is 64300 km^2. The Southern Bug basin is located in the territory of the following Ukrainian Oblasts (regions): Khmelnytsk, Vinnytsa, Kirovograd, Mykolaiv, Kyiv, Odesa and Cherkassy Oblasts.

The main tributaries of the Southern Bug are the rivers Bolshaya Vys, Gniloy Tikitch, Volk, Gornyi Tikitch, Zgar, Ingul, Kodyma, Mertvovod, Rov, Savranka, Sinyukha, Sob, Tchernyi Tashlyk, Chicheklya, Yatran.

There are a number of big water reservoirs on the Southern Bug River: Schedrivske, Ladyzhenske, Sabarovske, Glubochanske, Gaivoronivse, Pershotravneve and Oleksandrivske. Those are used mainly for power production. The Southern Bug does not have big tributaries. The biggest is the Sinyukha River (its catchment area is 16804 km^2 – 26% of the Southern Bug catchment); it is formed by confluence of the Tikitch and the Bolshaya Vys Rivers. The longest tributary is the Ingul, its length being 342 km.

The Southern Bug River hydrology is characterized by significant seasonal changes in water quantity. It is fed mainly with snowmelt and rainfall, but also with groundwater. High water period is from late February to mid-April – early May, low water period is from June to February, floods are seldom. Spring high water period brings 50 to 80 % of discharge. In spring and winter the river is low. Slight rise of water level is observed in autumn, which is due to rainfall. It freezes over almost regularly in November (December) – February and becomes clear of ice by mid-March; ice regime is not permanent, ice melting and freezing is often observed in winter. In the lower reach does not freeze over in warm winters.

According to model data from the Swedish Hydrometeorological Institute (HYPE database, https://hypeweb.smhi.se), average daily flow of the Southern Bug River for the period of 1981-2010 made 1111 m^3/sec with minimum of 2 (08.1992) and maximum of 2143 (28.10.2010) m^3/sec (Figure 4.26).

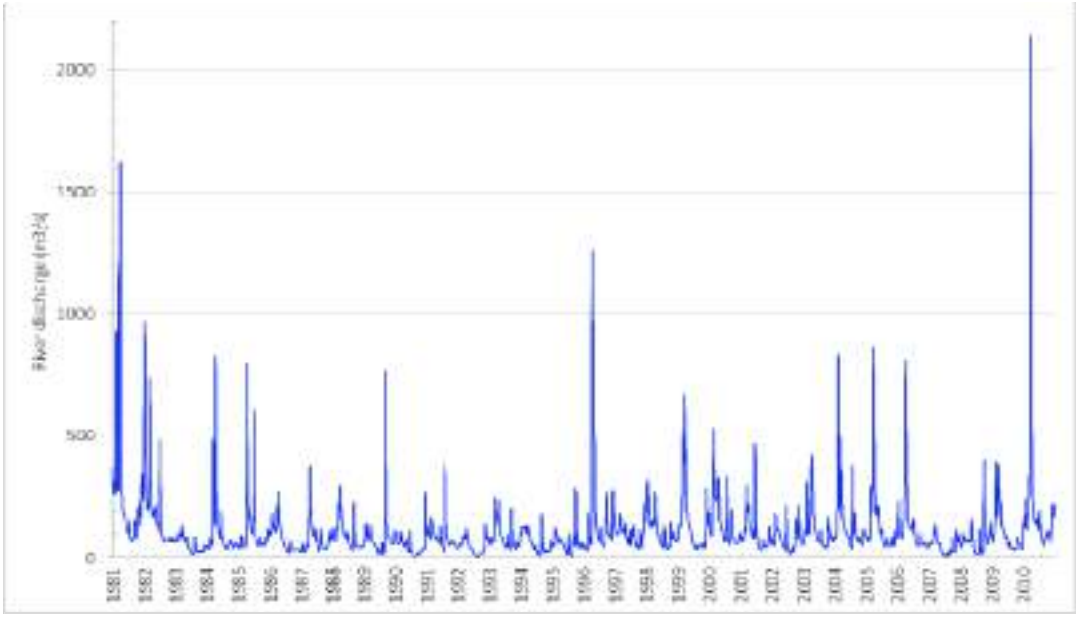

Figure 4.26. Temporal variability of daily discharge of the Southern Bug River (retrieved from HYPE database, 1981-2010, https://hypeweb.smhi.se)

About 90% of all the observations for the mentioned years have shown daily discharge less than 200 m^3/sec (Figure 4.27).

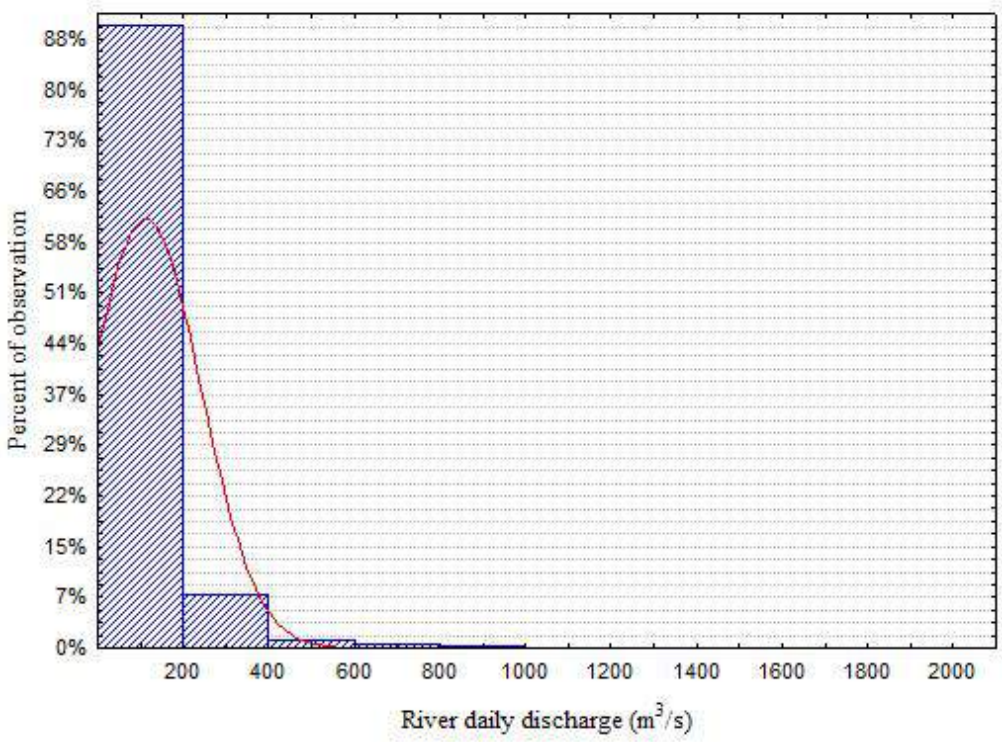

Figure 4.27. Frequencies of the Southern Bug River daily discharges (retrieved from HYPE database, 1981-2010, https://hypeweb.smhi.se) (red line - Gaussian distribution)

According to the data (HYPE database, https://hypeweb.smhi.se), minimal water flow in the Southern Bug River seasonal variation for 1981-2010 was observed in average in May-December, maximal – in spring, from March to April (Figure 4.28).

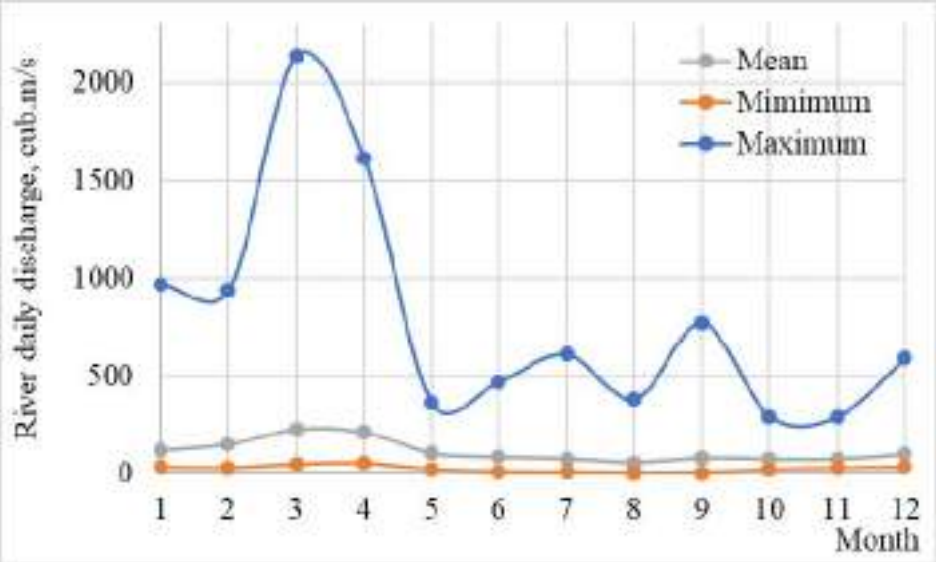

Figure 4.28. Long-term average monthly, minimal and maximal values of the Southern Bug River daily discharges (retrieved from HYPE database, 1981-2010, https://hypeweb.smhi.se) (red line - Gaussian distribution)

According to the data (HYPE database, https://hypeweb.smhi.se), for the period of 1981-2010, average value of the Southern Bug River annual discharge made 4 km^3/year with minimum of 2 (1983, 1986, 1987, 1990, 1992, 1994, 1995, 2007, 2008) and maximum of 9 (1981) km^3/year (Table 4.18.). Average value of the Southern Bug annual discharge according to instrumental measurements at hydrological stations in 1977-2010 (IMB data, 2018) made 3.0 km^3/year with minimum of 1.7 (1990) and maximum of 6.2 (1980) km^3/year.

Negative linear trend for the period of 1981-2010 was observed in both sources: - 0.01 km^3/year (IMB data, 2018) and – 0.003 km^3/year (HYPE database, https://hypeweb.smhi.se). For the period of 1977-2010, according to the data (IMB data, 2018), the linear trend of annual discharge was also negative and made – 0.04 km3/year.

Inter-annual fluctuations of the Southern Bug River discharge volume for the period 1990-2010, according to spectral analysis results (Gazyetov & Dyatlov, 2021) contain 7 harmonic constituents with the periods 2.3, 4.2, 6.0, 8.4, 14.0, 21.0 and 42.0 years.

Table 4.18. Average annual Southern Bug Rivers Discharges

	River Discharge (m^3/s)				
Year	Average	Minimum	Maximum	Standard deviation	Total Runoff (10^6 m^3/y)
1981	276.141	71.054	1624.518	0.903	8708.377
1982	198.174	72.651	969.604	0.683	6249.604
1983	57.184	16.201	134.757	0.203	1803.353
1984	110.043	40.102	832.975	0.626	3479.826
1985	122.454	43.661	800.399	0.575	3861.707
1986	78.478	25.719	277.806	0.315	2474.897

	River Discharge (m^3/s)				
Year	Average	Minimum	Maximum	Standard deviation	Total Runoff (10^6 m^3/y)
1987	77.693	28.343	377.714	0.358	2450.124
1988	95.754	34.701	298.789	0.324	3027.960
1989	86.032	15.921	768.506	0.516	2713.120
1990	53.966	7.847	275.480	0.298	1701.885
1991	89.408	25.118	378.068	0.290	2819.567
1992	51.551	2.366	148.158	0.258	1630.181
1993	90.345	35.735	246.083	0.281	2849.115
1994	63.945	9.164	180.894	0.269	2016.574
1995	62.226	6.513	290.454	0.276	1962.358
1996	159.800	34.055	1263.635	0.897	5053.274
1997	100.240	41.688	224.982	0.210	3161.171
1998	112.122	38.098	321.031	0.310	3535.880
1999	138.853	37.411	673.299	0.582	4378.876
2000	148.559	56.426	529.255	0.420	4697.797
2001	101.530	33.457	472.538	0.364	3201.863
2002	81.324	23.276	218.178	0.261	2564.639
2003	118.514	44.937	422.851	0.408	3737.450
2004	139.488	40.707	836.643	0.536	4410.937
2005	139.839	46.038	865.000	0.630	4409.965
2006	134.484	43.686	813.471	0.612	4241.080
2007	53.910	8.557	142.516	0.233	1700.091
2008	78.745	13.530	405.506	0.342	2490.094
2009	105.448	35.840	400.248	0.443	3325.414
2010	208.974	56.939	2142.836	1.090	6590.205